กลไกของสารพฤกษเคมีจากหอมแขกและหญ้าหวานในเซลล์โมเดลของโรคเบาหวาน เซลล์เพาะเลี้ยง มะเร็งตับและมะเร็งท่อน้ำดีในภาวะน้ำตาลสูง

นางสาวณัฐกานต์ หนูรุ่น

วิทยานิพนธ์นี้เป็นส่วนหนึ่งของการศึกษาตามหลักสูตรปริญญาวิทยาศาสตรดุษฎีบัณฑิต
สาขาวิชาชีวเคมีคลินิกและอณูทางการแพทย์ ภาควิชาเคมีคลินิก
คณะสหเวชศาสตร์ จุฬาลงกรณ์มหาวิทยาลัย
ปีการศึกษา 2560

MECHANISMS OF PHYTOCHEMICALS FROM MURRAYA KOENIGII AND STEVIA REBUADIANA IN CELL MODEL OF DIABETES, HEPATOCELLULAR CARCINOMA AND CHOLANGIOCARCINOMA UNDER HYPERGLYCEMIC CONDITIONS

Miss Nattakarn Nooron

A Dissertation Submitted in Partial Fulfillment of the Requirements
for the Degree of Doctor of Philosophy Program in Clinical Biochemistry and Molecular Medicine
Department of Clinical Chemistry
Faculty of Allied Health Sciences
Chulalongkorn University
Academic Year 2017

Thesis Title	MECHANISMS OF PHYTOCHEMICALS FROM MURRAYA KOENIGII AND STEVIA REBUADIANA IN CELL MODEL OF DIABETES, HEPATOCELLULAR CARCINOMA AND CHOLANGIOCARCINOMA UNDER HYPERGLYCEMIC CONDITIONS
By	Miss Nattakarn Nooron
Field of Study	Clinical Biochemistry and Molecular Medicine
Thesis Advisor	Anchalee Chiabchalard, Ph.D.

Accepted by the Faculty of Allied Health Sciences, Chulalongkorn University in Partial Fulfillment of the Requirements for the Doctoral Degree

.....Dean of the Faculty of Allied Health Sciences

(Assistant Professor Palanee Ammaranond, Ph.D.)

THESIS COMMITTEE

.....Chairman

(Associate Professor Rachana Santiyanont, Ph.D.)

.....Thesis Advisor

(Anchalee Chiabchalard, Ph.D.)

.....Examiner

(Assistant Professor Tewin Tencomnao, Ph.D.)

.....Examiner

(Tewarit Sarachana, Ph.D.)

.....External Examiner

(Warunya Arunotayanun, Ph.D.)

ณัฐกานต์ หนูรุ่น : กลไกของสารพฤกษเคมีจากหอมแขกและหญ้าหวานในเซลล์โมเดลของโรคเบาหวาน เซลล์เพาะเลี้ยงมะเร็งตับและมะเร็งท่อน้ำดีในภาวะน้ำตาลสูง (MECHANISMS OF PHYTOCHEMICALS FROM MURRAYA KOENIGII AND STEVIA REBUADIANA IN CELL MODEL OF DIABETES, HEPATOCELLULAR CARCINOMA AND CHOLANGIOCARCINOMA UNDER HYPERGLYCEMIC CONDITIONS) อ.ที่ปรึกษาวิทยานิพนธ์หลัก: อ. ดร. อัญชลี เฉียบฉลาด, 175 หน้า.

โรคเบาหวานเป็นโรคที่มีความผิดปกติในการเผาผลาญของร่างกาย ส่งผลให้ระดับน้ำตาลในเลือดสูงเป็นระยะเวลายาวนาน ซึ่งเกิดจากการผลิตอินซูลินจากตับอ่อนที่ลดลง หรือภาวะดื้อต่ออินซูลินจากอวัยวะต่างๆของร่างกาย ประชากรที่เป็นโรคเบาหวานมีความเสี่ยงที่เพิ่มขึ้นของภาวะแทรกซ้อนจากโรคหัวใจและหลอดเลือด และโรคมะเร็ง ภาวะน้ำตาลในเลือดสูงทำให้เกิดอนุมูลอิสระขึ้นภายในร่างกาย ซึ่งส่งผลต่อการบาดเจ็บของเซลล์และความเสียหายของอวัยวะ โดยเฉพาะอย่างยิ่งจะส่งผลต่อเซลล์ตับอ่อนชนิดเบต้าเซลล์ซึ่งมีหน้าที่ผลิตอินซูลิน นอกจากนี้ภาวะการดื้อต่ออินซูลินในเซลล์กล้ามเนื้อและเซลล์ไขมันก็เป็นอีกหนึ่งปัจจัยสำคัญในการบริหารกลูโคสในกระแสเลือด ดังนั้นการเพิ่มการนำกลูโคสเข้าสู่เซลล์ได้มากขึ้นจะสามารถลดภาวะดื้อต่ออินซูลินในผู้ป่วยโรคเบาหวานชนิดที่ 2 ได้อีกทางหนึ่ง นอกจากนี้หลายการศึกษาพบว่า โรคเบาหวานนั้นมีความสัมพันธ์กับมะเร็งท่อน้ำดีซึ่งเป็นมะเร็งที่มีความชุกสูงในภาคตะวันออกเฉียงเหนือของประเทศไทยอีกด้วย การศึกษาวิจัยนี้มีจุดประสงค์เพื่อศึกษาคุณสมบัติของสารพฤกษเคมีของหอมแขกและหญ้าหวานทางด้านเภสัชวิทยาในรูปแบบที่เกี่ยวข้องกับการรักษาเบาหวาน เช่น การลดระดับน้ำตาลในเลือด ลดภาวะดื้อต่ออินซูลิน รวมทั้งการรักษามะเร็ง จากการวิจัยพบว่า mahanine ซึ่งเป็นสารกลุ่ม alkaloid carbazole จากหอมแขกมีฤทธิ์ในการป้องกันการเกิดภาวะเครียดออกซิเดชันจากระดับน้ำตาลกลูโคสสูงในเซลล์ตับอ่อนชนิด RIN-m5F โดยการยับยั้งการแสดงออกของยีน NADPH oxidase จากการศึกษาพบว่า mahanine ยังช่วยเพิ่มการหลั่งอินซูลินด้วยการกระตุ้นการแสดงออกของยีน proinsulin (PRE-INS) glucose transporter 2 (GLUT2) และ glucokinase (GCK) นอกจากนั้น mahanine ยังช่วยกระตุ้นให้เพิ่มการนำกลูโคสเข้าสู่เซลล์กล้ามเนื้อและเซลล์ไขมันโดยการกระตุ้นโปรตีน GLUT4 เพื่อไปรับน้ำตาลที่ผิวเซลล์ผ่านทางการรับสัญญาณของโปรตีน Akt และ mahanine ยังแสดงให้เห็นถึงความเป็นพิษต่อเซลล์มะเร็งตับและเซลล์มะเร็งท่อน้ำดีสายพันธุ์ญี่ปุ่นและไทย ซึ่งสัมพันธ์กับระดับการแสดงออกที่เพิ่มขึ้นของ MITF การศึกษาสารพฤกษเคมีจากหญ้าหวาน ได้แก่ steviol, isosteviol และ 7 β-OHisosteviol พบว่าช่วยกระตุ้นให้เพิ่มการนำกลูโคสเข้าสู่เซลล์กล้ามเนื้อและเซลล์ไขมันผ่านการกระตุ้นการเคลื่อนโปรตีน GLUT 4 แต่มีฤทธิ์น้อยกว่า mahanine การศึกษาเหล่านี้ชี้ให้เห็นอย่างชัดเจนว่า mahanine มีศักยภาพที่จะสามารถนำไปใช้ในการรักษาโรคเบาหวานและโรคมะเร็งได้ในอนาคต

ภาควิชา เคมีคลินิก ลายมือชื่อนิสิต .....

สาขาวิชา ชีวเคมีคลินิกและอณูทางการแพทย์ ลายมือชื่อ อ.ที่ปรึกษาหลัก .....

ปีการศึกษา 2560

5576952937 : MAJOR CLINICAL BIOCHEMISTRY AND MOLECULAR MEDICINE
KEYWORDS: DIABETES MELLITUS / MURRAYA KOENIGII / STEVIA REBUADIANA / HEPATOCELLULAR CARCINOMA / CHOLANGIOCARCINOMA

NATTAKARN NOORON: MECHANISMS OF PHYTOCHEMICALS FROM MURRAYA KOENIGII AND STEVIA REBUADIANA IN CELL MODEL OF DIABETES, HEPATOCELLULAR CARCINOMA AND CHOLANGIOCARCINOMA UNDER HYPERGLYCEMIC CONDITIONS. ADVISOR: ANCHALEE CHIABCHALARD, Ph.D., 175 pp.

Diabetes mellitus (DM) is a group of metabolic disorders in which high blood glucose levels over a prolonged period, caused by deficiency of insulin production from the pancreas, or by the insulin resistance. Several epidemiological studies suggest that diabetic population is not only at increased risk of cardiovascular complications, but also at substantially higher risk of many types of malignancies. Hyperglycemia induced free radical reactive oxygen species (ROS) production, which is a major cause of cell injury and organ damage, especially affects pancreatic beta cells. Whereas insulin resistance in skeletal muscle tissue and adipocyte are the major sites of postprandial glucose disposal, and enhancing glucose uptake into this tissue may decrease insulin resistance in type 2 diabetes patients. Moreover, Hyperglycemia and hyperinsulinemia in DM also showed the strong relation with cholangiocarcinoma proliferation and migration, the high prevalence cancer in the Northeast of Thailand. The study of phytochemical chemistry form *Murraya koenigii* and *Stevia rebuadiana* were conducted to investigate their pharmacological properties in various model that related to DM such as hyperglycemia, insulin resistance as well as in cancer cell line. Mahanine, a carbazole alkaloid from *Murraya koenigii* showed the outstanding protective effects in high glucose induced oxidative stress in RIN-m5F pancreatic beta cells via suppression of NADPH oxidase gene expression. Moreover, mahanine increased the insulin secretion by stimulating the pancreatic duodenum homeobox-1(PDX-1) expression and translocation, proinsulin (PRE-INS), and glucose transporter 2 (GLUT2) and glucokinase (GCK) gene expression. In addition mahanine enhanced the insulin sensitizing effects in skeletal muscle and adipocyte cells by increased glucose uptake and promoted glucose transporter 4 (GLUT4) translocation via activation of the Akt signaling pathway. Furthermore, mahanine showed the potent cytotoxicity in HepG2 human hepatocellular carcinoma and HuCCT1 and KKU-100 human cholangiocarcinoma cells, which was associated with increased the expression levels of MITF. Whereas the phytochemical chemistry from *S. rebuadian;* steviol, isosteviol and 7 β-OHisosteviol, also presented the anti-diabetes effects by increased the glucose uptake and GLUT 4 translocation but least potent than mahanine. These study suggested that mahanine have anti-diabetic potential for treating diabetes and anti-cancer, which potentially to use as concomitant herbal medicine in cancer and/or diabetes patient without concerning of cancer treatment-induced DM and DM treatment-induced cancer.

Department: Clinical Chemistry Student's Signature .....
Field of Study: Clinical Biochemistry and Molecular Medicine Advisor's Signature .....
Academic Year: 2017

ACKNOWLEDGEMENTS

I would like to thank my major advisor, Dr. Anchalee Chiabchalard who provided me with excellent guidance, the opportunity to study in Ph.D. Program in Clinical Chemistry, Faculty of Allied Health Sciences, Chulalongkorn University. I would like to thank my oversea advisor Professor Shigeki Shibahara, Professor Soisungwan Satarug, Assoc. Prof. Dr. Kazuhisa Takeda and Asst. Prof. Dr. Koji Ohba, for his/her kind help with the formality of special research student at Tohoku University, School of Medicine. Special thanks go to Prof. Apichart Suksamrarn for kindly providing the valuable compounds and for many valuable suggestions.

My thanks go to the member of my advisory committee, Assoc. Prof. Dr. Rachana Santiyanont, for kindly providing valuable time to be a chair in the thesis examination. I would like to say thank you to Asst. Prof. Dr. Tewin Tencomnao, Dr. Tewarit Sarachana, and Dr. Warunya Arunotayanun for kindly providing valuable time to be a committee in the thesis examination.

I would like to thank a scholarship from 60/40 Support for Tuition Fee and research assistant fellowship from Graduate School and Faculty of Allied Health Sciences. This study was financially by the Overseas Research Experience Scholarship for Graduate Student, Graduate School and Faculty of Allied Health Sciences, Chulalongkorn University and the 90th Anniversary of Chulalongkorn University Fund (Ratchadaphiseksomphot Endowment Fund). This research was supported by National Research University Project, Office of Higher Education Commission (WCU-58-041-AS).

Many thanks for friends and colleagues from Clinical Biochemistry and Molecular Medicine Program for creating a warm environment during my work.

Lastly, and most importantly, I would like to thank my family for supporting me throughout all my studies at Chulalongkorn University. They always stand by me in every situation and encouraged me to do my best in all matters of life.

CONTENTS

Page

Page

Page

Page

Page

Page

Page

LIST OF TABLE

LIST OF FIGURES

CHAPTER I
INTRODUCTION

Background and rationale

The prevalence of diabetes mellitus worldwide has dramatically increased due to the modern lifestyle, reduced physical activity and increased dietary fat consumption [1]. Recently, the International Diabetes Federation, 2015 indicated that 415 million people have diabetes, and the number of people with the disease is set to rise beyond 642 million in 2040 and type 2 diabetes accounts for at least 90% of all cases. Type 2 Diabetes mellitus (T2DM) is a chronic disease characterized by insulin resistance of target tissues (skeletal muscles and adipocytes), caused by reduced communication of insulin signaling, combined with progressive functional deterioration and decreased insulin secreting from pancreatic beta cells [2]. These two pathological processes were showed by impaired glucose tolerance of the affected individuals, leading to hyperglycemia. Hyperglycemia can induce free radicals reactive oxygen species (ROS) production, which is a major cause of cell injury and organs damage, especially pancreatic beta cells that lead to the aggravation of type 2 diabetes. A key to successful management of diabetes is to control postprandial hyperglycemia in order to reduce short and long-term health complications including heart disease, nerve damage, retinopathy and nephropathy [3]. Moreover, epidemiological studies indicated that the risk of many types of cancer including pancreas, liver, and breast, is increased in diabetic patients. Hyperinsulinemia most likely favors cancer in diabetic patients since, insulin is

acting as growth factor and mitogenic effects. Obesity, hyperglycemia, and increased oxidative stress may also contribute to increased cancer risk in diabetes [4]. Hyperglycemia, insulin resistant, hyperinsulinemia, increased insulin-like growth factor-1 (IGF 1) level and inflammatory cytokines are potential mechanisms which believed act as a key member that associated with increased cell proliferation, migration and invasion and decreased apoptosis in cancer cell [5].

One of the major causes of type 2 diabetes is ROS and the NADPH oxidase (NOX) complex that play a crucial role. The NADPH oxidase induces, under high glucose, ROS production leading to insulin secretion and decreased insulin gene expression [6, 7]. Thus, the excessive or sustained production of ROS is negatively correlated with the insulin secretory process, leading to impairment of pancreatic beta cells function. In addition, oxidative stress mediated inhibition of insulin gene expression has been shown to stem in part from the well-established decrease of pancreatic duodenum homeobox-1 (PDX-1) binding to the insulin promoter [8]. Destruction of pancreatic islets leads to decreased insulin secretion, resulting in an abnormally high blood glucose and progressive generation of additional oxidative stress. The main signaling pathways affecting insulin secretion is glucose transport into pancreatic beta cells by glucose transporter 2 (GLUT2) which is then metabolized by glucokinase (GCK) to glucose-6-phosphate, resulting in ATP production, which in turn induces Ca^{2+} influx, and then the release of insulin. In parallel, PDX-1 is recognized as a key regulation factor in the cascade regulating insulin secretion. Translocation of PDX-1 into the nucleus induces

proinsulin (PRE-INS) expression [9]. Thus, the suppression of NOX may reverse glucose-induce insulin secretion. Another mechanism of diabetes type 2 is insulin resistance of target tissues which skeletal muscles and adipose play a major role. Skeletal muscles and adipose tissues are a major (80%) part of insulin-mediated glucose uptake from the body in the post-prandial state, and play important roles in maintaining glucose homeostasis [10]. In skeletal muscle and adipocytes, insulin increases glucose uptake through signaling that leads to the activation of phosphatidylinositol-3 kinase (PI3K) and Akt (also known as protein kinase B, PKB) resulting in increased translocation of glucose transporter 4 (GLUT4) to the plasma membrane [10]. Another GLUT4 translocation promoter is AMP-activated protein kinase (AMPK) [11].

Diabetes is chronic illnesses that depends on drugs for successful management. However, diabetes medicines are very expensive and can cause serious side effects such as kidney complications, increased risk of liver disease and increased anaemia risk [12]. Traditional medicines derived from medicinal plants are used as an alternative treatment by about 60% of the world's population. The World Health Organization (WHO) has listed 21,000 plants which are used for diabetes medicinal purposes around the world [13]. Studies of medicinal plants have clearly established clinical information to support anti-diabetes effect such as *Allium sativa, Panax ginseng, Gymnema sylvestre, Momordica charantia, Tinospora cordifolia and Murraya koenigii* (L.) Spreng. [14]. However, numerous herbal plants have limited evidence to support anti-hyperglycemic, side effect and long-term toxicity.

Many studies show the prevention and treatment of metabolic syndrome by using natural compounds. *Murraya koenigii* (Linn.) Spreng (curry leaf) is defined in folk medicine as a tonic, and for the treatment of stomach ache, and diabetes mellitus [15]. Several bioactive carbazole alkaloids have been isolated from the leaves of this plant, including mahanine, mahanimbine, isomahanimbine, koenigine, koenine, girinimbine, koenimbidine koenidine and murrayanine [15]. Carbazole alkaloids have been reported for their various pharmacological activities such as anti-tumor, anti-viral, anti-inflammatory, anti-diarrheal, diuretic, anti-oxidant and anti-diabetes activities [15]. Mahanine (3,11-dihydro-3,5-dimethyl-3-(4-methyl-3-pentenyl)-pyrano[3,2-a]carbazol-9-ol) has been reported to be the major bio-active alkaloid [16]. Mahanine present in the edible parts of some plants such as *Micromelum minutum* and *Murraya koenigii*, that are consumed in some parts of Southeast Asia, including Thailand [17]. However, evidence regarding the plant's mechanisms of action by the active compounds from *Murraya koenigii* has not been widely reported. Previous studies demonstrated the likely mechanism of mahanine is its antioxidant and free radical-scavenging activities [18]. There are many mechanisms for reducing hyperglycemia such as increasing insulin secretion, enhancing glucose uptake by skeletal muscle or adipose tissues and inhibiting glucose absorption from the intestine. Some researchers have also demonstrated a reduction of blood glucose and increased insulin sensitivity in obese rats [19], as well as suppression of glucose uptake when treated with *M. koenigii* [20, 21]. However, any anti-

diabetes effect and the molecular mechanism signaling pathways for glucose uptake by mahanine treatment still need investigation.

Currently, there are many studies on diabetes and cancer, such as using metformin for cancer treatment [22]. There are problems in type 2 DM from hyperglycemia, insulin resistant and hyperinsulinemia increased insulin-like growth factor-1 (IGF 1) stimulation and inflammatory cytokines release which resulting in promote cell proliferation, migration and invasion and decreased cell apoptosis which favour on cancer. Cholangiocarcinoma is a malignant tumor that is originated from the biliary epithelial cell, and is the second most common primary liver tumor, accounting for about 10-15% after hepatocellular carcinoma [23]. Both types of hepatic cancer are characterized by poor prognosis. Samatiwat et al. 2016 showed an inhibition of Hedgehog signalling can increase the expression of MITF (total MITF) levels in human hepatocellular carcinoma and cholangiocarcinoma cell lines [24]. In the presence of a Hedgehog ligand, it smoothened enhances nuclear translocation of glioma-associated transcription factors, glioma-associated oncogene 1 (GLI1) [25], thereby mediating the Hedgehog signal. The increasing of GLI1 found in cancer cell proliferation. Because Hedgehog signalling is required for normal development of RPE in the mouse [26], it is tempting to speculate the Hedgehog signalling may influence MITF expression in the liver. Mitf (transcription factors) ontains a basic helix-loop-helix and a leucine-zipper (bHLH-LZ) structure, and it has been established as a key regulator for development of melanocytes and the retinal pigment epithelium (RPE) [27-30]. However, subsequent

studies have suggested the pleiotropic functions of Mitf in various organs, including liver [31], pancreas [32], kidney [33], lung [34], olfactory bulb [35] and frontal cortex [33]. A first step to study the regulation of MITF in the liver by analysed the expression profile of gene in human hepatocellular carcinoma and cholangiocarcinoma. We thus show that MITF immunoreactivity is detected in subsets of human hepatocellular carcinoma and cholangiocarcinoma specimens that also express GLI1. Subsequently, we study MITF expression in human hepatic cancer cells treated with mahanine from *Murraya koenigii*. This plant is used as folk medicine in Thailand, where the liver fluke-associated cholangiocarcinoma is common [23]. In fact, the infection with the liver fluke (*Opisthorchis viverrini*) is a well-known risk factor of cholangiocarcinoma in Thailand [36, 37]. We found that mahanine show not only anti-diabetes effect but also anti-cancer via Microphthalmia-associated transcription factor (Mitf) pathway. The increase in MITF expression was found in human hepatic cancer cells treated with mahanine [38, 39]. A better understanding the regulation of MITF expression may contribute to developing a novel anti-hepatic cancer agent.

In this study determination of anti-oxidative effect and anti-hyperglycemic mechanisms of bioactive compounds from *Murraya koenigii* and *Stevia rebuadiana* were performed. The mechanisms of α-glucosidase and α-amylase inhibition activity, stimulation of glucose uptake in both fat cells (3T3-L1) and skeletal muscle (L6) cell were studied. The pancreatic beta cells protective effect of both compounds from free radicals damaged in high glucose conditions were also determined. The results were

that mahanine showed more effective than steveiol to increase glucose uptake in skeletal muscle and adipocyte cells. The effect of this compound to prevent hyperglycemic occur through mechanisms such as increased glucose transporter 4 (GLUT4) translocation to the plasma membrane via the AMPK pathway or stimulation of phosphatidylinositol 3-kinase (PI3K) Akt pathway. In addition, mahanine showed the effect on NADPH oxidase mediated oxidative stress and insulin secretion of pancreatic beta cells that response to high glucose condition and explored the underlying mechanisms. Moreover, anti-cancer effect of mahanine via Mift mechanism was also revealed in this study.

CHAPTER II
LITERATURE REVIEW

2.1 Epidemiology of diabetes mellitus

Nowadays, there are 382 million people living with diabetes mellitus. A more 316 million with impaired glucose tolerance are at high risk from the disease an disturbing number that is set to reach 592 million by 2035 [40].

2.2 Definition of diabetes mellitus

Diabetes mellitus is well-defined as an elevated blood glucose related with absent or inadequate pancreatic insulin secretion, with or without parallel impairment of insulin action. The disease situations underlying the diagnosis of diabetes mellitus are classified into four types: type1, insulin-dependent diabetes; type2, non-insulin-dependent diabetes; type3, other; type4, gestational diabetes mellitus [41]. However, type 2 diabetes mellitus is importance because 90% of diabetes mellitus developed to this type. In addition Type 2 diabetes mellitus leading to causes of diabetes complication such as retinopathy, neuropathy and cardiovascular disease. Therefore, prevention or treatment of type 2 diabetes is an importance to reduce complication and this study will be focused on treatment of type 2 diabetes mellitus.

2.3 Glucose homeostasis

The preservation of glucose homeostasis is regulated by multipart interaction between organs, hormone and the neuronal control system. Insulin and glucagon are recognized to hold leading roles for balancing blood glucose levels, in case of feeding and staving state [42, 43]. Insulin is a hypoglycemic hormone that increases glucose storage into the cells (feeding state), while glucagon is hyperglycemic hormone that stimulates the release of glucose from the liver (staving state) [43]. The rising of glucose levels after intake response to pro-insulin undergoes posttranslational processing into insulin and C-peptide secretion [44]. This process happens in the secretory vesicles just before useful insulin is secreted form the pancreatic beta cells into blood circulation. Insulin stimulates the uptake of glucose into outer tissue, mainly skeletal muscle and adipose cells, and encourages storage of glucose in the liver in the form of glycogen (glycogenesis); glycogen can be quickly released, broken down to glucose and used for energy as required [45]. As a rule, the body's energy supplies are met first, monitored by the formation and storage of glycogen; finally, if excess glucose is still presented, it is changed to fat and stored in adipose tissue. After the blood glucose level returns to the normal state, insulin secretion is inhibited [46].

The stimulation of glucose uptake into muscle and adipose cells needs to have insulin in process of translocation via glucose transporter (GLUT-4) [47]. Insulin starts the biological properties by binding to its receptor on muscle and/or adipose cell surface. The insulin receptor is a glycoprotein going to subfamily of tyrosine kinase

receptor, and is composed of two alpha-subunits and two beta-subunits. When insulin binds to alpha subunits of insulin receptor, tyrosine kinase activity be present in beta subunit. After that Beta subunits is stimulated and catalases the phosphorylation of an amount of cellular proteins such as insulin receptor substrate (IRS-1) and (IRS-2). In the basal state, GLUT-4 is stored within secretory vesicles in cytoplasm. Upon phosphorylation, these vesicles are released from intracellular site, letting trafficking of GLUT-4 to the surface via exocytosis, where the vesicles then fuse with the cell membrane and let glucose to move in the cell by facultative diffusion. This effect of insulin on translocation of GLUT-4 is reversible. When insulin levels decrease, GLUT-4 is removed from the cell surface and restored back to secretory vesicles in intracellular sites. In opposition, glucose uptake into intestine, kidney, liver, and brain tissues is not dependent on insulin. Glucose arrives the hepatocytes and pancreatic beta cells via GLUT-2 glucose transporters, whereas GLUT-3 together with GLUT-1 are involved in non-insulin mediated uptake of glucose into the brain [48]. During starvation, decreasing blood glucose levels reason secretion of glucagon from the pancreas. Glucagon stimulates the change of liver glycogen to glucose or glycogenolysis and synthesis of glucose from the non-carbohydrate molecules or gluconeogenesis. The hepatic glucose production reasons the releases of glucose into the blood circulation and gets blood glucose levels to the normal range. This process is required for maintaining blood glucose within homeostatic level to ensure a sufficient stock of glucose for normal organ function and survival, since the brain and other neuronal tissue use glucose at a constant rate.

Therefore, insulin is necessary endocrine hormone, which is importance for metabolic process in both normal and diabetes mellitus [47, 49].

2.4 Insulin

Insulin is small protein contains 51 amino acid arrange in two chain connected by disulfide bridges; there are species differences in the amino acid of both chain [50]. Proinsulin, a long single chain protein molecule, is managed with in the Golgi apparatus of beta cells and packaged into granules, where it is hydrolyzed into insulin and a residual linking segment called C-peptide by removed of four amino acid [50]. Insulin and C-peptide are secreted in equimolar amounts in response to all insulin secretagogues; a small quantity of unrefined or incompletely hydrolyzed proinsulin is released as well. Although proinsulin may have some mild hypoglycemic action, C-peptide has no know physiologic function. Granules within the beta cells store the insulin in the form of crystals involving of two atom of zinc and six molecules of insulin. Basal insulin standards of 5-15 μU/mL (30-90 pmol/L) are established in normal human, with a peak rise to 60-90 μU/mL (360-540 pmol/L) during meals [51].

Insulin is secreted from pancreatic beta cells at a low basal rate and at much higher stimulated rate on response to a variety of stimuli, especially glucose. Glucose-stimulated insulin secretion (GSIS) relates glucose oxidation in order to produce ATP and the anaplerotic/cataplerotic pathway which mediated generation of coupling factors that activate insulin secretion [52, 53]. In the fasting state, insulin is not secreted, glucagon derives out from the alpha cells to excite the liver to produce glucose, and

these tend to raise the blood sugar back up to normal levels. Food consuming is as the glucose goes up, that stimulates the beta cells in the pancreas to make insulin, which in turn locks off glucagon, with decreased glucose output from the liver and of course, peripheral tissues that are insulin-sensitive, such as muscle and adipose tissue, take up glucose. Therefor is what happens in the normal state. In diabetes, there are some major pathophysiologic defects in type 2 diabetes, and there is islet cell dysfunction. There is an unsuitable secretion of glucagon leading to enlarged hepatic glucose output; the beta cells is not making as much insulin as it should be so there is a relative insulin deficiency. In addition, of course, in type 2 diabetes we usually have insulin resistance as well, so that the insulin-sensitive tissues are not picking up glucose like they should. These situation results in elevated levels of glucose in bloodstream. One mechanism of stimulated insulin release is show on the Figure 1, hyperglycemia result in increased intracellular ATP levels, which adjacent the ATP dependent potassium channels. Decreased external potassium efflux results in depolarization of the beta cells and opening of voltage gated calcium channels. The resulting improved intracellular calcium triggers secretion of insulin. However, in type 2 diabetes mellitus represent abnormal insulin secretion or insulin resistance in skeletal muscle cell.

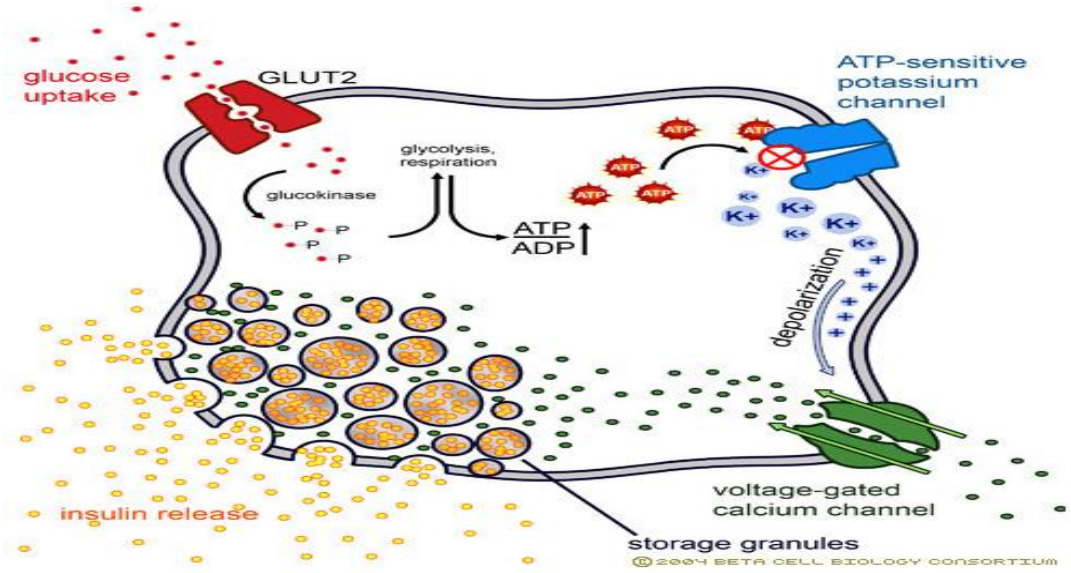

Figure 1: Mechanism of insulin secretion in beta cells [54].

2.5 Insulin resistance

Insulin resistance is a situation in which target tissues decrease sensitivity to normal circulating heights of insulin. In the insulin resistant specific, the cell- surface receptor on skeletal muscle, liver and adipocyte cells no longer muddles insulin appropriately and/or responds to the insulin signal with the importance of reduce glucose uptake. Consequently, the pancreas tried to reward by increasing insulin secretion for maintaining glucose homeostasis. Many persons with insulin resistance have increased heights of both glucose and insulin circulation in their blood concurrently [55, 56].

2.6 Insulin signal transduction in type 2 diabetes

In the physiological condition, insulin regulates the blood glucose level, cell growth and cell metabolism. When insulin bind to the insulin receptor, which is transmembrane tryrosine kinase receptor it course receptor remodeling by

phosphorylated the substrate protein such as Gab1, CbI - CAP and insulin receptor substrate (IRS) protein. The activated receptor send the signal transduction to the cell by two major pathways. First, mitogen activated protein kinase pathway, Ras activate MAPK cascade that involve in cell growth [57, 58]. Second is phosphoinositide 3-kinase (PI3K) pathway, insulin receptor substrate (IRS) protein induced PI3K, phosphatidylinositol (3,4,5)-triphosphase (PIP3) and PDK1 activation. The downstream signal transduction send to Protein serine/threonine kinase B (PKB) or AKT, P70S6K and Protein kinase C leading to glucose transporter (GLUT) vesicles fuse with the cell membrane and let glucose enter to the cell by facultative diffusion [57, 58].

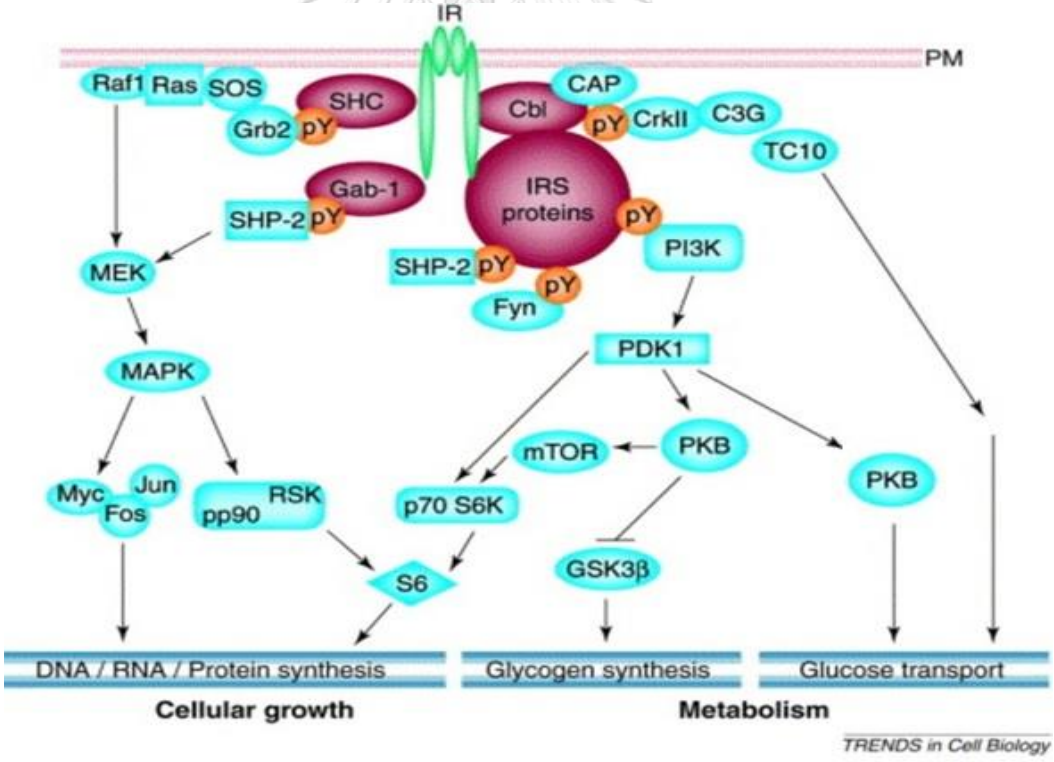

Figure 2: Insulin signal transduction [59]

2.7 Cause of insulin resistance

Circumstances, insulin resistance is a risk of causing type 2 diabetes and found that insulin resistance is associated with physical abnormalities such as obesity, high blood pressure and infectious diseases. The mechanism of insulin resistance is caused by the phosphorylation at serine or threonine of IRS proteins leading to send a negative feedback to stop responding to insulin (Figure 3). Increasing of tumor necrosis factor α (TNF α), cellular stress (ROS) and fatty acid (FFA) has been reported as the cause of insulin resistance [60]. The increased free fatty acid passes through the cell by fatty acid transporter protein and accelerates the process of metabolism of fatty acids and stimulate protein kinase C (PKC). Induction of protein kinase C by the phosphorylation at serine or threonine of IRS proteins lead to inhibition of PI3K signaling pathway caused the reduction of intracellular glucose transport [58].

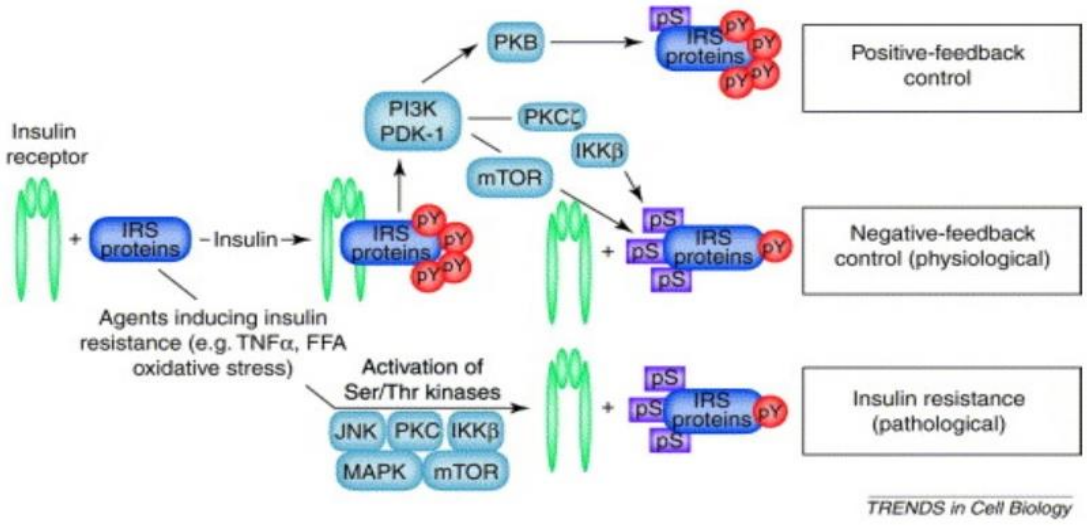

Figure 3: Ser/Thr-phosphorylated insulin receptor substrate (IRS) proteins as modulators of insulin action and insulin resistance [59].

In addition, diabetes type 2 patients found the abnormalities of beta cells function and quantity. The mechanism that causes the death of the beta cells is the high level of blood glucose that stimulates the creation of reactive oxygen species (ROS). The occurrence of ROS, resulting in the activation of cytokine leading to beta cells destruction while the pancreas has low antioxidant property and easy causing further damage [61].

2.8 Insulin signaling in skeletal muscle and adipocyte

Total body glucose homeostasis is controlled by hormone insulin, which is secreted from beta cells in the pancreatic islets in response to a rise of glucose concentration. Insulin stimulates glucose transport, oxidation and regulates protein glycogen in target tissue such as skeletal muscle and adipose tissue. Skeletal muscle and adipocyte is responsible for approximated 80% of whole body glucose uptake in insulin-stimulated conditions, thus it is essential tissue to study the defect mechanism of insulin signaling transduction and action [62].

2.9 Glucose transporter

Glucose transporter (GLUT) plays a crucial roles in glucose metabolism [10]. Glucose transporter isoform-4, a member of the GLUT family, is mainly articulated in skeletal muscle, heart, and adipose tissues. When target cell was stimulated by insulin, GLUT-4 from the intracellular pool will transfer to the plasma membrane resulting glucose uptake [62].

Table 1: The glucose transporter (GLUT) family of facilitative sugar

The glucose transporter (Glut) family of facilitative sugar			
Isoform	Main tissue location	Insulin sensitive	Functional characteristics
GLUT1	erythrocyte, brain, muscle	No	Glucose
GLUT2	liver, pancreas, intestine, kidney	No	Glucose
GLUT3	brain	No	Glucose
GLUT4	heart, muscle	Yes	Glucose
GLUT5	intestine, kidney, testis	No	Glucose/Fructose
GLUT6	brain, spleen, leucocyte	No	Glucose
GLUT8	testis, brain	No	Glucose
GLUT9	liver, kidney	No	Glucose
GLUT10	Liver, pancreas	No	Glucose
GLUT11	heart,	No	Glucose/Fructose
GLUT12	heart, prostates, small intestine	Yes	Glucose

2.10 Signaling pathway and glucose uptake in skeletal muscles and adipocyte

The skeletal muscles and adipocytes are the majority (80%) part of insulin-mediated glucose uptake from whole body in post-prandial state which play an important role in maintaining glucose homeostasis [10]. In skeletal muscle and adipocyte, insulin increases glucose uptake through a signaling that leads to activation of phosphatidylinositol-3 kinase (PI3K), Akt and atypical PKCs (aPKCs) resulting in

increased translocation of glucose transporter 4 (GLUT4) to the plasma membrane [10]. Another GLUT4 translocation promoter is AMP activated protein kinase (AMPK) [11]. Two different signals exist as AMPK activators; passing increase in intracellular Ca^{2+} concentration contributes to activation of AMPK, and AMPK-dependent pathway leads to contraction-induced glucose uptake [11], which is linked to enhanced GLUT4 genesis and translocation to the cell membrane [11].

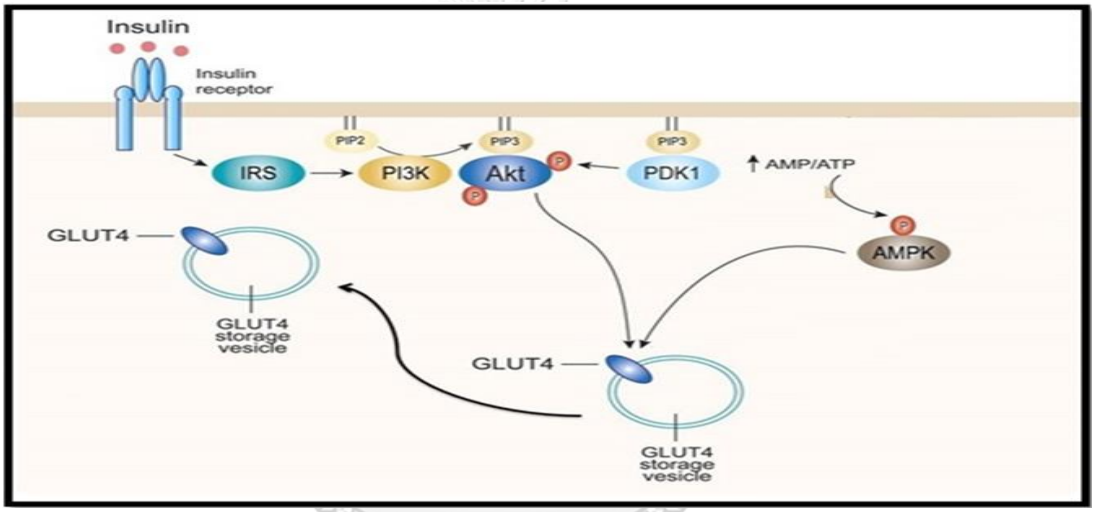

Figure 4: Glucose uptake signaling pathway [63].

2.11 Defects in insulin signaling and metabolism in skeletal muscle and adipocyte

Skeletal muscle and adipocyte insulin resistance is an early defect in type 2 diabetes. Therefore, deeper empathetic of the mechanisms which lead to dysregulation of insulin action in muscle may play a significant role in drug improvement. IRS-1 and IRS-2, the major downstream target of IR, are the major IRS isoforms that expressed in skeletal muscle. Reduced insulin-stimulated phosphorylation of IRS-1 has been established in muscle from type 2 diabetes patients [64]. The phosphorylation of IRS at

this serine residue lead to decreased IRS tyrosine phosphorylation with consequent impaired activation of PI3K [64]. The phosphatidyl inositol-3 kinase (PI3K) plays a critical role in insulin-mediated signal transduction, control glucose uptake and GLUT4 translocation. Significant defects in phosphorylation of AKT has been reported in human primary muscle cell from Type 2 diabetes patients [65]. AS 160 is a downstream target of AKT, and link PI3K/AKT signaling to GLUT4 translocation. The insulin-encouraged phosphorylation of AS 160 is significantly decreased in skeletal muscle and adipocyte from type 2 diabetes subjects [65].

2.12 AKT protein

AKT/PKB (a serine/threonine kinase with α, β and γ isoforms) is an importance key enzyme that regulating of insulin function [66, 67]. AKT α has a function in fat metabolism, stimulates glycogen synthesis in muscle and a function of insulin in adipocytes [68, 69]. AKT β is a main isoform in skeletal muscles [69, 70]. The lack of AKT γ activity showed in skeletal muscle of obese and insulin resistant persons [71, 72]. Therefore AKT is play a key role in insulin target tissues to activate the glucose uptake [73].

2.13 AMPK protein

AMPK, the most important molecule that controlling energy metabolism and maintain glucose balance, is recognized as a core in type 2 diabetes and other metabolic syndromes [74]. AMPK is expressed in various organs that could be induced hormones stimulations, cellular stress and movement and substances effecting cellular

metabolism. The activation of AMPK could ameliorate metabolic dysfunctions triggered by type 2 diabetes. AMPK exists as a heterotrimer complex consisting of a catalytic subunit α and two further regulatory subunits β and γ. Each of these subunits has isoforms expressed by different genes [75]. N-terminal of α subunit consists of a conservative site Thr172, the phosphorylation of which is integrant in the activation of AMPK. Subunit γ bind to adenosine triphosphate (ATP) or adenosine monophosphate (AMP) [75, 76] lead to the increased ratio of AMP and ATP and activates AMPK. Therefore, all metabolic stresses disturbing energy balance through interfering ATP production can induce AMPK activation [75, 76]. AMPK reduction show the pathologic level of type 2 diabetes and may make glycogen synthesis in skeletal muscle [77]. Metformin, a well-known drug to treat diabetes, is an activator of AMPK. Metformin show various mechanisms in treatment of diabetes, including suppressing hepatic gluconeogenesis, decreasing appetite of patients, reducing intestinal carbohydrate absorption and increasing glucose uptake [78]. McBride A. et al. [79] found that AMPKα2 knockout mice appear a systematic insulin resistance, indicating the important function of AMPK in regulating insulin sensitivity. Additionally skeletal muscle of AMPK mutation appears to respond normally to insulin *in vitro*. Consequently, the future drug discovery should not only concentrate on the activation of particular molecules contributing to the traditional insulin signaling pathway, but also pay attention to insulin-resistant tissue while responding to insulin.

2.14 The effect of insulin resistance on beta cells failure

Though insulin resistance plays an importance role in the pathogenesis of T2DM, beta cells failure is also important factor and accountable for the evolution of impaired glucose tolerance (IGT) to T2DM. Many factors including age, genetic factors, and developed factors like glucotoxicity contribute to beta cells failure. Early inhibition of development of T2DM protect against the loss of beta cells mass and function. Pancreatic islet cells are more subject to oxidative stress than cells in other tissue as they produce less antioxidant enzymes. This balance is lost in diabetic persons where enhanced ROS formation overcome and/or decreased the antioxidant defenses of the organism. The link between oxidative stress and glucotoxicity has been submitted by earlier studies in beta-cell cell lines, secluded islets, and diabetic animal models showed that antioxidants can protect beta-cells against the toxic effects of high glucose levels on insulin secretion, islet insulin content, insulin gene expression, and survival [80]. The NADPH oxidase (NOX) complexes induce in high glucose increased ROS production process [81, 82] and lead to insulin secretion, insulin gene expression decreased. In addition, oxidative stress mediated inhibition of insulin gene expression has been shown to stem in part from the well-established decrease of PDX-1 binding to the insulin promoter [83]. Demolish pancreatic islets result in decreased insulin secretion, resulting in hyperglycemic condition and continuous generation of additional oxidative stress. The main signaling pathways affecting insulin secretion is glucose transported into pancreatic beta cells by GLUT2, and then metabolized by GCK to glucose-6-phosphast, resulting in

ATP production, which induces Ca^{2+} influx, followed by the release of insulin. In parallel, PDX-1 is recognized as a key regulation factor in the cascade regulating insulin secretion. The translocation of PDX-1 to nuclease induced PRE-INS expression [84].

The various indications showed that oxidative stress was a central role of pathogenesis in T2DM, hence antioxidant therapy should be hypothetically very helpful to these patients. Antioxidant (pre) action of diabetic animal models (STZ-induced diabetic mice and rats) provided some encouraging results over the last decade with respect to the defense against diabetic complications [85]. Interestingly, clinical trials using seed extracts of *Silybum marianum* (Silymarin) alone or in combination with glibenclamide were very encouraging and showed a marked progress of glycemic control in T2DM patients [86]. Some reports proposed that selenium and vitamin E supplementation may increase T2D risk and all-cause mortality [87]. Therefore, traditional medicines derived from medicinal plants which have antioxidant could to find scientific research to support anti-hyperglycemic, side effect and long-term toxicity.

2.15 Cancer and diabetes

The prevalent of type 2 diabetes mellitus (T2DM) and obesity is becoming increasingly globally. Over the past decades, many studies showed the evidences that diabetes patient, especially type 2 diabetes increase the risk of several cancer such as kidney, colorectal, breast, liver, pancreatic cancer [88]. The potential mechanisms that proposed to contribute to the increased the risk of cancer in DM type 2 consist of hyperglycemia, insulin resistant, hyperinsulinemia, increased insulin-like growth factor-1

(IGF 1) level, dyslipidemia, and inflammatory cytokines. The physiological process that might link obesity, diabetes and neoplasia was represented in Figure 5. Intake over energy consumption for long time can lead to insulin resistance in insulin-target tissues such as adipocytes and skeletal muscle resulting in hyperglycaemia. Obesity that might influence neoplasia include increased levels of inflammatory cytokines, which stimulate various processes in cancer development, and reduced levels of adiponectin which normally inhibits cell proliferation via activation of AMP-activated protein kinase (AMPK) [89].

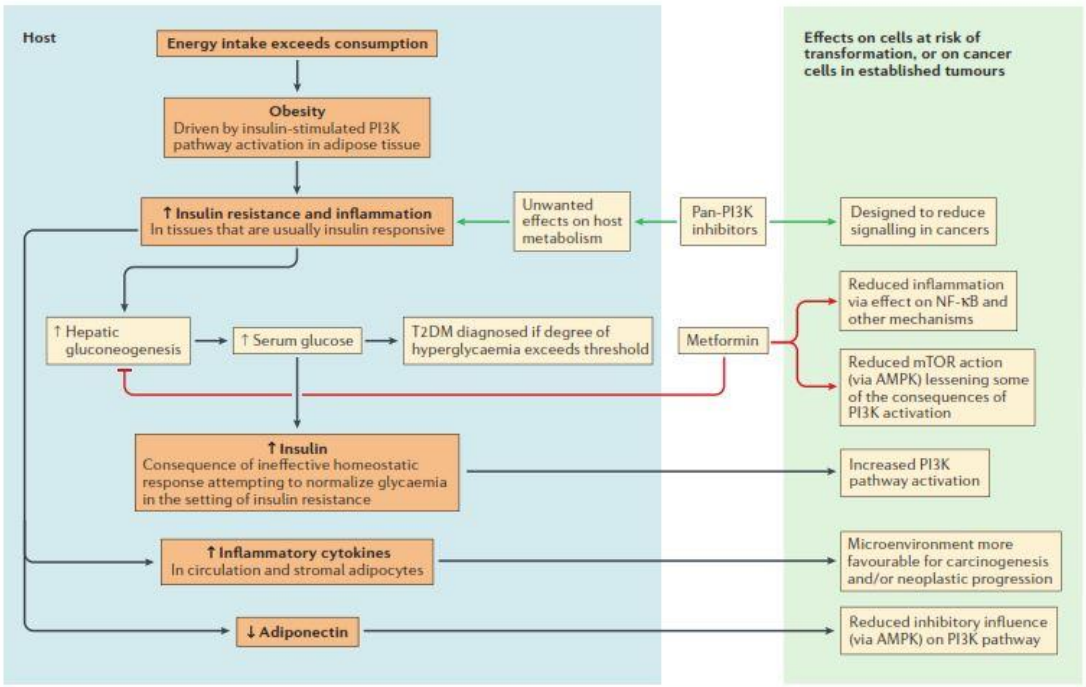

Figure 5: The physiological process that might link obesity, diabetes and neoplasia [89].

The direct link between cancer and diabetes is cancer cell needed the extra energy to promote cell growth and cell proliferation which the major source of energy

is glucose, whereas hyperglycemia was normally found in DM patient. The overall potential mechanisms of diabetes and cancer are represent in Figure 6.

Hyperinsulinemia was believed act as a key member that associated with increase the risk of cancer. Insulin and insulin-like growth factors (IGF) bind to the insulin receptor (IR) and IGF receptor with different affinities. IGF-binding proteins (IGFBP) are decreased by insulin and may result in increased bioavailable IGF-1 and IGF-2. Insulin binding to IR activates the phosphoinositide 3-kinase (PI3K)–Akt–mammalian target of rapamycin (mTOR) signaling pathway. Binding of IGF-1 and IGF-2 to IGF-1R stimulates the PI3K-Akt-mTOR and Ras-Raf-MAPK pathways that resulting in increased cell proliferation, migration and invasion and decreased apoptosis [5].

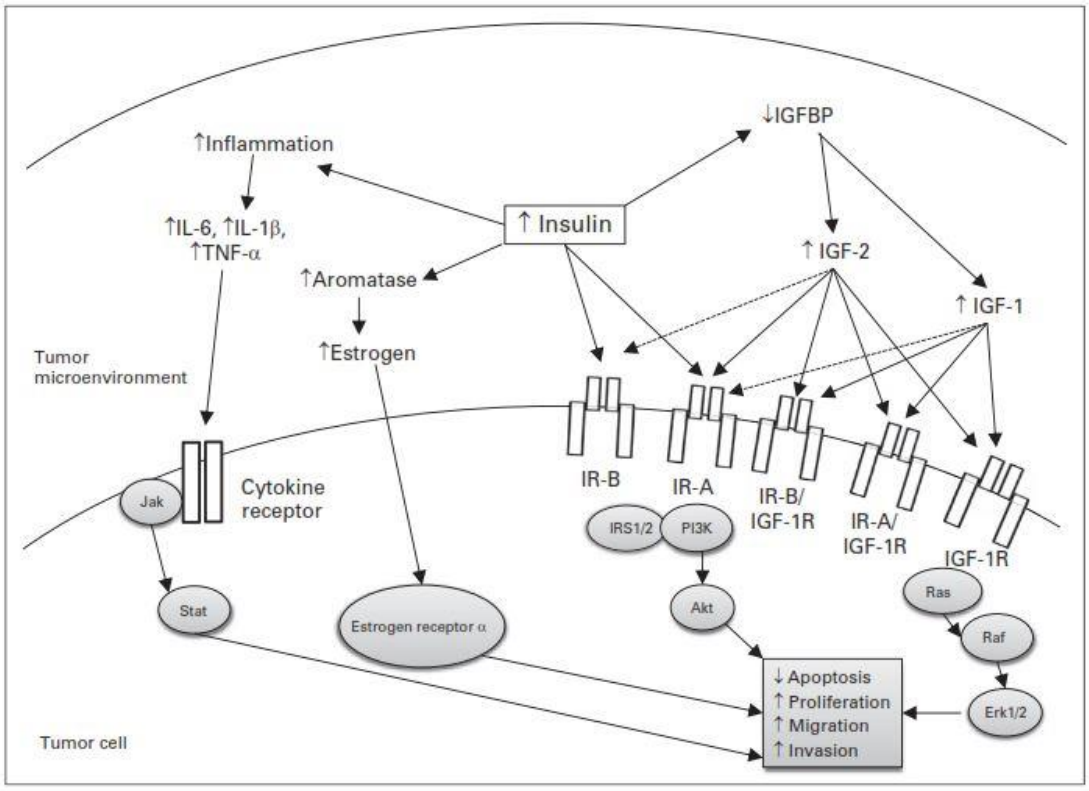

Figure 6: Effects of hyperinsulinemia on the tumor cell microenvironment and intracellular signaling that contribute to tumor growth and progression.

Cholangiocarcinoma (CCA) is a malignancy that arises from bile duct epithelia that highly prevalent in Northeast Thailand. It hypothesized that chronic infection of parasites such as *Opisthochis viverrini* may initiate the carcinogenesis via parasite factors like mitogenic substances antigen coupled with immunological response that promotes chronic inflammatory, leading to DNA damage and development of CCA. However, the infection of *O. viverrini* alone may not produce CCA, but other carcinogens of risk factor may also require to develop CCA. Several studies indicated that the common factor such as smoking, obesity, alcohol consumption and DM as risks of CCA. The data from several epidemiological strongly revealed that DM is a risk factor of CCA [90, 91], however the extract mechanism of DM and CCA is unclear. Recent study represented that high glucose enhanced CCA metastasis via modulation of O-GlcNAcylation, through the expressions of glucosamine-fructose-6-phosphate amidotransferase (GFAT) and vimentin [92].

2.16 Hedgehog signaling, MITF and Cholangiocarcinoma

Microphthalmia-associated transcription factor (Mitf) contains a basic helix-loop-helix and a leucine-zipper (bHLH-LZ) structure, and it has been established as a key regulator for development of melanocytes and the retinal pigment epithelium (RPE) [27-30]. However, subsequent studies have suggested the pleiotropic functions of Mitf in various organs, including liver [31], pancreas [32], kidney [33], lung [34], olfactory bulb

[35], and frontal cortex [33]. In particular, the Mitf vitiligo mouse, *Mitf*^{vit}/*Mitf*^{vit}, is characterized by retinal degeneration and the accumulation of retinyl palmitate in RPE and the liver [31]. The *Mitf*^{vit} protein carries the Asp222Asn substitution [30] and its mutant protein is predicted to show the decrease in Mitf function [93]. Thus, Mitf may be involved in the metabolic function of hepatocytes and/or cholangiocytes. However, the immununohistochemical analysis of the mouse liver revealed that Mitf immunoreactivity was detected only in Kupffer cells, but not detectable in hepatocytes, cholangiocytes, and other cell types [33]. In addition, the expression levels of Mitf mRNA were 10-fold lower in the mouse liver than those in the mouse eyeball, as judged by the real-time RT-PCR analysis [33]. Likewise, expression levels of MITF mRNA were marginally detected in the human liver [24]. MITF represents a human orthologue of Mitf. We therefore hypothesize that the expression of Mitf/MITF may be maintained at the low level in hepatocytes and cholangiocytes.

Cholangiocarcinoma is a malignant tumor that is originated from the biliary epithelial cell, and is the second most common primary liver tumor, accounting for about 10-15% after hepatocellular carcinoma [23]. Both types of hepatic cancer are characterized by poor prognosis. Hedgehog signaling plays a critical role in growth of many cancer [94, 95], including hepatocellular carcinoma [95-98] and cholangiocarcinoma [95] [99]. In addition, Hedgehog signaling is required for normal development of RPE in the mouse [26]. It is therefore tempting to speculate the regulatory role of Hedgehog signaling for MITF expression in the liver. In this context,

we found that cyclopamine, an inhibitor of Hedgehog signaling, increased the expression levels of MITF in human hepatocellular carcinoma and cholangiocarcinoma cell lines [24]. Importantly, cyclopamine is a natural teratogen, contained in the plant *Veratrum californicum,* and it causes craniofacial birth defects in sheep, such as cyclopia [100]. Cyclopamine acts on a signal transducer, Smoothened, located in plasma membrane [100] to inhibit the Hedgehog signaling. In the presence of a Hedgehog ligand, Smoothened enhances nuclear translocation of glioma-associated transcription factors, glioma-associated oncogene 1 (GLI1) [25], thereby mediating the Hedgehog signal. In particular, GLI1 is expressed in normal bile duct [95] and is overexpressed in hepatocellular carcinoma [98] and cholangiocarcinoma [95] [99], suggesting that the Hedgehog signaling pathway may be activated in hepatic cancer cells.

2.17 Diabetes pharmacotherapy and cancer

The blood glucose level in diabetes type 2 can be controlled by oral or injected medication, while in diabetes type 1 require injection of insulin. Several studies indicated that medication that used for DM treatment may increase or decrease the risk factor of cancer development. Summarize of studies was represented in the Figure 7. Many studies pay attention to metformin, an oral biguanide that is the first line treatment of diabetes type 2. The mechanism of metformin on anti-cancer is unclear. There are two hypothesis to explain the antineoplastic effect of metformin. First, it sensitizes the body to insulin that reduce insulin production from beta-cell and decrease insulin in blood. Second its decrease hepatic glucose production resulting in inhibit cancer growth [101].

Mechanisms of Diabetes Medications and Potential Risks and Benefits in Oncology Patients

Drug Class (available in the United States)	Mechanism of Action	Preclinical Evidence of Effects on Cancer	Clinical Evidence of Potential Effects on Cancer
Biguanides (metformin)	↓ HGP ↓ Insulin resistance	Indirect effects ↓ Circulating insulin[22] ↓ Glucose levels[22] Direct effects ↑ AMPK activation[26] ↓ Signaling via mTOR[26] ↓ Cancer cell glycolysis[27] ↓ Hexokinase activity and tumor cell glucose uptake[28] ↓ Inflammatory signals in cancer cells[29]	↓ Pancreatic cancer,[19] HCC,[19,20] lung cancer,[20] CRC,[20] and breast cancer[21] ↓ Cancer-related mortality and all-cause mortality in cervical cancer,[23] PC,[24] and CRC[25]
Sulfonylureas (glipizide, glimepiride, glyburide)	↑ Insulin secretion	No direct mitogenic activity found[30]	↓↑ Overall cancer incidence[31,32]
TZDs (rosiglitazone, pioglitazone)	↓ Insulin resistance	↓ Lung tumor size in a rodent model[33]	↓ PSA levels in PC[34] ↓ CRC with rosiglitazone and breast cancer with pioglitazone[35] ↑ Bladder cancer[36-39] (conflicting data)
GLP-1 RA (exenetide, liraglutide, albiglutide, dulaglutide)	↓ Appetite	↑ Thyroid C-cell hyperplasia and calcitonin secretion in rats[40]	No evidence in humans for thyroid C-cell hyperplasia and calcitonin secretion[40]
DPP-IV inhibitors (sitagliptin, linagliptin, saxagliptin, alogliptin)	↓ Insulin resistance ↑ Insulin secretion ↓ HGP ↓ Glucagon secretion	↑ Small and large bowel tumor growth[41]	↔ Pancreatic cancer[42-44]
SGLT2 inhibitors (dapagliflozin, canagliflozin, empagliflozin)	↑ Urinary glucose excretion	Overexpressed in pancreatic,[45] PC,[45] and CRC[46] ↔ Mammary tumors (dapagliflozin)[48] ↑ Renal tubules, adrenal glands, and testicular Leydig cell tumors (canagliflozin)[49]	↔ Overall cancer rates (dapagliflozin)[47] ↔ Bladder, breast, renal, and malignant adrenal tumors (canagliflozin)[47]
Insulin analogs (glargine, detemir, degludec, aspart, lispro, glulisine)	↑ Insulin	↑ Proliferation of breast cancer cell lines (insulin AspB10)[50] ↔ Mammary gland neoplastic lesions development (glargine)[52]	↔ Cancer incidence (glargine)[51]

Abbreviations: AMPK, adenosine monophosphate kinase; CRC, colorectal cancer; DPP-IV, dipeptidyl peptidase IV; GLP-1 RA, glucagon-like peptide-1 receptor agonist; HCC, hepatocellular carcinoma; HGP, hepatic glucose production; mTOR, mammalian target of rapamycin; PC, prostate cancer; PSA, prostate-specific antigen; SGLT2, sodium glucose cotransporter 2; TZD, thiazoledinedione.

Figure 7: Mechanisms of diabetes medication and potential risks and benefits in oncology patients [5].

2.18 Oral anti-diabetes agents

The mechanism of oral anti-diabetes are cassified into three groups; insulin secretagugue, increses insulinsensitivity or reduce insulin resistance (insulin sensitizer) and Alpha glucosidase inhibitor [102]**.** Some side effects and diabetes drug- drug interactions have been reported as shown in table 2.

Table 2: Drugs used for diabetes patients [102]

Subclass	Mechanism of action	Effect	Toxicities, interaction
Insulin secretagogue			
Sulfonylureas	- Insulin secretagogue : Close K+ channels in beta cells and increase insulin release	The patients with functioning beta cells and increased glycogen, fat and protein formation	Toxicities : hypoglycemia, weight gain, Liver cirrhosis GFR < 30 mL/min
Glinide	- Insulin secretagogue : Similar to sulfonylureas with some overlap in binding sites and Close K channels in beta cells rapid and short action	The patients with functioning beta cells and increased glycogen, fat and protein formation	Toxicities: hypoglycemia, weight gain, hyperinsulinemia
DPP-4 inhibitor	- Blocks degradation of GLP-1,raise circulation GLP-1 level	Prevents degradation of incretin (GLP-1) due to stimulate insulin secretion and inhibit glucagon secretion	Toxicities: hypoglycemia, headache, nausea, hypersensitivity and skin reactions
Insulin sensitizer			
Biguanide (Metformin)	- Reduced hepatic gluconeogenesis -Enhanced glucose transport in skeletal muscle and adipose tissue	Decreased endogenous glucose production	Toxicities: gastrointestinal symptom, lactic acid, and cannot use if impaired renal/hepatic function
Thiazolidinedione	- Regulates gene expression by to PPARγ	Reduce insulin resistance	Toxicities: edema, weight gain cannot use hepatic disease
Alpha glucosidase inhibitor			
Acarbose	- Inhibit intestinal α glucosidase	Reduce conversion of starch and disaccharides to monosaccharide and reduce postprandial hyperglycemia	Gastrointestinal symptom cannot use if hepatic function, intestinal disorder

2.19 Pharmaceutical activators of insulin sensitizer

Metformin is a usually used as antidiabetic agent that mainly actions as a suppressor of glucose production in liver [103]. It also improves glucose transport in skeletal muscle. A decade ago, it was show that metformin activates the AMPK pathway in rat hepatocytes [104]. In addition, AMPK activation by metformin in rat skeletal muscle leads to an increase in glucose transport. Metformin has been exposed to increase phosphorylation of AMPK in skeletal muscle of type 2 diabetes subject [105]. However, the main side effect of metformin is gastrointestinal symptom, lactic acid, and cannot use if impaired renal/hepatic function [106].

Thiazolidiones (TZDs), such as rosiglitazone or pioglitazone, were widely used as therapeutic agents to treat type 2 diabetes before the worries regarding cardiovascular risks led to removal of rosiglitazone [107]. TZDs are known to increase insulin sensitivity by improving glucose disposal and obstructing gluconeogenesis. TZDs improve insulin action through activation of proliferator-activated receptor-γ (PPAR-γ), a transcription factor that is extremely expressed in adipocyte [108, 109]. The activation of PPAR-γ in adipose tissue leads to enlarged differentiation of adipocyte and formation of smaller adipocytes that are more sensitive to insulin. In addition, it has been suggested that TZDs have direct metabolic effect on skeletal muscle independent of the activation of PPAR-γ [110]. However, the main side effect of thiazolidinediones is water retention, edema, decompensation of heart failure and could not use in hepatic disease [111]. Since side effects of diabetes drug have been reported. Therefore, traditional medicines

derived from medicinal plants that used as an alternative treatment by about 60% of the world's population become more interesting. However, numerous herbal plants have limit document to support anti-hyperglycemic properties, side effect and long-term used toxicity.

2.20 *Stevia rebaudiana* Bertoni

Stevia rebaudiana Bertoni is one of 150 known species of the genus *Stevia* that produce sweet steviol glycosides. It generally known as stevia, sweet leaf, sweet herb of Paraguay, honey leaf, candy leaf or Yawan in Thailand. In an ancient times, the Guarani Indians of South America used this plant as tea sweetens. Today steviol glycosides which extracted from this plant are commonly used as a food additive by the Japanese and Brazilians as a non-caloric sweetener [112]. This non-caloric sweetening agent is sweet around 300 times higher than sucrose. Vast of study noticed the biological activities of the sweetening compound such as reducing blood pressure and cardioprotective, antitumor effects and especially anti-hyperglycemic [113]. It is essential to noted that there are many steviol glycosides that can be extracted from *Stevia rebaudiana* Bertoni plant, generally are stevioside, rebaudioside A, rebaudioside C and dulcoside which exert difference biological activities [114].

Figure 8: *Stevia rebaudiana* Bertoni [112]

Some study believed that the antihyperglycemic activity of steviol is due to its antioxidant properties. Further supported by the evidence that the leaves extracted have a greater ability to scavenge free radicals and prevent lipid peroxidation than hydroxytoluene [115]. Other than antioxidant activities it exert many biological effects such as help maintenance blood-glucose levels, anti-inflammatory and influence on insulin secretion. The data were reported that stevioside can affect both α and β-cells. In α-cells, stevioside inhibits glucagon hyper-secretion induced by palmitate [116]. In beta cells, stevioside and steviol stimulate insulin secretion in the presence of high levels of glucose (16.7 mM). The stimulation of stevioside is independent of ATP-sensitive K channel [117]. Research on the molecular level showed that stevioside improves pancreatic beta cells function during glucotoxicity (16.7 mM glucose) [118] via regulation of acetyl-CoA carboxylase (ACC) [119]. In STZ-induced diabetic rats, an insulin-resistant animal model, feeding with stevioside increases the response to exogenous insulin. This

result suggests that stevioside may be suitable as an adjuvant for diabetic patients [120]. Several tetracyclic diterpenoids have important biological activities. Isosteviol, a tetracyclic diterpenoid from the beyerane series, was obtained from acid hydrolysis of stevioside, aditerpenoid glycoside from leaves of *stevia rebaudiana* Bertoni. Many studies noticed that this isosteviol processes many biological activities consist of reducing blood pressure and cardioprotective, anti-tumor effects and anti-hyperglycemic [113]. Some study demonstrated that the mechanism of anti-diabetic effects in diabetes rat of isosteviol is insulinotropic effect [121]. Other study illustrated anti-hyperglycemic effects of isosteviol could enhance utilization of glucose in the periphery and reduce beta cells damage induced by dyslipidemia. It might be due to the potential enhancement of liver PPARα mRNA expression of isosteviol [122]. Moreover, isosteviol can improves glucose and insulin sensitivity as well as improving the lipid profile and upregulates the gene expression of key beta-cell genes, including insulin regulatory transcription factors [123]. The data show isosteviol has greater activity than steviol. Supplementation of diabetic KKAy mice with 20 mg/kg isosteviol for 9 weeks reduced the plasma LDL cholesterol. In the test, it was noticed that isosteviol only affects the metabolites that differed between healthy control mice and obese type 2 diabetic mice [124]. It is likely that isosteviol also elicits its beneficial effect by stimulating insulin release only in the diabetic stage, just as stevioside does [125]. Even though, there are many unknowns of insulin-signalling pathways, the mechanisms of glucose uptake, GLUT4 translocation, and insulin resistance and the mechanism of isosteviol that

involving in these matters should be investigated. Plant-derived compounds and synthetic derivatives of natural products have been an important source of several clinical useful anti diabetes agents [126]. It has been recognized for a long time that natural-product structures have the characteristics of high chemical diversity, biochemical specificity and other molecular properties that make them favourable as lead compounds for drug discovery. These characteristics serve to differentiate them from libraries of synthetic and combinatorial compounds [127]. The biotransformation of isosteviol has been investigated extensively. The researchers used isosteviol as a substrate for *Fusarium verticilloides* (Sacc.) to select for therapeutic metabolites of isosteviol [128]. Hydroxyl groups were introduced to isosteviol by fungi. This reaction may enhance the existing properties of isosteviol or lead to new biological activities. The metabolites of isosteviol metabolized microbial transformations of isosteviol by fungus *Cunninghamella echinulate* NRRL 1386 elongate have yielded metabolites exhibiting more potent inhibition effects on vasorelaxant promotion [113]. Isosteviol was also metabolised by *Cunninghamella echinulate* NRRL 1386 to yield compounds that are effective in the treatment of inflammation and immunomodulation [129]. Even though, there are many unknowns of insulin-signalling pathways, the mechanisms of glucose uptake, GLUT4 translocation, and insulin resistance and the mechanism of sevioside, isosteviol and microbial transformation of isosteviol to analogs that involving in these matters should be investigated.

2.21 *Murraya koenigii*

Murraya koenigii know as curry leaf in English. It belongs to family Rutaceae which have more than 150 types and 1600 species. This plant is the richest source of carbazole alkaloids [130]. *Murraya koenigii* is widely used in Indian cooking and have an adaptable role to play medicine. Fresh leaves, essential oil and dried leaf powder are widely used for flavoring soups, curries fish, traditional curry powder blends and seasoning. Mature leaves contain 63.2% moisture and a maximum of hot water soluble extractive 33.45% [131]. A number of chemical ingredients from every part of the plant extract of *M. koenigii* leves including carbazole alkaloids, namely murrayanine, mahanimbine, girinimbine, murrayacine, isomurrayazoline, isomahanimbine, koenimbidine mahanine, koenine, koenigine, koenidine, koenimbine and 8,8-biskoenigine [132]. Form the hexane extract of leaves has isolated mahanimbine, isomahanimbine, koenimbidine, and murrayacine. Methanolic extract of *M. Koenigii* was subjected to qualitative thin-layer chromatography and HPLC using different solvent system [130, 133]. Then the structures of these 6-bioactive compounds confirmed as carbazole alkaloids-mahanimbine, mirinimbine, isomahanimbine, murrayazoline, murrayazolidine, and mahanine by the spectrometric data. From stem bark Murrayazolinol (a minor carbazole alkaloid), mahanimbinol, murrayazolidine, murrayacinine, mukonidine, murrayazolinine, murrayanine, girinimibine and mahanimbine, girinimbinol and mahanimbilol has also been identified and isolated [18, 134]. Normal and semi-synthetic carbazole alkaloids have been establish useful as a new

class of therapeutic agents for many diseases related with tissue damage due to the generation of free radicals, inflammation, rheumatoid arthritis and diabetes mellitus [135, 136]. Several pharmacological activities and medicinal properties of various parts of *M. koenigii* are well known. Biological activity of *M. koenigii* is informed with the crude extracts and their different fraction form leaf, bark, roots, seed and oil.

Figure 9: *Murraya koenigii* (Linn.) Spreng [112]

2.21.1 Antioxidant

Antioxidant activity of carbazole alkaloids, one of the potential bioactives, has been informed by a number of workers. The antioxidative properties of 12 carbazole alkaloids isolated form *M. koenigii* leaves were evaluated on the basis of Oil Stability Index (OSI) together with their radical scavenging ability against 1, 1- diphenyl, 2- picryl hydrazyl (DPPH). Moreover, antioxidant activity of various extracts of *M. koenigii* as measured by in-vitro nitric oxide scavenging activity follows the order seeds aqueous> leaf aqueous> leaf CHCl2: MeOH> seed CHCl2: MeOH [18]. The aqueous extracts of *Murrya koenigii* leaf showed significant antioxidant activity defense to rat cardiac tissue

against cadmium-induced oxidative stress by increasing the levels of lipid peroxidation, glutathione level, and protein carbonyl content. So this antioxidant activity of *Murrya koenigii* could be helpful to people who are exposed to cadmium either globally or occupationally [137].

2.21.2 Anticancer activity

The effects of *M. koenigii* extracts in *in-vitro* show anticancer in lymphoma cell line and *in-vivo*. The anticancer models have been estimated in male Swiss albino mice. The *in-vitro* anti-tumour encouraging activity and antioxidant properties of girinimbine isolated from the stem bark of *Murraya koenigii* was studied by Yih et.al [138]. The ethanolic extract displayed significant anti-inflammatory effects as compared with petroleum ether and chloroform extracts. Curry leaf have been described to show potent cytotoxic activity against human leukemia cells, prostate cancer cell lines [139, 140], viral and clinical pathogens [141, 142]. Girinimbine, acarbazole isolated from the bark of *Murrya koenigii* significantly induced programmed cell death in HepG2 cells telling the necessity for further calculations in preclinical human hepatocellular carcinoma models [143]. The results from the study conducted by Bhattacharya *et al.* 2010 [144] offers indication for the involvement of death receptor mediated extrinsic pathway of apoptosis in mahanine-induced anticancer activity in MOLT-3 cells [144]. Furthermore, 3 carbazole alkaloids mahanine, pyrayafoline and murrafoline, showed significant activity against HL-60 cells by inducing apoptosis through of capsase-9/capsase-3 pathway, via mitochondrial dysfunction [145]. Down regulation of cell

survival factors by activation of capsase-3 through mitochondrial dependent pathways and interruption of cell cycle evolution could be an additional mechanism [17]. The mean number of neoplasms in the colon and intestines were significantly low as demonstrated by morphological and histological studies in the *Murrya koenigii* treated animals [146]. The methanolic extract of *Murrya koenigii* leaves demonstrated a significant increase in the phagocytic index by the rapid removal of carbon particles from blood stream. It also demonstrated an increase in the antibody titer against ovalbumin and protection against cyclophosphamide-induces myelosuppression. Thus, *Murrya koenigii* holds promise as an immunomodulatory agent acting by stimulating humoral immunity and phagocytic function. However, these extracts were unable to stimulate cellular immunity [147].

2.21.3 Antiobesity and Antihyperlipidemic activities

The dichloromethane and ethyl acetate extracts of *Murraya koenigii* leaves significantly reduced the body weight gain, plasma total cholesterol (TC) and triglyceride (TG) levels significantly. The experiential antiobesity and antihyperlipidemic activities of these extract are connected with the carbazole alkaloids, mahanimbine. When mahanimbine was assumed orally significantly dropped the body weight gain as well as plasma TC and TG levels. These answers prove the excellent pharmacological potential of mahanimbine to prevent obesity [19].

2.21.4 Lipid-lowering

Murrya koenigii leaves in dichloromethane and ethylacetate extracts show significantly reduced the body weight gain, total cholesterol (TC) and triglyceride (TG) levels in obese rats. These results suggest the potential role of *Murrya koenigii* to prevent obesity [19]. Moreover the effect of one month oral administration of *Murrya koenigii* aqueous leaves extract in normal and streptozotocin (STZ)-induced severe diabetic rats were studied. The results demonstrated that the fasting blood glucose (FBG) level of treated animals decreased total cholesterol (TC) and triglycerides (TG), increased the HDL-cholesterol levels and reduced serum alkaline phosphatase values. Additionally the serum creatinine levels reduced in the *Murrya koenigii* treated group. Thus the results indicate that besides lipid-lowering activity the aqueous extract of *Murrya koenigii* also reduced the severity of diabetes and its associated nephropathic complications [148].

2.21.5 Antidiabetic and islet protective

Hypoglycemic activity, serving the leaves to rats formed hypoglycemia by increasing the hepatic glycogenesis as obvious by increased activity of glycogen synthetase. A significant decrease in fasting blood sugar and postprandial blood sugar was observed by feeding (12 gm) leaves powder to the Non Insulin Dependent Diabetes Mellitus patients (NIDDM). Aqueous and methanolic extracts of leaves and fruits of *M. koenigii* displayed very good antidiabetic activity in alloxan-induced diabetic rats. Plasma insulin was perceived with significantly high levels on the 43rd and 58th days of treatment in aqueous and methanol extracts of *M. koenigii* -treated groups. Fruit juice

decreased blood glucose level at the 10th and 15th days of running in alloxan-induced diabetic mice. Blood glucose level was reduced with the extreme fall of 14.68% in normal and 27.96% in mild diabetic animals when aqueous extract of leaves at a dose of 300 mg/kg was used. These results submitted that *M. koenigii* treatment uses a therapeutically protective outcome in diabetes by decreasing oxidative stress and pancreatic beta cells damage [149]. Extracts of *Murrya koenigii* resulted in pancreatic beta cells protection and increase function of pancreatic islets that produce insulin. The level plasma insulin and C-peptide levels after treatment in streptozotocin-induced diabetic Swiss mice has become normalized. Additionally, the histochemical and immunohistochemical analysis suggest and islet protective and insulin productive role. Moreover, extracts of *Murrya koenigii* increased the heights of glucose-6-phosphate dehydrogenase enzyme, normalized hepatic and muscle glycogenesis, subsequent in appropriate glucose consumption. The levels of post-prandial hyperglycemia were similarly reduced due to the pancreatic and intestinal glucosidase inhibitory activity of the extracts of *Murrya koenigii* [150, 151].

2.21.6 Immunomodulatory

The leaf extracts of *Murrya koenigii* can regulate immunology related to oxidative stress metabolism. This immunomodulatory and anti-inflammatory activity was marked by interleukin (IL)-2, 4, 10 and tumor necrosis factor alpha (TNF-alpha) expression [151].

2.21.7 Hepatoprotective

Hydroethanaolic leaf extracts of *Murrya koenigiii* proved significant decrease in the levels of alanine aminotransferases, aspartate aminotransferases, alkaline phosphatase and total bilirubin in CCl4-treated hepatotoxic rats. Moreover, *Murrya koenigii* treated rats also increase the hepatic superoxide dismutase, catalase, reduced glutathione and decrease in lipid peroxidation. The tannins and carbazole alkaloids from the aqueous extracts showed first-rate hepatoprotective activity against ethanol-induced hepatotoxicity [140, 152]. This study proved that *M. Koenigii* is encouraging and a rich source of free radical quenchers, which have been intermediated through hepatocyte membrane stabilizing activity along with the reduction of fat metabolism [153]. The usual morphology of cell was continued after ethanolic challenge when aqueous extract enclosing tannins and carbazole alkaloids of *M. Koenigii* was assumed. All three extracts of dichloromethane, ethanolic and methanolic of *M. koenigii* leaves exhibited antilipase activity greater than 80% [154]. Mahanine (3,11-dihydro-3,5-dimethyl-3-(4-methyl-3-pentenyl)-pyrano[3,2-a]carbazol-9-ol) has been reported to be the major bio-active alkaloid [16]. It is present in the edible parts of some plants such as *Murraya koenigii*, which are expended in some parts of Southeast Asia, including Thailand [38]. The current study is therefore targeting to further study the role of the carbazole alkaloidal extract from *Murraya koenigii* leaves (MK) with respect to its antihyperglycemic effect.

CHAPTER III

OBJECTIVES

3.1 Objectives

1. Screening for highest antioxidative ability of bioactive compounds from herbal extracts

2. Screening for highest antihyperglycemic ability of bioactive compounds from herbal extracts through inhibition of α-glucosidase and α-amylase activity

3. To investigate the antioxidative mechanisms of bioactive compounds from *Murraya koenigii*

4. To investigate the antihyperglycemic mechanisms of bioactive compounds from *Murraya koenigii* and *Stevia rebuadiana*

5. To investigate the protective effect of bioactive compounds from *Murraya koenigii* on diabetes (hyperglycemia) related hepatocellular carcinoma and cholangiocarcinoma

3.2 Research Questions

1. Do the chosen herbal extracts contain antioxidant compounds, and do they show antioxidant activity?

2. Do one or more herbal extracts would protect pancreatic beta cells from ROS stress in culture?

3. Does any of herbal extracts process ability of inhibiting of α-glucosidase and α-amylase activity?

4. Does any of herbal extracts process ability in glucose metabolism through the study on molecular mechanisms for glucose uptake using cultured L6 myocytes and 3T3-L1 adipocyte?

5. Does any of herbal extracts process protective ability in diabetes (hyperglycemia) related hepatocellular carcinoma and cholangiocarcinoma?

3.3 Hypotheses

1. One or more of herbal extracts contain antioxidant compounds and possess antioxidant properties.

2. Some of the chosen herbal extracts would protect pancreatic beta cells from ROS stress.

3. Some of the chosen herbal extracts possess ability of inhibiting of α-glucosidase and α-amylase activity.

4. Some of the chosen herbal extracts possess ability on glucose metabolism through the study on molecular mechanisms for glucose uptake using cultured L6 myocytes and 3T3-L1 adipocyte.

5. Some of the chosen herbal extracts possess protective ability in diabetes (hyperglycemia) related hepatocellular carcinoma and cholangiocarcinoma.

3.4 Conceptual framework

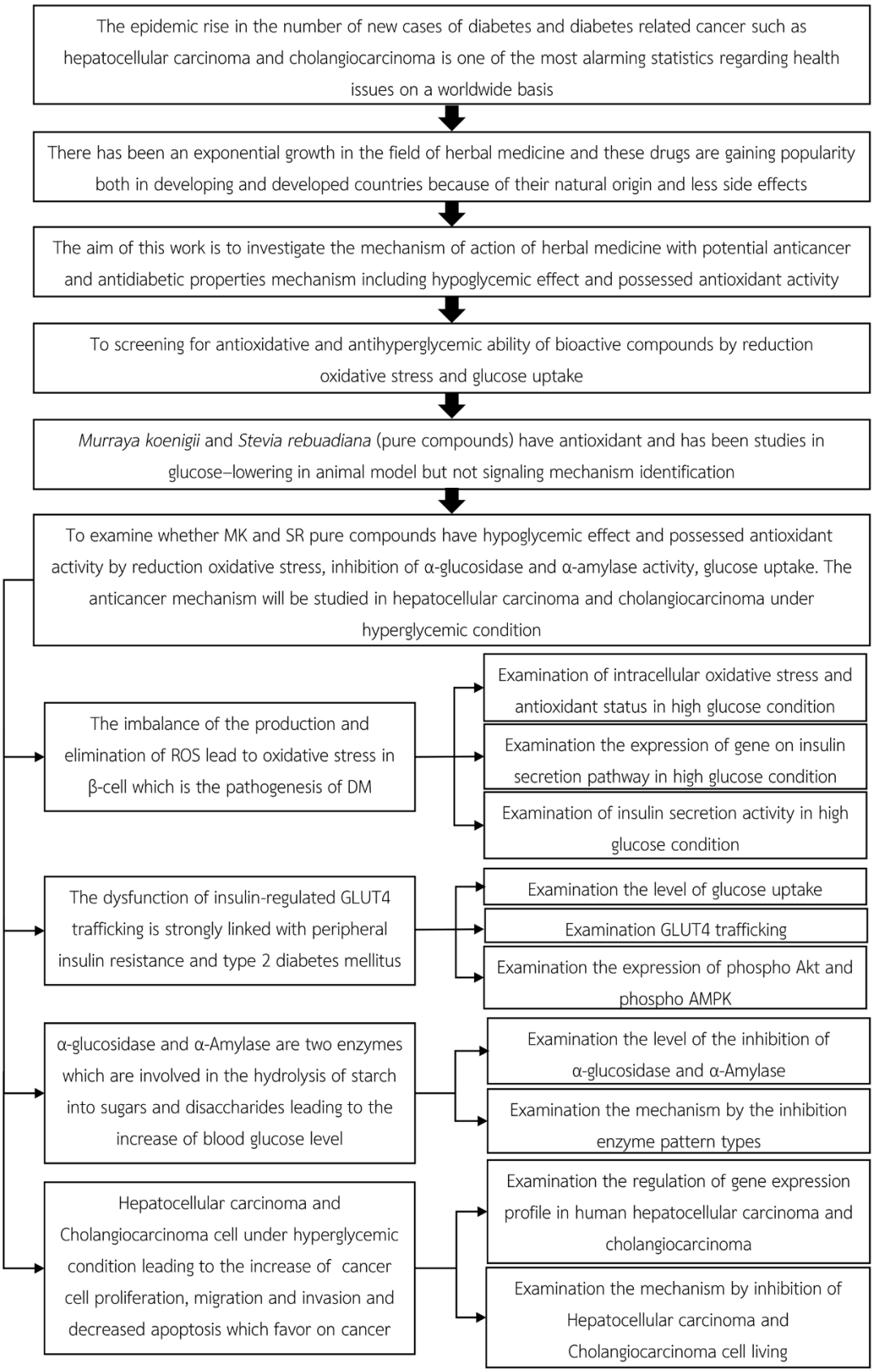

3.5 Experimental design

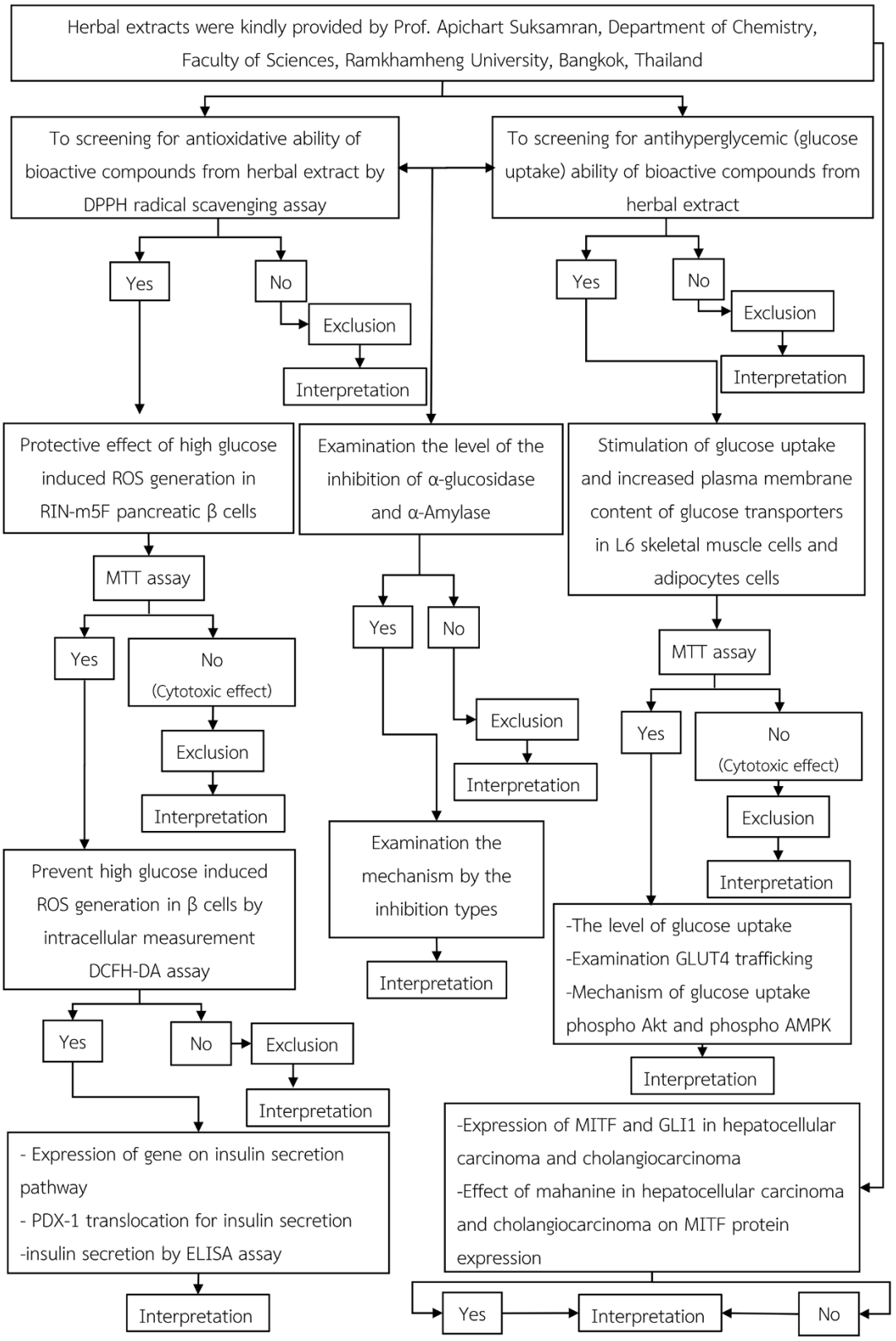

CHAPTER IV

MATERIALS AND METHODS

4.1 Materials

4.1.1 Reagents

Accupower RT premix	Bioneer, Korea
Accupower 2X Greenstar qPCR Master Mix	Bioneer, Korea
Adenosine 5'-triphosphate disodium salt	Sigma Aldrich, USA
Akt (pan) (C67E7) Rabbit mAb	Cell Signaling Technology, USA
Anti-MITF (C5) Mouse mAb	Thermo Scientific, USA
Anti-GLI1 Rabbit pAb	Cell Signaling Technology, USA
Anti-*Heme Oxygenase-1* Rabbit mAb	Cell Signaling Technology, USA
Anti-mouse IgG, HRP-linked Antibody	Cell Signaling Technology, USA
Anti-rabbit IgG, HRP-Linked Antibody (1 mL)	Cell Signaling Technology, USA
AMPK (D63G4) Rabbit mAb	Cell Signaling Technology, USA
Aluminium chloride	Sigma Aldrich, USA
Ascorbic acid	Merck, Germany
Beta-actin mouse mAb	Sigma Aldrich, USA
Beta-actin (13E5) Rabbit mAb	Cell Signaling Technology, USA
B-nicotinamide adenine dinucleotide phosphate	Sigma Aldrich, USA
DPPH (1,1-diphenyl-2-picrylhydrazyl)	Merck, Germany
Dimethyl Sulphoxide (DMSO)	Merck, Germany

Dulbecco's Modified Eagle Medium/High glucose (DMEM: with 4 mM/L Glutamine, 4500 mg/L Glucose Without Sodium Pyruvate)	HyClone, USA
Dorsomorphin	Sigma Aldrich, USA
Diaphorase	Sigma Aldrich, USA
1,1-Dimethylbiguanide, hyfrochloride	Sigma Aldrich, USA
2-Deoxy-d-glucose	Sigma Aldrich, USA
3-(4,5-dimethylthianisol-2-yl)-2,5-diphenyl-2H-tetrazolium bromide (MTT)	Calbiochem, Germany
Ethanol	Merck, Germany
EDTA-Trypsin 0.25% (1X)	HyClone, USA
Folin Ciocalteu's phenol reagent	Sigma Aldrich, USA
Fetal Bovine Serum (FBS)	HyClone, USA
Gallic acid	Sigma Aldrich, USA
Glut4 (1F8) Mouse mAb	Cell Signaling Technology, USA
G6PDH	Sigma Aldrich, USA
Hexokinase	Sigma Aldrich, USA
Insulin solution	Sigma Aldrich, USA
3-Isobutyl-1-methylxanthine	Sigma Aldrich, USA
Krebs–Ringer bicarbonate buffer	Sigma Aldrich, USA
Maltose	Merck, Germany

Mem-PER Plus membrane Protein Extraction kit	Thermo Scientific, USA
Mercodia High Range Rat Insulin ELISA Kit (10-1145-01)	Sigma Aldrich, USA
methanol	Merck, Germany
O-dianisidine dihydrochloride	Sigma Aldrich, USA
Oil red O	Sigma Aldrich, USA
OMNIPUR HEPES, FREE ACID	Sigma Aldrich, USA
PdX1 (D59H3) XP Rabbit mAb	Cell Signaling Technology, USA
Penicillin-Streptomycin Solution (10,000 units/mL Peniciliin/10,000 µg/mL Streptomycin)	HyClone, USA
PGO enzyme	Sigma Aldrich, USA
Phospho Akt (Ser473) (D9e) XP Rabbit mAb	Cell Signaling Technology, USA
Phosphate Buffered Saline (PBS: without calcium without magnesium)	HyClone, USA
Phospho Akt (Ser473) (D9e) XP Rabbit mAb	Cell Signaling Technology, USA
Phospho-AMPK (Thr172) (40H9) Rabbit mAb	Cell Signaling Technology, USA
Pierce ECL Western Blotting Substrate	Biorad, USA
Potassium chloride	Sigma Aldrich, USA
Potassium persulfate	Merck, Germany
Protease inhibitor Cocktail	Cell Signaling Technology, USA

Protein marker	Thermo Scientific, USA
Quercetin	Sigma Aldrich, USA
Rat intestinal acetone powder	Sigma Aldrich, USA
Resazurin sodium salt	Sigma Aldrich, USA
RIBOZOL RNA EXTRACTION REAGENT	*Amersco, Canada*
Rosilglitazone	Sigma Aldrich, USA
RPMI 1640 Medium	HyClone, USA
Sodium acetate	Sigma Aldrich, USA
Sodium carbonate	Merck, Germany
Sodium Chloride	Merck, Germany
Sodium phosphate dibasic anhydrous	Sigma Aldrich, USA
Sodium phosphate monobasic anhydrous	Sigma Aldrich, USA
Sucrose	Merck, Germany
Supersignal West Femto Substrate Trial kit	Biorad, USA
Spectra Multicolor Broad Range Protein Ladder	Thermo Scientific, USA
Sterile Water (deionized water)	General Hospital Products
Triethanolamine hydrochloride	Sigma Aldrich, USA
Trypan Blue Stain 0.4%	Invitrogen, USA
Wortmanin	Sigma Aldrich, USA

4.1.2 Tools and Devices

Analytical Balances	Mettler Toledo, Switzerland
Auto pipette	GILSON, France
Block heater	Wealtec Corp., USA
Cell Culture Flask (25, 75 cm^2)	Corning Inc., USA
Centrifuge tube (15, 50 mL)	Corning Inc., USA
CO_2 incubator	Sheldon Manufacturing, USA
Cryovial tube 2.0 mL	Corning Inc., USA
Confocal Microscopes	Zeiss, Germany
Disposable Serological pipette (5, 10 mL)	Corning Inc., USA
Electrophoresis power supply	Biorad laboratories, USA
Exicycler™ 96	Bioneer, Korea
Fluorescence microscope	Zeiss, Germany
Glassware	Pyrax, USA
Hemocytometer	Hausser Scientific, USA
Incubator	Memmert, Germany
Inverted microscope	Olympus Optical, Japan
Larminar Flow Cabinet	E.S.I. Flufrance, France
Light microscope	Olympus Optical, Japan
Liquid Nitrogen Tank	Taylor-Wharton, USA
Multichannel pipette	GILSON, France

Microcentrifuge tube (0.2 and 0.6 mL)	Axigen scientific, USA
Microcentrifuge tube (1.5 mL)	Biologix Research company, USA
Micro refrigerated centrifuge	Vision Scientific, South Korea
Multichanel pipette	GILSON, France
Mini Trans-Blot® Electrophoretic Transfer cell	Bio-Rad Laboratories, USA
0.2 mL Opaque White 8-Strip PCR tube, 250 strip	Bioneer, Korea
Pipette tips (10, 200, 1000 µL)	Sorenson™ BioScience, Inc., USA
Sonicator	Soniclean, USA
Sterile aerosol pipette tip (10, 200, 1000 µL)	Corning Inc., USA
Vortex Mixer	FINEPCR, Korea
Vortex Mixer (FINE VORTEX)	FINEPCR, Korea
Water Bath	Memmert, Germany
-20 °C Freezer	Sanyo Electric, Japan
-80 °C ULT Deep Freezer	Shin Lab, Korea
1.5 mL microcentrifuge tube	Eppendorf, Germany
2 mL Cryovial tube	Corning Inc., USA
4 °C Refrigerator	Sharp, Japan
6 well cell culture plate flat bottom with lid	Corning Inc., USA
96 well cell culture plate flat bottom with lid	Corning Inc., USA

4.2 Method

4.2.1 To Study the effect of bioactive compounds from herbal extract in regulation of anti-hyperglycemic mechanism

4.2.1.1 Investigation for the effect of bioactive compounds from herbal extract in regulation of antioxidant mechanism

4.2.1.1.1 Pure Compound

Mahanine from *Murraya koenigii*, steviol, isosteviol and 7 *β*-OHisosteviol from *Stevia rebuadiana* were kindly provided by Prof. Apichart Suksamran, Department of Chemistry, Faculty of Sciences, Ramkhamheng University, Bangkok, Thailand. Preparation and identification of mahanine was described as previously reported [39]. Briefly, dried *Murraya koenigii* leaves were pulverised and extracted with dichloromethane and methanol. The extract was filtered and concentrated to give the total alkaloid residue. The residue was chromatographed over silica gel and the eluates were examined by thin-layer chromatography. The selected fraction was chromatographed on Sephadex LH-20 and silica gel. Mahanine was acquired after purified by recrystallisation and column chromatography. The purity of mahanine was more than 90% after NMR identification [39]. The structure of mahanine (Table 3) was identified by nuclear magnetic resonance spectroscopy. Steviol, isosteviol and 7 *β*-OHisosteviol from *Stevia rebuadiana* were prepared as previously reported [113]. Briefly, dried *Stevia rebuadiana* leaves were pulverised and extracted with methanol. The residue was chromatographed over silica gel and the eluates were examined by thin-layer chromatography to get stevioside, a diterpenoid glycoside from the leaves.

Isosteviol (ent-16-ketobeyeran-19-oic acid), a tetracyclic diterpenoid from the beyerane series was obtained from acid hydrolysis of stevioside. Then Isosteviol was chosen as the parent compound for structural modification to its analogs. Microbial transformation of isosteviol with *Cunninghamella echinulata* NRRL 1386 (fungi) produced the 7 β-OHisosteviol. The isolated metabolites were characterized by nuclear magnetic resonance spectroscopy and the purity of three compounds were more than 90%. Mahanine, steviol, isosteviol and 7 *β*-OHisosteviol were dissolved in dimethyl sulfoxide (DMSO) at 100 mM as stock solution and then further diluted with serum free media for cell treatment, however the final concentration of DMSO in treatment medium was not more than 0.01 %. Mahanine, steviol, isosteviol and 7 *β*-OHisosteviol were stored at -20 °C until the experiment was performed.

Table 3: Chemical structures of mahanine from *Murraya koenigii*, steviol, isosteviol and 7-beta-OH isosteviol from *Stevia rebuadiana*.

Plant	Structure	Formula (M.W.)	Pure compounds
Murraya koenigii	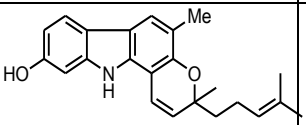	$C_{23}H_{25}NO_2$ (347.19)	mahanine
Stevia rebuadiana	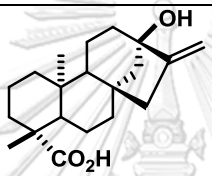	$C_{20}H_{30}O_3$ (318.45)	steviol
Stevia rebuadiana	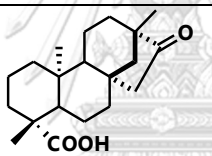	$C_{21}H_{33}O_3$ (333.2)	isosteviol
Stevia rebuadiana	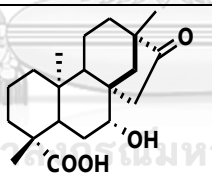	C20H30O4 (334.45)	7-β-OH - isosteviol
	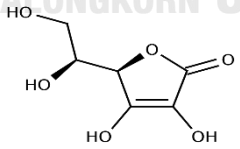	$C_6H_8O_6$ (176.12)	Ascorbic acid

4.2.1.1.2 Measurement of antioxidant activity by using DPPH Assay

All fraction of herbal extracts were screened for antioxidant activity by measuring the ability to scavenge the free radical 2, 2-diphenyl-1-picrylhydrazyl (DPPH) compared with ascorbic acid (positive control). Briefly, DPPH and herbal extracts were dissolved in

dimethyl sulfoxide (DMSO) to 1 mM and 100 mM, respectively. Then the herbal extracts were prepared to the ratio of 1:10 with DPPH solution in 96-well plate. The absorbance will be measured at 517 nm after 30 min of incubation using a microplate reader. The results will be represented as 50 % inhibition concentration (IC50).

4.2.1.1.3 Cell culture

Rat pancreatic beta cells (RIN-m5F) were purchased from the American Type Culture Collection (ATCC, Manassas, VA). RIN-m5F cells were maintained in RPMI-1640 supplemented with 10% fetal bovine serum (FBS) as described previously [155].

4.2.1.1.4 Measurement of cell viability by using MTT reduction assay

The effect of mahanine on RIN-m5F cell viability was determined by the MTT assay, which is a measure the enzyme activity that reduce (3-(4, 5-Dimethylthiazol-2-yl)-2, 5-diphenyltetrazolium bromide (MTT) to purple formazan. MTT was dissolved in phosphate buffer saline (PBS), filtered and protected from light and stored at 4 °C. RIN-m5F cells were seeded in 96-well flat-bottom culture plates at a density of 2×10^4 cells/well. Cells were treated and incubated with mahanine for 24 h. Then media was removed and new RPMI was added. MTT at a final concentration of 0.5 mg/mL was added into each well in the 96-well plate which was incubated for another 3 h in a humidified atmosphere at 37 °C, 5 % CO_2. After that the medium was removed and 100 µL DMSO was added to dissolve the formazan crystals. The absorbance was measured at 550 nm using a microplate reader. After subtraction of background, cell viability was

expressed as a percentage relative to control that was designated as 100 %. DMSO treated cells and untreated cells were positive and negative controls, respectively.

4.2.1.1.5 Measurement of intracellular oxidative stress

Intracellular ROS levels were monitored using the fluorescent probe 2',7'-dichlorodihydrofluorescein diacetate (H_2DCFDA) according to manufacturer's protocol with some modifications as described previously [156]. In briefly RIN-m5F cells were seeded in 96-well flat bottom culture plates at a density of 2×10^4 cells/well. Cells were pre-incubated in RPMI-1640 medium at either a maintenance glucose conditions (11 mM) or a high glucose conditions (33 mM) for 48 h, after which time, cells were treated or not treated with mahanine. The medium was removed and 20 μM of H_2DCFDA was then added. After an additional 30 min of incubation in the dark at 37 °C, cells were washed twice with PBS and then maintained in phenol-red free RPMI without fetal bovine serum. The results were analyzed immediately using a fluorescence microplate reader (Bio-Tek Instruments) at 485 and 528 nm, respectively. H_2O_2 (50 μM) was used as a positive control. After measurement of 2',7'-dichlorofluorescein (DCF) fluorescence, an MTT assay was performed immediately according to the procedures described above. The ratio of the DCF fluorescence and MTT absorbance was taken as the extent of intracellular ROS generation normalized to the absorbance of the cell viability. The result are presented as a fold of control. In parallel, intracellular ROS was also observed directly under a fluorescent microscope. RIN-m5F cells were seeded into a 35 mm culture dish at a density of 2×10^5 cells/well and allowed to grow for 2 days under

maintenance glucose conditions (11 mM) or high glucose conditions (33 mM) before switching to Krebs-Ringer bicarbonate buffer containing 25 mM glucose (fed state condition) cotreated with mahanine for 2 h. The medium was then removed and 50 μM of H_2DCFDA was added. After an additional 30 min incubation in the dark at 37 °C, cells were washed twice with serum free medium and observed under a Zeiss Axio Observer A1 inverted microscope with a QImaging Retiga CCD.

4.2.1.1.6 Assessment of quantitative – reverse transcription polymerase chain reaction (qPCR)

RIN-m5F cells were seeded in 60 mm culture dishes and treated with mahanine as described above. After treatment, total RNA was extracted from the cells using TRI reagent (Favorgen Biotech Corp, Ping-Tung Taiwan) according to the manufacturer's instructions with some modifications. The total RNA was reverse transcribed to cDNA using oligo (dT) primers and a reverse transcriptase kit (Bioneer, Daejeon, Korea) following the manufacturer's protocol. Quantitative - reverse-transcription polymerase chain reaction was performed in 96-well plates using the Exicycler™ 96 Real time Quantitative Thermal Block (Bioneer, Daejeon, Korea). The SYBR green system was used to analyze PDX-1, PRE-INS, GLUT2, GCK, NADPH oxidase (NOX1, NOX4), and GAPDH expression using gene specific primer pairs as listed in table 4. All sample mRNA levels were normalized to the values of GAPDH and the results expressed as fold changes of threshold cycle (Ct) value relative to controls using the $2^{-\Delta\Delta Ct}$ method.

Table 4: Specific primer pairs used.

Pair	Name	Sequence 5'-3'	T (°C)	Fragment size (bp)
1	PDX-1-F	CGGACCTTTCCCGAATGGAA	56	314
	PDX-1-R	TCCACTTCATGCGACGGTTT		
2	PRE-INS-F	AGGCTTTTGTCAAACAGCACCTT	60	212
	PRE-INS-R	ATCCACAATGCCACGCTTCTG		
3	GLUT2-F	TTAGCAACTGGGTCTGCAAT	54	343
	GLUT2-R	GGTGTAGTCCTACACTCATG		
4	GCK-F	GCTTTTGAGACCCGTTTCGT	54	119
	GCK-R	CGCACAATGTCGCAGTCA		
5	NOX1-F	CTTCCTCACTGGCTGGGATA	58	219
	NOX1-R	CGACAGCATTTGCGCAGGCT		
6	NOX4-F	GTTAAACACCTCTGTCTGCTTG	64	454
	NOX4-R	CACCTGTCAGGCCCGGAACA		
7	GAPDH-F	CAGGGCTGCCTTCTCTTGTG	57	359
	GAPDH-R	TCTCGTGGTTCACACCCATC		

4.2.1.1.7 Assessment of PDX-1 protein expression

PDX-1 protein expression in RIN-m5F cells was examined by western blotting. Cells were seeded in 60 mm culture dishes and allowed to grow overnight (80-90%

confluence), and then incubated with vehicle (DMSO), Insulin (0.1 μM) or mahanine (5 or 10 μM) under 11 and 33 mM glucose as appropriate. The treated cells were washed twice with ice-cold PBS, detached with cell scrapers and pelleted by centrifugation at 5,000 g at 4℃ for 3 minutes. The pelleted cells were lysis with RIPA buffer (Merck Millipore, Billerica, USA) containing protease/phosphatase inhibitor cocktail (Cell Signaling Technology, Boston, USA). The cell lysate supernatants were collected after centrifugation at 14,000 g for 15 minutes at 4 ℃. Cell lysates (30 μg protein per lane) were subjected to western blot analysis. Equal amounts of total cellular protein were resolved by SDS–PAGE and transferred onto polyvinylidene difluoride (PVDF) membranes [Millipore (Billerica, MA, USA)], and probed with a primary antibody against PDX-1 (1:2000 dilution) overnight at 4 ℃, followed by incubation with a horseradish peroxidase (HRP)-conjugated secondary antibody (1:5000 dilution for 1 hour). Immunoblots were exposed to X-ray film to produce bands in the linear range. Equal loading was confirmed by analysis of the internal control of beta-actin, and bands were quantified using densitometry by the Image J Software (NIH, Bethesda, MD, USA).

4.2.1.1.8 Assessment of the intracellular localization PDX-1

The intracellular localization of PDX-1 in RIN-m5F cells was examined by immunofluorescence staining. Cells were seeded on a coverslip that was placed in the well of a 6-well plate at 37 ℃ overnight, pre-incubated in RPMI-1640 medium at either maintenance glucose (11mM) or high glucose (33 mM) for 48 h. After incubation, cells were treated in the absence or presence of mahanine. Ascorbic acid and H_2O_2 were

used as positive controls. Cells were washed with PBS and fixed in 4% paraformaldehyde for 15 minutes, washed with PBS with 0.5% Triton X-100 5 times, and then blocked with 1% FBS-BSA for 1 hour. Cells were incubated with primary antibodies for PDX-1 at a 1:500 dilution in 1% BSA–PBS (v/v) at 4 ℃ overnight. Cells were washed three times with PBS, and incubated with a goat anti-rabbit IgG-Alexa Fluor 488 secondary antibody at a 1:3000 dilution in 1% BSA–PBS (v/v), for 1 hour at room temperature. Coverslips were washed with PBS three times, incubated with DAPI (4′,6-diamidino-2-phenylindole) at 0.2 μg/mL in PBS (v/v) for 10 minutes. Thereafter, samples were washed with PBS three times, and mounted on microscope slides with Prolong® Gold antifade reagent (Invitrogen, Carlsbad, USA). The localization patterns of PDX-1 proteins were analyzed using a LSM700 laser confocal scanning microscope (Carl Zeiss Microscopy GmbH, Oberkochen, Germany). Fluorophores were excited with a 405-nm laser for DAPI and a 561-nm laser for Alexa 488. PDX-1 immunofluorescence staining images were analyzed by ImageJ v 1.50 software (National Institute of Health, USA) [157]. The data are presented as the average fluorescence intensity for each image from cells or nuclei.

4.2.1.1.9 Measurement the glucose stimulated insulin secretion (GSIS)

RIN-m5F cells (2×10^5 cells/well) were seeded in 24-well plates. After 2 days, cells were pre-incubated with glucose (11 or 33 mM) for 48 hour and then cells were washed twice with Krebs–Ringer bicarbonate buffer [25 mM HEPES, 115 mM NaCl, 24 mM NaHCO3,5 mM KCl, 2.5 mM CaCl2, and 1 mM MgCl2 supplemented with 0.1% bovine serum albumin, pH 7.4]. Subsequently, the medium was replaced and cells were

incubated in KRB 25 mM glucose (simulated fed state with glucose-stimulated insulin secretion) with or without mahanine (5 μM and 10 μM), and then the cells were incubated for 2 h at 37 ℃. The supernatant was collected for measurement of secreted insulin using a high range rat insulin ELISA kit (Mercodia Inc., Uppsala, Sweden).

4.2.1.2 Investigation for the hypoglycemic effect of herbal extract through inhibition of α-glucosidase and α-amylase activity

4.2.1.2.1 Pancreatic α-amylase inhibitory activity

The pancreatic α-amylase inhibition assay was performed follow by a previous report [12]. Porcine pancreatic α-amylase (3 units/mL) was dissolved in 0.1 M phosphate buffer saline, pH 6.9. The various concentrations of the extract (10 μL) were added to a solution containing starch (1 g/l). The reaction was started by adding enzyme solution (10 μL) to the incubation tube. After 10 min of incubation, the reaction was stopped by adding 10 μL dinitrosalicylic (DNS) reagent (1% 3,5-dinitrosalicylic acid, 0.2% phenol, 0.05% Na_2SO and 1% NaOH in aqueous solution) to the reaction mixture. The mixtures were heated at 100˚C for 10 min in order to stop the reaction. Afterward, 200 μL of 40% potassium sodium tartarate solution was added to the mixtures to stabilize the color. After cooling to room temperature in a cold water bath, the absorbance was recorded at 540 nm using a microplate reader. Acarbose was used as positive control

4.2.1.2.2 Intestinal α-glucosidase inhibitory activity

The valuation of intestinal α-glucosidase inhibitory activity was followed by the previously modified method [12]. Briefly, rat intestinal acetone powder was homogenized in 0.9% NaCl solution at concentration 100 mg/mL. The solution was

centrifuged at 14,000 rpm for 30 min and then was subjected to assay. The crude enzyme solution (as maltase assay, 10 µL; as sucrase assay, 40 µL) were incubated with 30 µL maltose (86 mM) or 30 µL sucrose (120 mM) respectively. 10 µL of the extract was added at various concentrations, followed by the addition of 0.1 M phosphate buffer, pH 6.9 to give a final volume of 100 µL. The reaction was incubated at 37 °C for 30 min for maltase assay and 60 min for sucrase assay. Next, the mixtures were incubate at 100 °C for 10 min to stop the reaction. The concentrations of glucose unobstructed from the reaction mixtures were determined by glucose oxidase method with absorbance at a wavelength of 450 nm. Intestinal α-glucosidase inhibitory activity was expressed as percentage inhibition. Acarbose was used as positive control.

4.2.1.3 Investigation for the hypoglycemic effect of herbal extract through glucose uptake by using cultured myocytes and adipocyte

4.2.1.3.1 Cell culture and differentiation

The muscle myoblast cell line L6 (ATCC CRL 1458) and a murine preadipocytes cell line 3T3-L1 (ATCC CL 173) were purchased from the American Type Culture Collection (ATCC, Manassas, VA). L6 cells were maintained in DMEM containing 10% (v/v) FBS and 1% penicillin-streptomycin, cultured in a humidified atmosphere of 5% CO_2 at 37 ℃. To differentiate the myoblast cell into myotubes, the medium was switched to DMEM containing 2% (v/v) FBS for 7 days to induce to myotube formation. The differentiation medium was replaced every 2 days prior to use as describe previously [155, 158]. Total RNA was used to assess the mRNA expression of myogenin, a myotubes marker and beta-actin was used to normalize the expression as a house keeping gene

(data not shown). 3T3-L1 cells were maintained in DMEM, supplemented with 10% fetal bovine serum (FBS). To induce differentiation of 3T3-L1 cells, they were cultured as described previously [158, 159]. The differentiated adipocytes were confirmed by determination of lipid accumulation as assessed by Oil Red O staining. Briefly, the differentiated cells were washed with phosphate-buffered saline (PBS) and fixed with 10% formalin-PBS solution for 1 h. After air drying, the plates were stained with Oil Red O dye (Sigma Aldrich, St. Louis, MO) for 30 min at room temperature. The plates were rinsed four times with distilled water. Cell images were obtained using a Zeiss Axio Observer A1 inverted microscope with a QImaging Retiga CCD at 10 X magnification.

4.2.1.3.2 Measurement of cell viability by using MTT assay

The effects of mahanine, steviol, isosteviol and 7 β-OHisosteviol on L6 and 3T3-L1 cell viability were determined by the MTT assay. L6 and 3T3-L1 cells were seeded into 96-well plates at a density of 2×10^3 cells/well and 0.5×10^3 cells/well respectively. After differentiation, myotube and adipocyte cells were incubated with mahanine, steviol, isosteviol and 7 β-OHisosteviol for 24 hour in a humidified atmosphere at 37 °C, 5 % CO_2.Cell viability was expressed as a percentage relative to control that was designated as 100 %. DMSO treated cells and untreated cells were positive and negative controls, respectively.

4.2.1.3.3 Glucose uptake assay

Glucose uptake by myotubes and adipocyte cells was analyzed by measurement of 2-NBDG uptake [160]. Briefly, differentiated cells were cultured under serum starvation conditions (DMEM with 0.1% BSA) overnight in a CO_2 incubator. Then cells were washed and starved in Krebs-Ringer phosphate HEPES (KRPH) buffer containing [NaCl 118 mM, KCl 5 mM, KH_2PO_4 1.2 mM, $CaCl_2$ 1.3 mM, $MgSO_4$ 1.2 mM and HEPES 30 mM (pH 7.4)] for 1 hour. The cells were treated with or without 5 or 10 μM mahanine for 30 min and with or without 50 μM steviol, isosteviol and 7 β-OHisosteviol for 60 min in KRPH buffer, with insulin used as a positive control. Then 2-NBDG (100 μM in KRPH buffer) was added to each well followed by incubation for 30 min at 37 °C. After washing the fluorescence intensity of cells containing 2-NBDG were analyzed immediately using a fluorescence microplate reader (Bio-Tek Instruments) with excitation at 485 nm and emission at 535 nm.

4.2.1.3.4 Assay for GLUT4 translocation

For measuring the amount of GLUT4, membrane-and-cytoplasmic protein fractions of cultured myotubes cell were obtained with a Mem-PER Plus Membrane Protein Extraction Kit (Catalog number 89842). Myotubes cells were treated with 5 or 10 μM mahanine for 30 min and with or without 50 μM steviol, isosteviol and 7 β-OHisosteviol for 60 min. A 15 min-incubation with insulin (0.1 μM) served as positive control. The levels of GLUT4, Na+/K+ ATPaseα-1 (membrane protein marker) and an internal control (beta-actin) were determined by western blot analysis. The membrane

protein was probed with primary antibodies to either GLUT4 (1:1000 dilution) *or Na+/K+ ATPase*α-1 (1:1000 dilution) overnight at 4 °C then incubated with an HRP-conjugated anti-mouse IgG secondary antibody or an HRP-conjugated anti-rabbit IgG antibody (1:2000, dilution) for 1 hour at room temperature. The membranes were analyzed by ECL detection reagents with ImageJ Software (NIH, Bethesda, MD, USA). The level of GLUT4 in the plasma membrane was calculated by the ratio of the levels of GLUT4 to beta-actin.

4.2.1.3.5 Assay for phosphorylations of both Akt and AMPK

The cells were treated with or without 5 or 10 μM mahanine and with or without 50 μM steviol, isosteviol and 7 β-OHisosteviol in KRPH buffer together with the presence or absence of 0.1 μM wortmannin (an Akt inhibitor) and 20 μM compound C (an AMPK inhibitor) as per the previous protocol [161]. The inhibitors were incubated with cells for 30 min prior to sample treatment. After the incubation time the treated cell were washed and lysed with cell lysis buffer (RIPA buffer). The amounts of p-Akt, Akt, p-AMPK and AMPK proteins were determined by western blot analysis. The PVDF membrane was probed with the primary antibodies for either p-Akt (1:5000 dilution) or p-AMPK (1:2500 dilution) overnight at 4 °C then incubated with a HRP-conjugated anti-rabbit IgG secondary antibody (1:5000 dilution) for 1 hour at room temperature. The membrane was analyzed by ECL detection reagents with ImageJ Software (NIH, Bethesda, MD, USA). The relative band intensities of p-Akt, p-AMPK, Akt and AMPK were expressed as a fold of the untreated control.

4.2.2 Investigation for the antihyperglycemic mechanisms of bioactive compounds from *Murraya koenigii* and related anticancer

4.2.2.1 Immunohistochemical analysis of human hepatic cancer arrays

The liver cancer tissue array contained 40 cases of hepatocellular carcinoma and 8 cases of cholangiocarcinoma (LV484, US Biomax, Inc.), and two arrays of the same lot were used for analyzing the expression of MITF and GLI1. However, one hepatocellular carcinoma specimen and one cholangiocarcinoma specimen were excluded, because one of the tissue specimens derived from a same patient was peeled from a slide glass during the immunohistochemical procedure with either anti-MITF antibody or anti-GLI1 antibody. In addition, one hepatocellular carcinoma specimen was excluded, because its grade in Pathology Diagnosis was not available. Accordingly, the remaining 38 hepatocellular carcinoma cases and 7 cholangiocarcinoma cases were analyzed. The specificity of polyclonal anti-MITF antibody was reported [35] [162]. Dilutions of primary antibodies were 1:400 for anti-MITF and 1: 100 for anti-GLI1 (BIOSS, Woburn, MA 01801 U.S.A). For simplicity, the presence of detectable immunoreactivity was defined as positive, irrespective of the staining intensity, while the absence of detectable immunoreactivity was defined as negative. In case of positive specimens, almost all cancer cells were reactive with a given polyclonal antibody (anti-MITF or anti-GLI1 antibody). As negative control, the tissue sections were incubated with normal rabbit IgG (DAKO), instead of a primary antibody (data not shown).

4.2.2.2 Cell culture

Human cholangiocarcinoma cell lines, KKU-100 and HuCCT1, were obtained from JCRB Cell Bank (Osaka, Japan) and RIKEN Cell Bank (Tsukuba, Japan), respectively. KKU-100 cells were cultivated in Dulbecco's Modified Eagle's Medium (DMEM) containing 10% fetal bovine serum (FBS), and HuCCT1 cells were cultivated in RPMI1640 medium containing 10% FBS. HepG2 hepatocellular carcinoma cells were cultivated in DMEM containing 10% FBS.

4.2.2.3 Assessment of cytotoxicity

Cytotoxicity of mahanine was determined in KKU-100 and HuCCT1 cholangiocarcinoma cells and HepG2 hepatocellular carcinoma cells by MTT assay. Cells were seeded and grown in 96 well flat bottom culture plates at a density of 1×10^4 cells/well for 24 h before were treated with varying concentrations of mahanine for 24 h. After treatment, culture medium was removed and fresh medium was added. MTT at a final concentration of 1 mg/mL was added into each well in the 96-well plate and incubated for 4 h in a humidified atmosphere at 37°C, 5% CO_2. After that, the medium was removed and 100 µL acidic isopropanol was added to dissolve the formazan crystal. The amount of formazan was determined based on absorbance at 570 nm, using a plate reader (FlexStation 3 Microplate Reader, Molecular Devices). After subtraction of background, cell viability was expressed as a percentage relative to control that was designated as 100%.

In another series of experiments, cells were seeded in 60-mm culture dishes and allowed to grow overnight (80-90% confluence), then incubated with vehicle (DMSO) or mahanine (up to 25 μM) in fresh medium containing 10% FBS for 24. Treated cells were washed twice with ice-cold PBS, detached with cell scrapers, and pelleted by centrifugation at 5,000 g at 4°C for 3 minutes. The cell lysate supernatants were collected after centrifuged at 14,000 g for 15 minutes at 4°C. Cell lysates (30 μg protein per lane) were subjected to Western blot analysis. The relative intensity of a specific protein band was assessed with the intensity of beta-actin (loading control).

4.2.2.4 Western blot analysis

Whole cell lysates were prepared from KKU-100 and HuCCT1 cholangiocarcinoma cells and HepG2 hepatocellular carcinoma cells, as described previously [24]. Cell lysates (30 μg protein per lane) were fractionated by SDS-PAGE and blotted to a polyvinylidene fluoride membrane (Immobilon™-P, Millipore Corporation) in the buffer containing 20% methanol, 48 mM Tris, 39 mM glycine, and 0.037% SDS. The membranes were treated with Tris-buffered saline (TBS) with 0.1% Tween 20 (TBS-T), containing 5% non-fat dried milk for 1 h at room temperature, exposed with each antibody in TBS-T for 2 h at room temperature, and were washed three times each for 10 min in TBS-T at room temperature. The antibodies used were mouse monoclonal anti-MITF antibody (C5) (NeoMarkers, Fremont, CA), anti-heme oxygenase (HO)-1 antibody (ADI-SPA-896) was from Enzo Life science (Farmindale, NY, USA), and anti-beta-actin antibody (Sigma-Aldrich, St. Louis, MO). Finally, immunoreactive proteins were

detected with a Western blot kit (Millipore Corporation). Horseradish peroxidase (HRP)-conjugated donkey anti-rabbit immunoglobulin (NA9340) and HRP-conjugated sheep anti-mouse immunoglobulin (NA931) were from GE Healthcare (Buckinghamshire, UK).

4.2.2.5 Statistical analysis

The results are expressed as mean ± SD of at least three independent experiments in which triplicate sample were performed. Statistical significance was assessed by Student t-test, Chi-Square and one-way ANOVA followed by a Tukey comparison test and Dunnett's post hoc comparison test using the GraphPad Prism program version 5 (GraphPad software, San Diego, CA, USA). A value of $p < 0.05$ was considered as statistically significant.

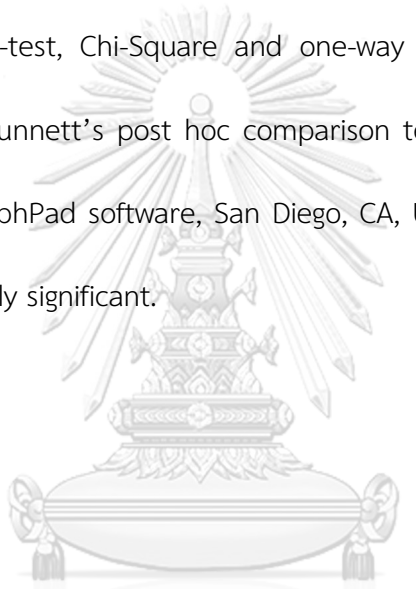

CHAPTER V
RESULTS

5.1 Investigation for the effect of bioactive compounds from herbal extract in regulation of antioxidant mechanism

5.1.1 Antioxidant activity of from *Murraya koenigii* and *Stevia rebuadiana* crude extraction determined by DPPH assay

Antioxidant activity of from *Murraya koenigii, Stevia rebuadiana* were determined by DPPH assay the result were shown in table 5. *Murraya koenigii* and *Stevia rebuadiana* possess different degrees of antioxidant capacity. *Murraya koenigii* possessed high antioxidant capacities was 45.75 ± 2.1 mg vit C / g Dry weigh of sample, while *Stevia rebuadiana* showed 15.49 ± 1.85 mg vit C / g Dry weigh of sample. *Murraya koenigii* showed stronger antioxidant activity than *Stevia rebuadiana*.

Table 5: Antioxidant activities of *Murraya koenigii*, *Stevia rebuadiana*. The data were represented in mg vit C / g Dry weigh of sample and performed in triplicate and determined at 10 min

Scientific Name	Part Used	Solvent	mg vit C / g Dry weigh of sample (Mean ± SD)
Murraya koenigii	Leaf	Methanol	45.75 ± 2.1
Stevia rebuadiana	Leaf	Methanol	15.49 ± 1.85

5.1.2 Antioxidant activity of pure compounds from *Murraya koenigii*, *Stevia rebuadiana* and ascorbic acid determined by DPPH assay

Antioxidant activity of pure compounds from *Murraya koenigii*, *Stevia rebuadiana* and ascorbic acid were determined by DPPH assay as shown in table 6. All fractions possess different degrees of antioxidant capacity. Mahanine possessed the highest antioxidant capacities; IC50 was 49.00 ± 1.67 μM, while Steviol, isosteviol and 7 *beta*-OH-isosteviol showed no antioxidant activity. Based on these results, mahanine were used to examined the protective effect on pancreatic beta cells from high glucose induce ROS damage in cell culture.

Table 6: Antioxidant activities of mahanine from *Murraya koenigii*, steviol, isosteviol and 7 beta-OH –isosteviol from *Stevia rebuadiana* and ascorbic acid.

The data were represented in 50% inhibition concentration (IC50) and performed in triplicate and determined at 10 min. NA; no antioxidant activity (the absorbance of DPPH does not change).

Plant	Pure compounds	IC50 (μM) (Mean ± SD)
Murraya koenigii	Mahanine	49.00 ± 1.67
Stevia rebuadiana	Steviol	NA
Stevia rebuadiana	isosteviol	NA
Stevia rebuadiana	7-*β*-OHisosteviol	NA
	Ascorbic acid	35.79 ± 1.61

5.1.3 Mahanine protect RIN-m5F pancreatic beta cells death in high-glucose condition

To determine the cytotoxic effect of high-glucose treatment on pancreatic beta cells, RIN-m5F cells were treated with glucose at the concentrations of 11, 22 and 33 mM and incubated for 48 hour. A glucose concentration of 33 mM showed a significantly decreased cell viability to 81.98± 7.96 % of control (Figure 10A). To determine the cytotoxic effect of mahanine on pancreatic beta cells viability, RIN-m5F cells were cultured and treated with various concentrations of mahanine for 24 h followed by MTT assay Figure 10B. Treatment with mahanine at concentrations of 25, 50 and 100 μM significantly decreased cell viability to 69.65 ± 7.01, 11.58 ± 2.54 and 9.45 ± 4.65 %, respectively Figure 10B. Based on these results, glucose at the concentration of 33 mM and mahanine at the concentrations up to 12.5 μM was used in the subsequent experiments. Moreover, it was found that exposure of the RIN-m5F cells to 33 mM glucose together with mahanine at 5 and 10 μM showed cyto-protective effects when compare to the treatment with 33 mM glucose alone as shown in Figure 10C. At 33 mM glucose cell viability was 75.10 ± 3.00 %, while co-treatment with mahanine at 5 and 10 μM showed cell viability of 88.91± 4.99 % and 95.36± 1.00% compared to the high glucose conditions.

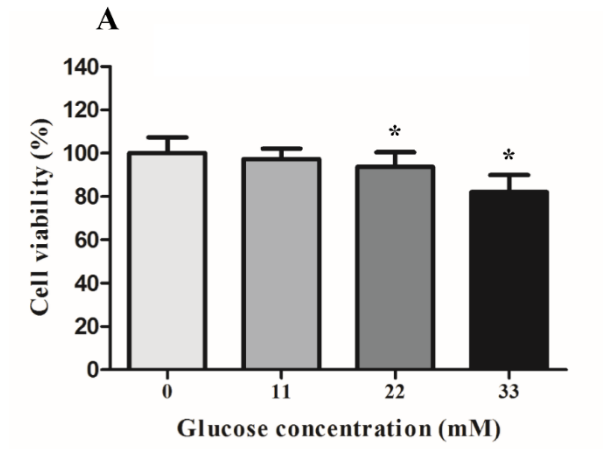
A
Cell viability (%)
140
120
100
80
60
40
20
0
*
*
0
11
22
33
Glucose concentration (mM)

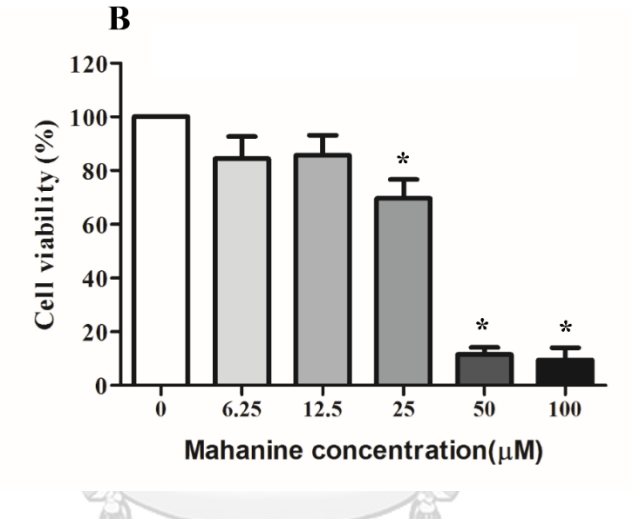
B
Cell viability (%)
120
100
80
60
40
20
0
*
*
*
0
6.25
12.5
25
50
100
Mahanine concentration(μM)

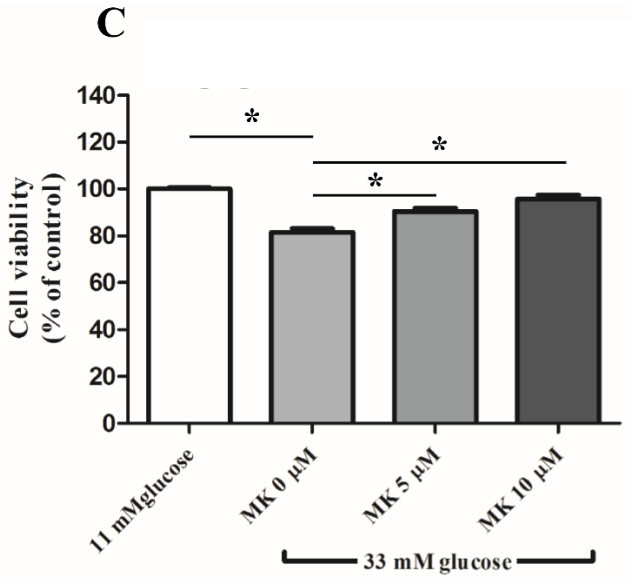
C
Cell viability
(% of control)
140
120
100
80
60
40
20
0
*
*
*
11 mMglucose
MK 0 μM
MK 5 μM
MK 10 μM
33 mM glucose

Figure 10: Mahanine protects against RIN-m5F pancreatic beta cell death in high-glucose condition.

(A) RIN-m5F cells were incubated with various concentration of glucose for 48 hour and cell viability determines by MTT assay. (B & C) RIN-m5F cells were incubated with mahanine (MK) at different concentrations for 24 hour and cell were exposured to 33 mM glucose for 48 h together with increasing concentration of mahanine and cell determines by MTT assay. Data represent mean ± S.D. of three independent experiments. $^{*}P < 0.05$ compared to control.

5.1.4 Mahanine reduce intracellular ROS generation in high glucose-treated RIN-m5F pancreatic beta cells

The protective effect of mahanine against pancreatic beta-cells damage from high glucose conditions induced ROS production was investigated. To confirm that high glucose induced ROS production, RIN-m5F cells were treated with glucose at concentrations of 11, 22 and 33 mM for 48 hour. The result are shown in Figure 11A. The 33 mM glucose treatment group showed significantly increased ROS levels of 1.52 ± 0.46 fold as compared to maintenance glucose (11 mM). Therefore, incubation of cells with 33 mM of glucose for 48 hour was used to further study ROS induced beta cells damaged. To investigate the ROS inhibition effect of mahanine, RIN-m5F cells were treated with mahanine at concentrations of 5 or 10 μM, for 2 h after exposure to high glucose (33 mM) for 48 hour. Treatment with 50 μM H_2O_2 for 30 min was used as a positive control. The ROS levels showed 2.11 ± 0.35 fold of control in the H_2O_2 treated

group. Mahanine at the concentrations of 5 and 10 μM, and ascorbic acid showed significantly reduced levels of ROS production to 1.29 ± 0.31, 1.16 ± 0.34 and 1.05 ± 0.64 fold, respectively as compared to the high glucose treatment (33 mM) as shown in Figure 11B and 11C. These results indicate that mahanine possesses antioxidant activity.

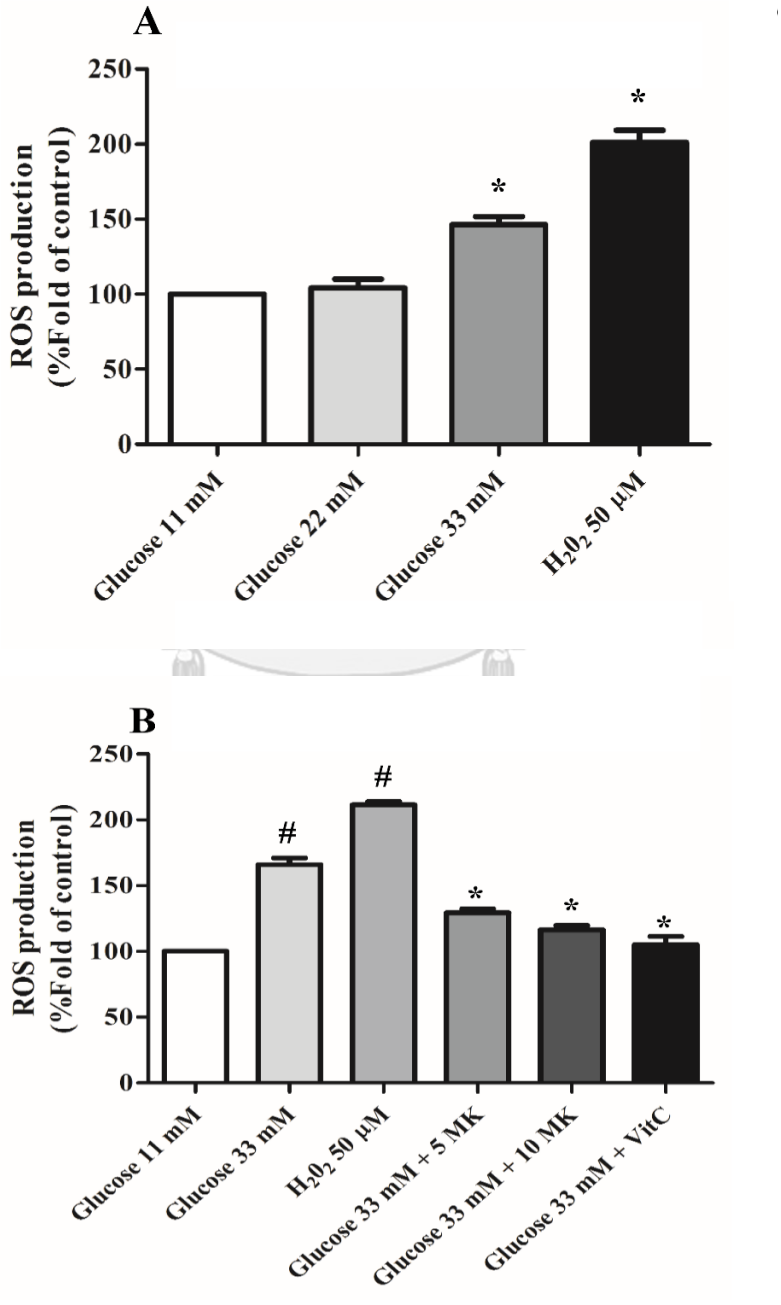

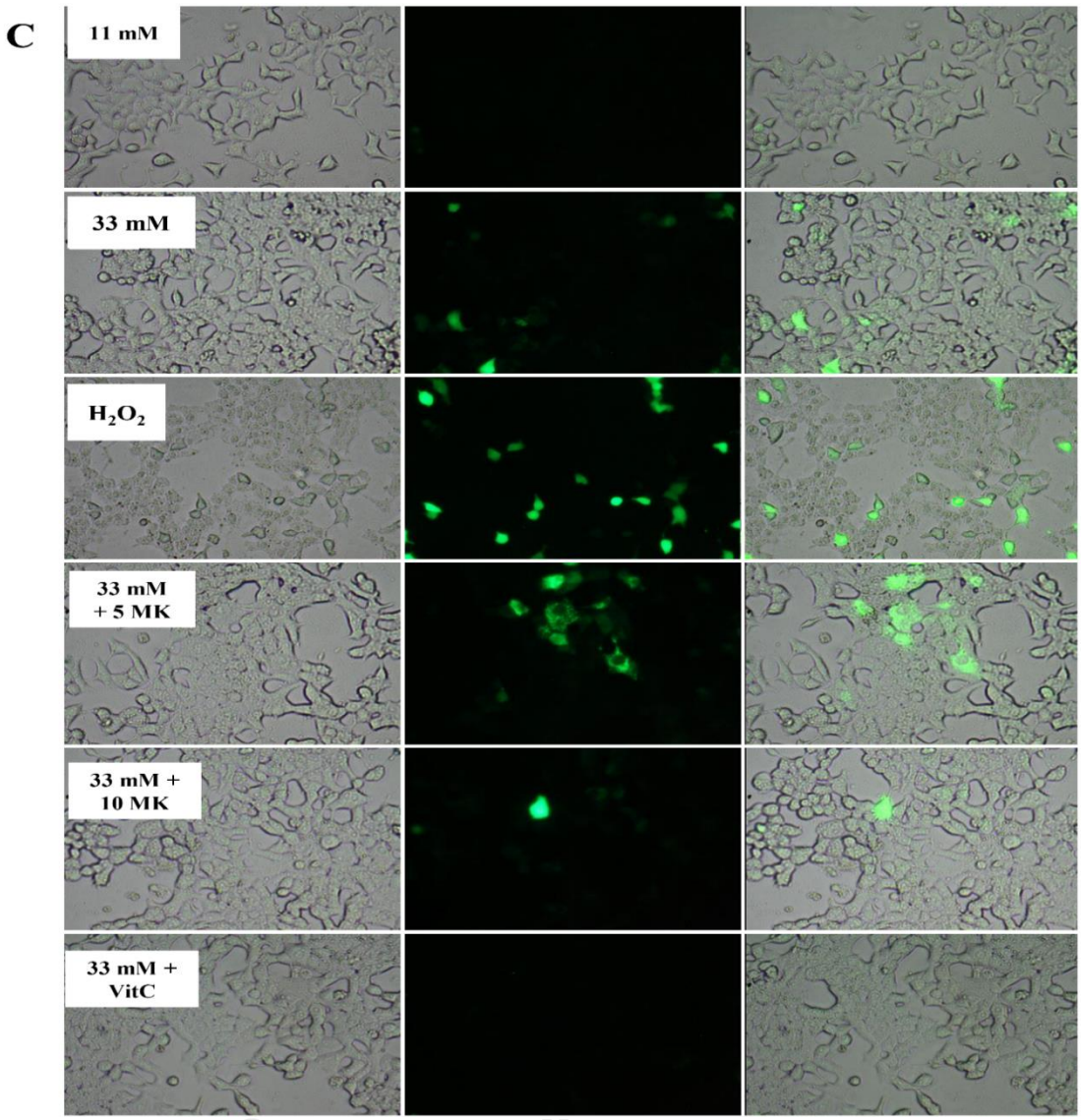

Figure 11: Mahanine reduces intracellular ROS generation in high glucose (33 mM) - treated RIN-m5F pancreatic beta cells.

(A) Effect of high glucose on intracellular ROS generation in RIN-m5F pancreatic beta cells. (B) Effect of mahanine (MK) on intracellular ROS generation in 33 mM glucose treated RIN-m5F pancreatic beta cells. (C) Intracellular ROS production in cells was observed under a fluorescence microscope after staining with H_2DCF-DA. Results are

presented as the mean ± SD (n=3) of three independent experiments. # P < 0.05, compared with cells exposed to maintenance glucose conditions (11mM). *P < 0.05 compared with cells exposed to high glucose conditions (33 mM).

5.1.5 Effect of mahanine involved in gene expression of insulin secretion pathway

To investigate the levels of gene expression of regulators of the insulin secretion pathway, mRNA levels of insulin transcription factor PDX-1, preinsulin (PRE-INS), glucose transport 2 (GLUT2), and glucokinase (GCK) were determined by qPCR. RNA of RIN-m5F was collected after exposure to maintenance glucose conditions (11mM) or high glucose conditions (33mM) and co-treatment for 48 hour with or without mahanine treatment. The result are shown in Figure 12. The 33 mM glucose treatment group significantly downregulated transcription levels of regulatory genes in the insulin secretory pathway as compared to the maintenance glucose conditions (11 mM). The 11 mM glucose treatment group showed no statistically significant difference in the expression of target genes after treatment with 5 or 10 μM mahanine. However, under 33 mM glucose, 5 and 10 μM mahanine significantly increased expression of PDX-1, PRE-INS, GLUT2, and GCK gene as compared with the 11 mM maintenance glucose condition. These results indicate that mahanine can ameliorated beta cells function in high glucose induced beta cells damage. We next analyzed the expression profile of the NOX family genes which are potential sources of ROS production in pancreatic beta cells. Real time RT-PCR showed the expression of NOX1 and NOX4 were significantly increased in expression in

high glucose treated cells Figure 12E and 12F. Importantly, in high glucose treated cells NOX1 and NOX4 were significantly decreased in the mahanine co-treatment groups. This data demonstrates that mahanine suppresses ROS levels, reverses high glucose–induced impaired synthesis and secretion of insulin via inhibition of NADPH oxidase.

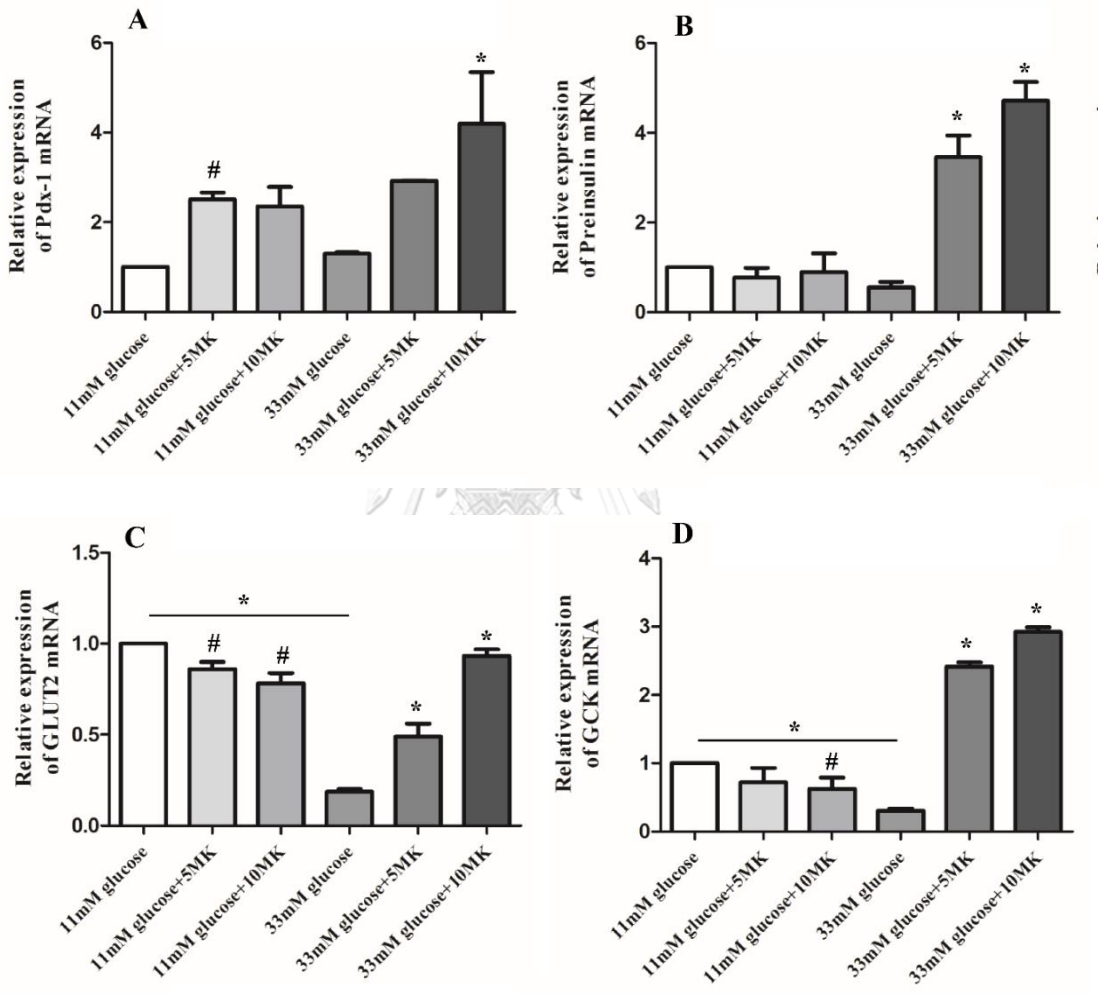

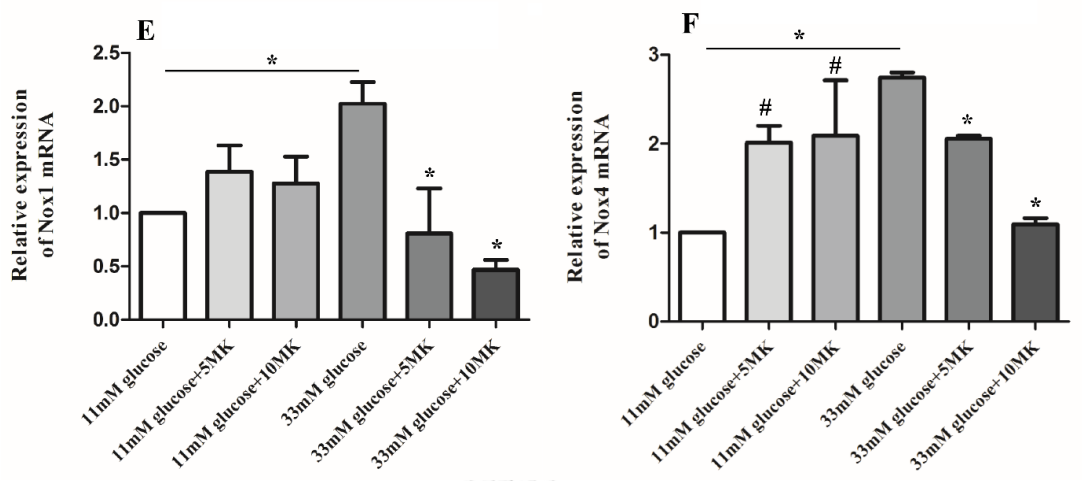

Figure 12: Relative mRNA expression gene expression of insulin secretion pathway.

Relative mRNA expression of PDX-1, PRE-INS, GLUT2, GCK, NOX1 and NOX4 at glucose doses of 11 and 33 mM with or without treatment of 5 μM (5 MK) and 10 μM (10 MK) mahanine. The data are shown as fold change compared with 11 mM glucose maintenance condition. Values are shown as mean ± SD (n = 3) of three independent experiments. The data values were analyzed by one-way ANOVA followed by Tukey's post hoc multiple comparison tests, and significantly different values are represented as # $P < 0.05$, compared with cells exposed to maintenance glucose conditions (11 mM). *$P < 0.05$ compared with cells exposed to high glucose conditions (33 mM).

5.1.6 Effect of mahanine on PDX-1 protein level and translocation

Western blot analysis and immunocytochemistry were performed to investigate the effect of mahanine on PDX-1 protein expression and translocation. Under high glucose conditions (33 mM) PDX-1 protein level was significantly decreased as compared to cells treated the maintenance glucose condition (11 mM). PDX-1 protein level in maintenance condition and co-treatment with mahanine at 5 or 10 μM showed no

statistically significant difference. In high glucose condition co-treatment with mahanine, PDX-1 protein showed a significant increase Figure 13A and 13B. Translocation of PDX-1 was determined using a confocal microscope. In the high glucose condition, PDX-1 was significantly translocated from the nucleus to the cytoplasm, similar to H_2O_2 treatment (positive control). Co-treatment with mahanine at 5 and 10 μM reversed the translocation of PDX-1 Figure 13C and 13D. This result indicates that mahanine is able to restore PDX-1 protein levels under high glucose conditions. Moreover, mahanine increased PDX-1 translocation from the cytoplasm to the nucleus leading to PDX-1 gene expression and finally increased insulin secretion.

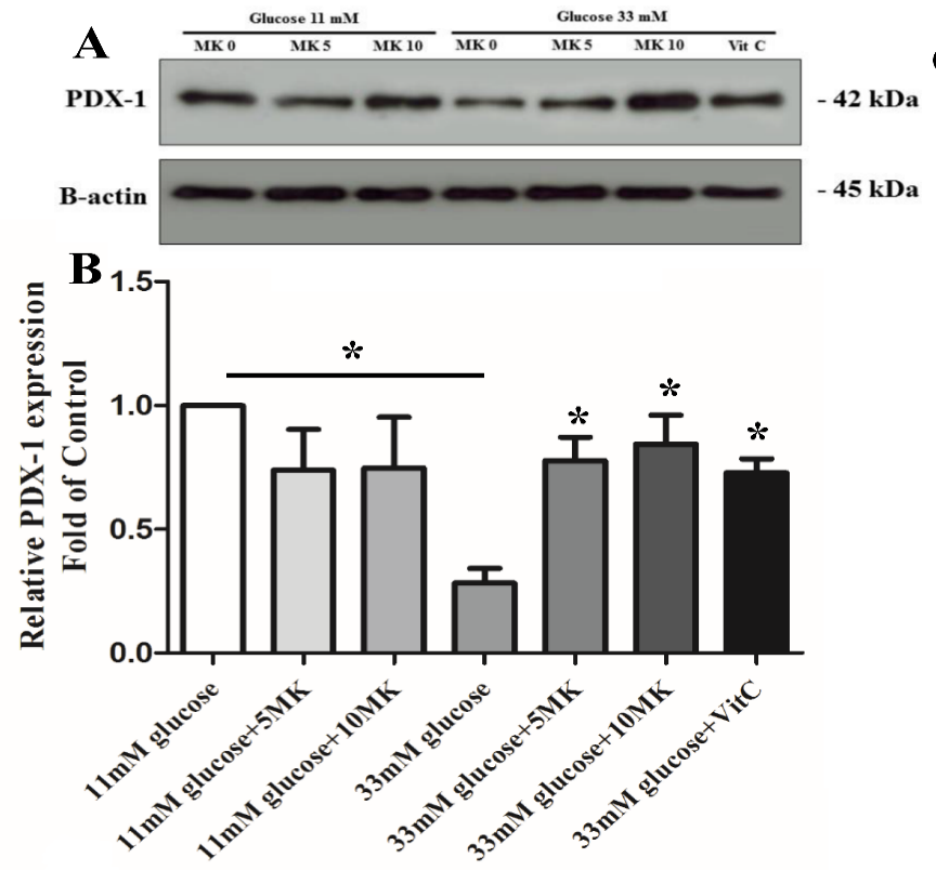

C

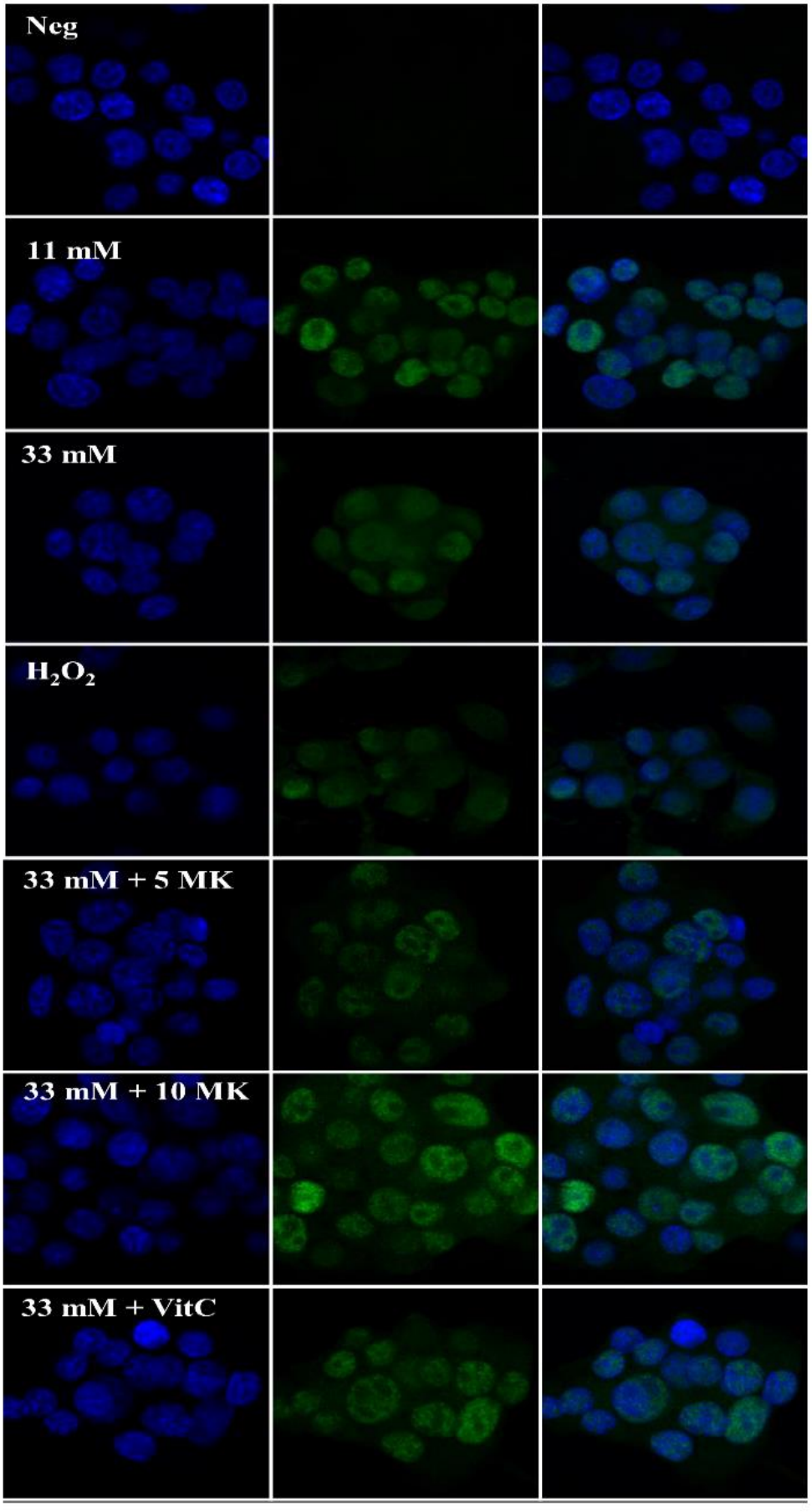

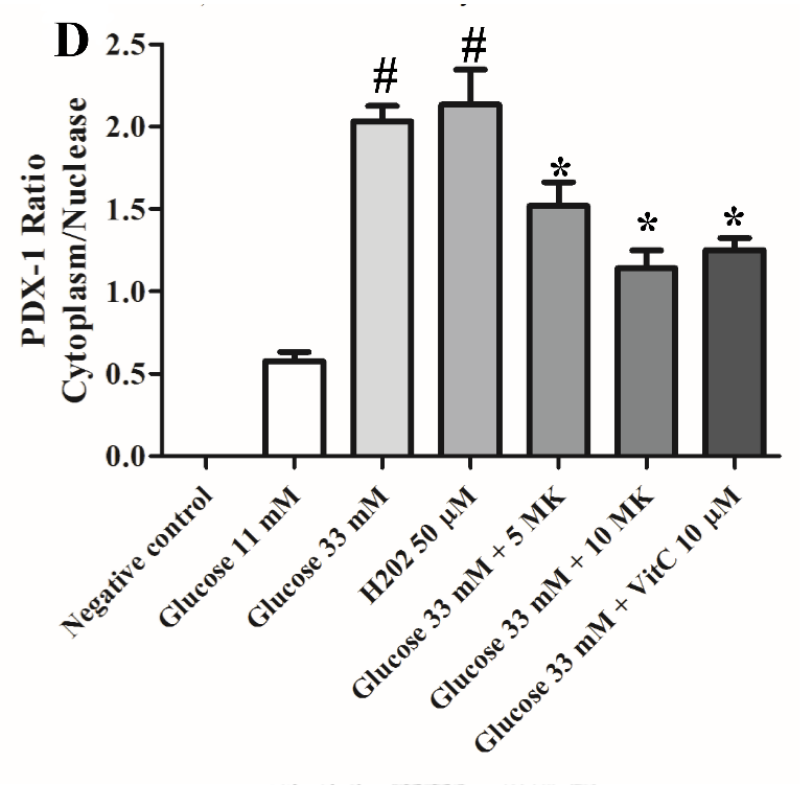

Figure 13: Western blot analysis of PDX-1. RIN-m5F cells were incubated with glucose at 33 mM or vehicle for 48 h.

Cells were incubated with mahanine (MK) at different concentrations for 2 h before stimulation with glucose at 25 mM (the data are shown from three independent experiments). Each lane contained cell extracts (30 µg protein) (A). A 10% gel was used for detecting PDX-1 and beta-actin (top and bottom). (B) Quantification of PDX-1 protein expression. Molecular mechanisms involved in PDX-1 of pancreatic beta cells induced glucose 11 and 33 mM with or without the treatment mahanine (MK) stimulated the PDX-1 translocation glucose dose of 11 and 33 mM with or without the treatment of 5 µM (5 MK) and 10 µM (10 MK) mahanine (C&D). The values are presented as the cytoplasm/nuclear ratio. # $P < 0.05$, compared with cells exposed to maintenance

glucose conditions (11mM). *P < 0.05 compared with cells exposed to high glucose conditions (33mM).

5.1.7 Effect of mahanine to maintained the glucose-stimulated insulin secretion (GSIS) potential of RIN-m5F pancreatic beta cells chronically exposed to high glucose levels

To confirm the effect of mahanine on PDX-1 nuclear translocation, insulin gene expression and secretion, an ELISA was performed. Insulin secretion was significantly decreased by around 50% under high glucose conditions as compared to the maintenance glucose conditions. When co-treated with 5 and 10 μM of mahanine, no effect was observed under maintenance glucose conditions. However, under high glucose conditions co-treatment with mahanine 10 μM and vitamin C (positive control) showed a significant increase in insulin secretion as compared to 33 mM glucose treated group. This data suggests that mahanine is able to restore the effect of insulin secretion, under high glucose conditions, but has no effect on insulin secretion under maintenance glucose conditions.

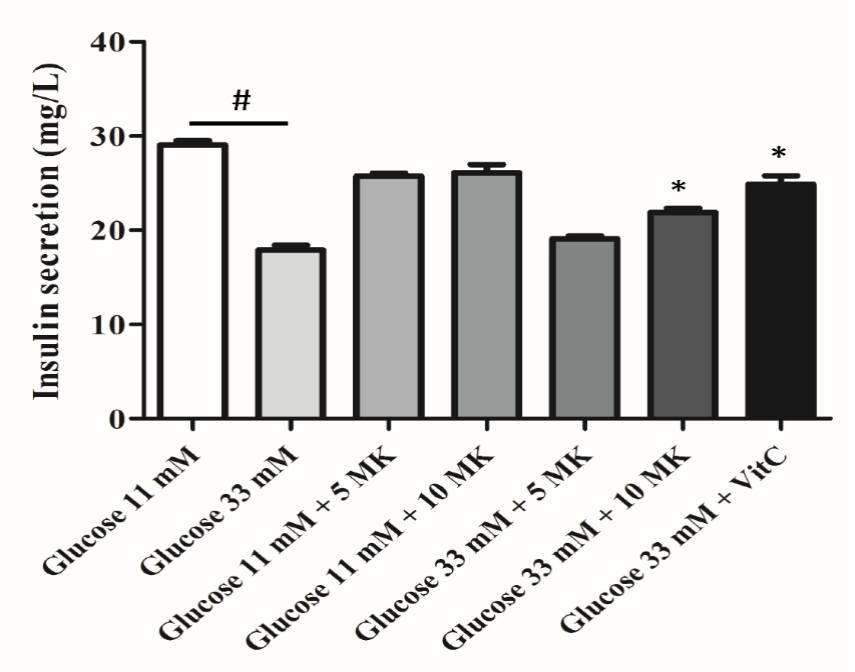

Figure 14: The effect of mahanine on maintenance glucose conditions (11 mM glucose) and high glucose conditions (33 mM glucose) stimulated insulin secretion.

The supernatant was collected for measurement of secreted insulin using a high range rat insulin ELISA kit .Each value is expressed as mean± SD (n=3). # P < 0.05, compared with cells exposed to maintenance glucose condition (11mM). *P < 0.05 compared with cells exposed to high glucose conditions (33mM).

5.2 Investigation for the hypoglycemic effect of herbal extract through inhibition of α-glucosidase and α-amylase activity

5.2.1 The effect of *Murraya koenigii* and *Stevia rebuadiana* crude extraction determined *by* α- Amylase activity

Both plants have been evaluated the effect on α-Amylase activity and results were showed in table 7. Acarbose was used as the positive control. *Murraya koenigii* (1mg/mL) showed less potential on α- Amylase inhibition which inhibit 15 ± 3.6% while

Stevia rebuadiana inhibit 23 ± 4.1%. Acarbose displayed 70 ± 51% of inhibition at 0.25 mg/mL. This results concluded that crude extracts from the *Murraya koenigii* and *Stevia rebuadiana* are showed inhibition effect on α-Amylase, but may not the main mechanism. Therefore, the pattern of enzyme activity form crude extracts and pure compounds were not studied.

Table 7: the inhibitory effect of *Murraya koenigii*, and *Stevia rebuadiana* on pancreatic α-amylase activity.

The data were represented in percentage inhibition and performed in triplicate. The absorbance was recorded at 540 nm using a microplate reader. Acarbose was used as positive control.

Scientific Name	Treatment (mg/mL)	% Inhibition of α Amylase activity (Mean ± SD)
Murraya koenigii	1 mg/mL	15 ± 3.6
Stevia rebuadiana	1 mg/mL	23 ± 4.1
Acarbose	0.25 mg/mL	70 ± 5.1

5.2.2 The effect of *Murraya koenigii* and *Stevia rebuadiana* crude extraction determined by α- glucosidase activity

Evaluation of carbohydrate digestive enzyme inhibition have beneficial to diabetes mellitus patient. Therefore in table 8 showed the inhibition effect on α - glucosidase activity (maltase and sucrase). Acarbose was used as the positive control.

Murraya koenigii (1mg/mL) showed less potential α -glucosidase activity which inhibit 12 ± 2.53% of maltose enzyme and 4 ± 2.01% of sucrose enzyme while *Stevia rebuadiana* inhibit 33 ± 5.67% and 21 ± 8.45% respectively. Acarbose displayed 47 ± 2.5% inhibition of sucrose enzyme and 55 ± 0.6% at 0.25 mg/mL. This results concluded that crude extracts from the *Murraya koenigii* and *Stevia rebuadiana* are showed inhibition effect on α -glucosidase, but may not the main mechanism. Therefore, the pattern of enzyme activity form crude extracts and pure compounds were not studied.

Table 8: the inhibitory effect of *Murraya koenigii*, and *Stevia rebuadiana* on intestinal α-glucosidase (maltase and sucrase).

Intestinal α-glucosidase inhibitory activity were expressed as percentage inhibition and performed in triplicate. The absorbance was recorded at 450 nm using a microplate reader. Acarbose was used as positive control.

Scientific Name	Treatment (mg/mL)	% Inhibition of maltase activity (Mean ± SD)	% Inhibition of sucrose activity (Mean ± SD)
Murraya koenigii	1 mg/mL	12 ± 2.53	4 ± 2.01
Stevia rebuadiana	1 mg/mL	33 ± 5.67	21 ± 8.45
Acarbose	0.25 mg/mL	47 ± 2.5	55 ± 0.6

5.3 Investigation for the hypoglycemic effect of herbal extract through glucose uptake by using cultured myocytes and adipocyte

5.3.1 Cell differentiation

Skeletal myoblast were cultured in differentiation medium for 7 days. L6 cells morphologically changed in term of the placement, elongation, and fusion of mononucleated myoblasts into multinucleated myotubes as shown in Figure 15A. The expression of a myotube specific marker (myogenin) was used to evalutate myotube formation as determined by RT-PCR (data not shown). In contrast, 3T3-L1 preadipocytes differentiation to mature adipocyte cells was evaluated by lipid accumulation as assessed by Oil Red O staining. The adipocyte cells that present lipid accumulation more than 80 % positive were used for further experiments as show in Figure 15B.

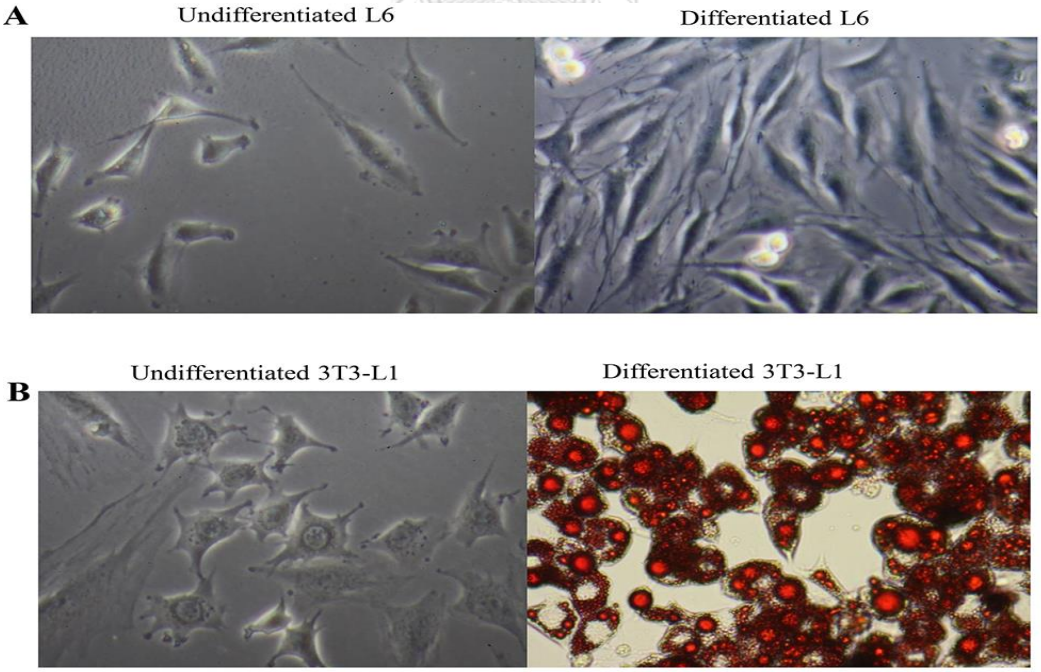

Figure 15: Differentiation of muscle myoblasts (A) and murine pre-adipocytes (B).

5.3.2 Effect of mahanine on cell viability

To determine the optimal concentration of mahanine, we assessed the viability of mahanine in L6 myotube and 3T3-L1 adipocyte cells using the MTT assay. The results of myotubes and adipocytes are shown in Figure 16A and 16B, respectively. Mahanine at a concentration up to 10 μM was appropriate to use in glucose uptake assays for both L6 myotubes and adipocytes cells because this concentration did not affect cell viability after 24 hours of treatment.

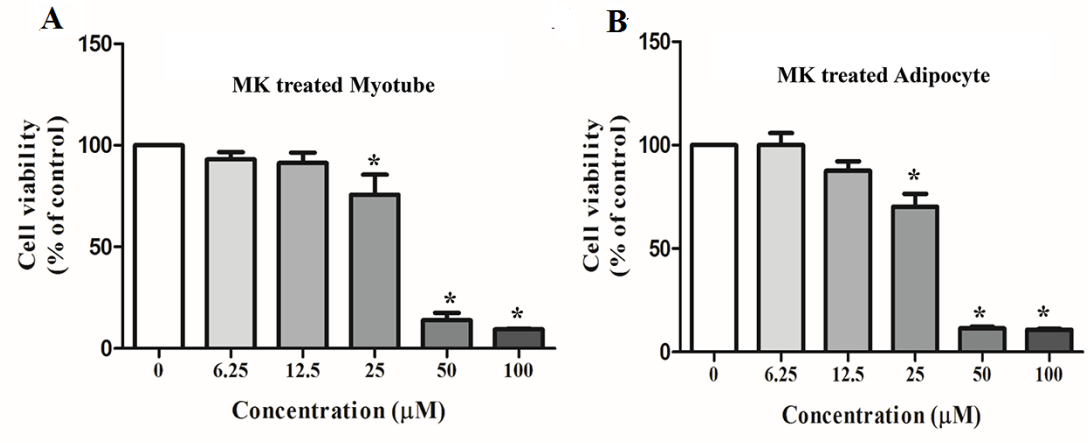

Figure 16: Myotube cells were treated with various doses of mahanine.

Myotube cells were treated with various doses of mahanine 0–100 μM for 24 h (A). Adipocyte cells were treated with various doses of mahanine 0–100 μM for 24 h (B).

5.3.3 Mahanine stimulates glucose uptake in myotubes and adipocyte cells

The effect of mahanine induced glucose uptake into the cell was determined using a fluorescent glucose analogue (2-NBDG). Differentiated myotubes and adipocytes were treated with various concentrations of mahanine for 30 min or with 0.1 μM of insulin for 15 min, then 2-NBDG uptake was measured as in a previous described

protocol [161]. The results showed that mahanine increased uptake of glucose. In myotubes, it was observed that 5 and 10 μM of mahanine increased the glucose uptake by 128.3 ± 5.4 % and 138.0 ± 8.4 %, respectively. In adipocyte cells, it was observed that glucose uptake increased by 131.0 ± 14.6 % and 180.0 ± 12.7 %, respectively when compared with control (Figure 17).

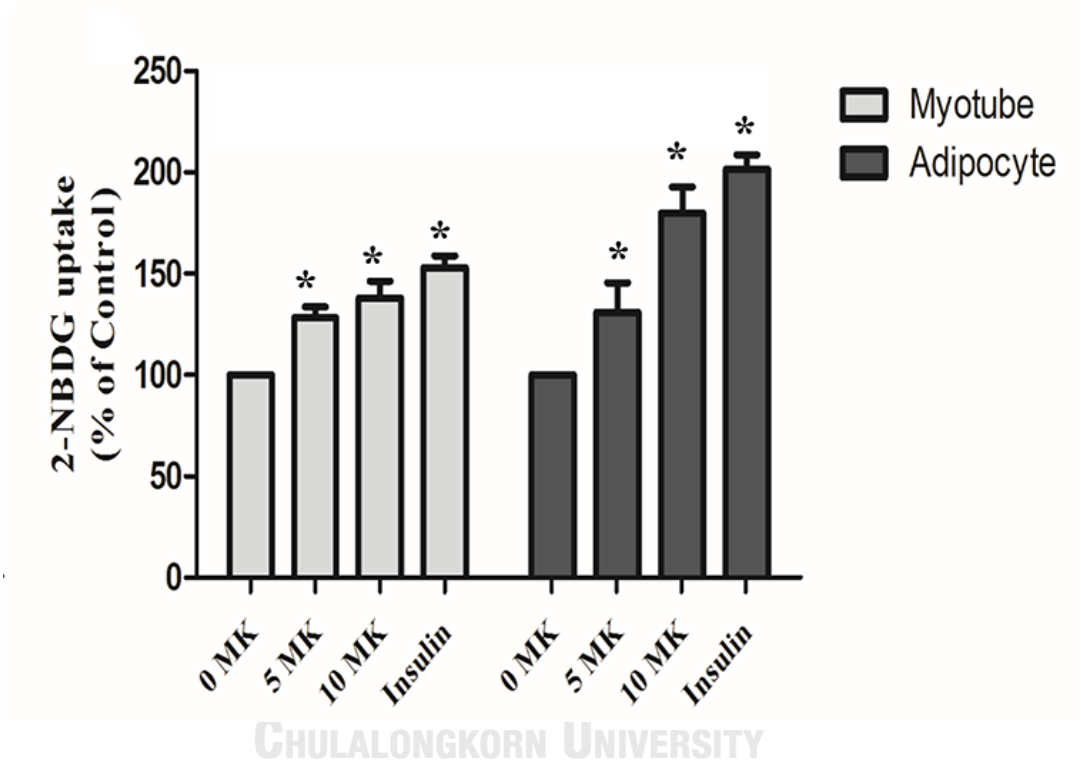

Figure 17: The effect of mahanine on 2-NBDG glucose uptake assay.

The effect of mahanine on 2-NBDG glucose uptake assay was performed in both myotube and adipocyte cell using insulin (0.1 μM) as a positive control. Data represent the mean ± standard error of five separate experiments, each performed in triplicate, *$p < 0.05$ vs. control.

5.3.4 Mahanine stimulates on GLUT4 translocation in myotubes

The effect of mahanine on GLUT4 translocation to the cell membrane was determination by western blot analysis. The results are shown in Figure 18, insulin and mahanine significantly increased GLUT4 translocation to the cell membrane as 2.06 ± 0.40 and 1.42 ± 0.07 fold of control, respectively. The Na/K ATPase, membrane protein marker and GLUT4 protein in cytosol fractions showed no significant difference when compared with the control group.

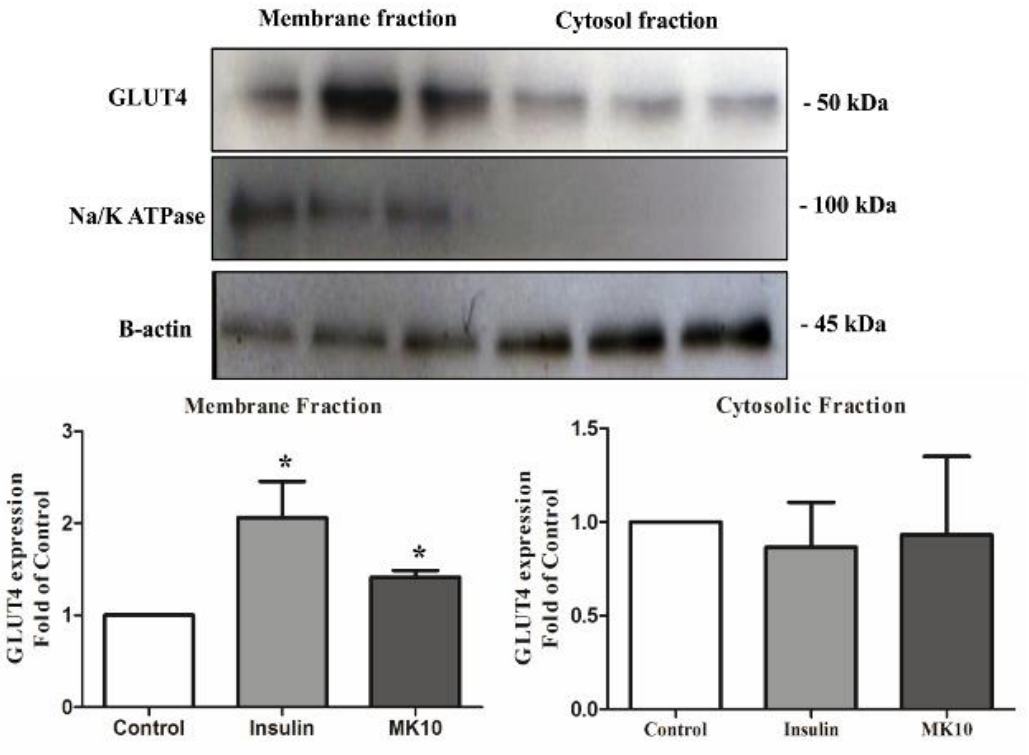

Figure 18: Effects of mahanine on GLUT4 translocation.

Myotubes were treated with 10 μM of mahanine for 30 min or 0.1 μM of insulin for 15 min. Plasma membrane and cytosolic fractions were used to assess the GLUT4 expression using western blot analysis. Treatment with 0.1 μM insulin for 15 min was

used as a positive control. Data are presented as the mean ±SD of three independent experiments. *p < 0.05, compared to the control.

5.3.5 Effects of mahanine on p-Akt, and p-AMPK protein level

5.3.5.1 p-Akt

To investigate the effect mahanine on the time-course of phosphorylated p-Akt protein level in myotube and adipocyte cells. Myotube and adipocyte cells were incubated with mahanine (10 μM) for indicated times (30, 60, 90, 120, 180 and 240 min). Then, the p-Akt protein level was assessed by western blot analysis. As illustrated in Figure 19, p-Akt protein level significantly increased at every time points of Mahanine incubation. The maximum p-Akt level was observed at 30 min. Hence based on these results, exposure to mahanine (10 μM) for 30 min will be used in other related experiments.

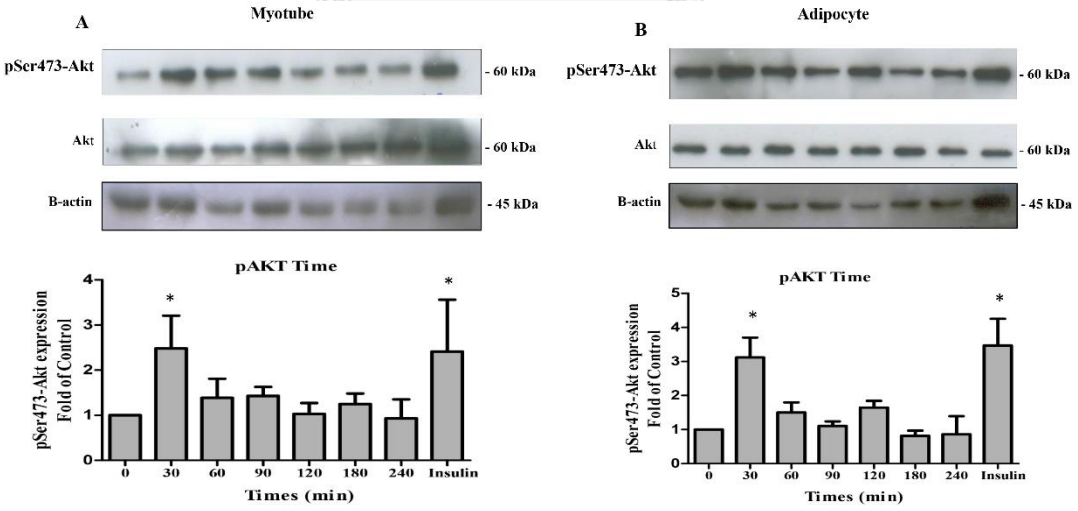

Figure 19: Effects of mahanine on p-Akt protein level.

Myotube and adipocyte cells were incubated with 10 μM mahanine for indicated times. The p-Akt protein level was measured using Western blot analysis. Total Akt

protein level was used as internal control. The values were expressed as mean ± SD from at least three separate experiments;*p<0.05 compared with control group.

5.3.5.2 p-AMPK

To investigate whether the stimulation effect of mahanine on glucose uptake was associated with the increasing of p-AMPK. Myotube and adipocyte cells were treated with mahamine at the concentration of 10 μM for indicated times (30, 60, 90, 120, 180 and 240 min). As illustrated in Figure 20, Mahanine increased p-AMPK protein level significantly increased the p-ampk protein compared with untreated group. Based on these results, exposure to mahanine (10 μM) for 240 min will be used in other related experiments.

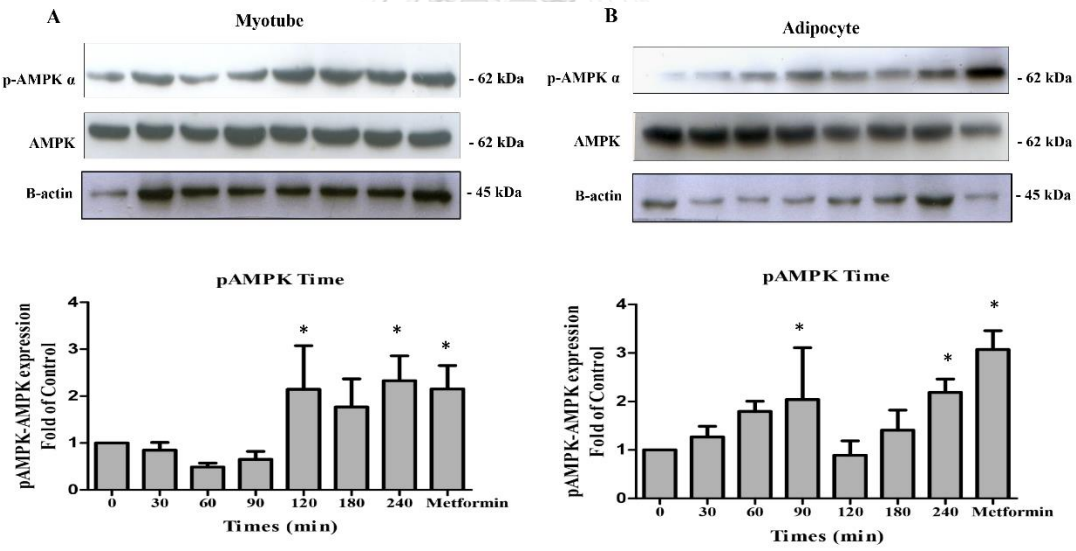

Figure 20: Effects of Mahanine on p-AMPK protein level.

Myotube and adipocyte cells were incubated with 10 μM of mahanine for indicated times. The p-AMPK protein level was measured using western blot analysis. Total AMPK protein level was used as internal control. The values were expressed as

mean ± SD from at least three separate experiments; * $p^{<}0.05$ compared with control group.

5.3.6 Mahanine stimulates glucose uptake through the Akt pathway

The involvement of mahanine in insulin-signaling pathways was examined next. The previous experiment showed that mahanine promoted 2-NDBG uptake in both myotubes and adipocytes in the presence of 0.1 μM insulin ($P < 0.05$), revealing the possibility of an insulin dependent or independent pathway. Subsequent studies on the Akt pathway supported this finding as presented in Figure 21A and Figure 21B. Insulin at a concentration of 0.1 μM promoted Akt phosphorylation in both myotubes and adipocytes cells. This result is with mahanine, which significantly increased Akt phosphorylation. Moreover, the effect of mahanine and insulin were abolished by wortmanin. This suggests that the stimulation of glucose uptake induced by mahanine in both myotubes and adipocytes involves the Akt pathway.

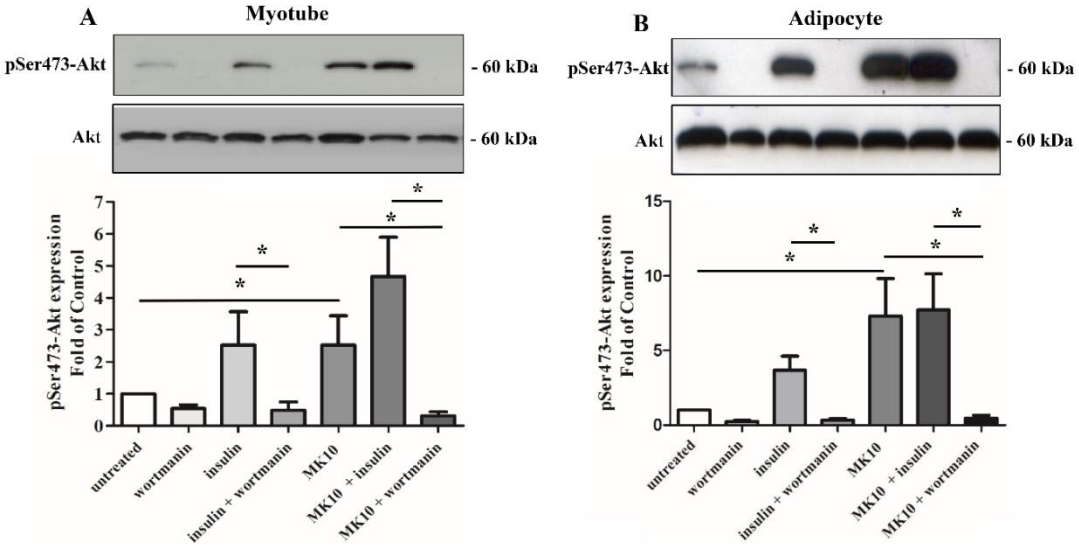

Figure 21: Effects of mahanine on the phosphorylation of Akt at Ser473 in myotube and adipocyte cells.

To study effect of mahanine on Akt signaling pathway**,** cells were treated with 10 μM of mahanine in the absence or presence of 0.1 μM of wortmanin (an Akt inhibitor). Treatment with 0.1 μM insulin for the indicated time was used as a positive control. Data are presented as the mean ±SD of three independent experiments. *$p < 0.05$, compared to the control

5.3.7 Mahanine stimulates glucose uptake is not regulated by the AMPK pathway

To study the effect of mahanine on the AMPK pathway signaling pathway, the phosphorylation levels of AMPK α at Thr172 was examined. Metformin, the AMPK activator, was used as a positive control with treatment for 2 hour [163]. Results showed that mahanine treatment showed no significant difference when compared to the untreated group, while the effect of metformin was abolished by compound C. This data suggests that mahanine stimulated glucose uptake in myotubes and adipocyte does not involve in the AMPK pathway (Figure 22A), (Figure 22B).

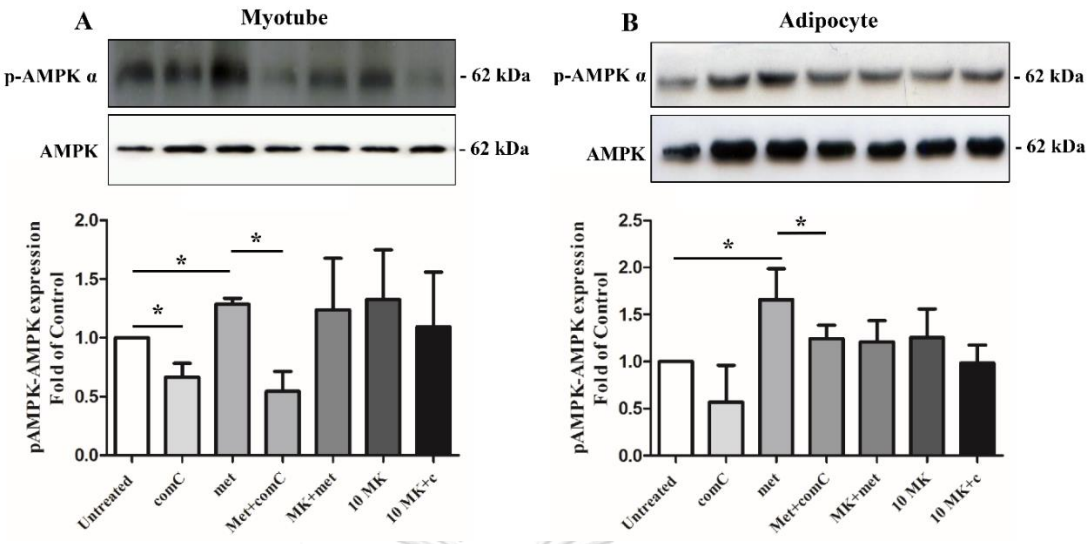

Figure 22: Effects of mahanine on the AMP-activated protein kinase AMPK α at Thr-172 in myotube and adipocyte cells.

To study the effect of mahanine on AMPK signaling pathway, cells were treated with 10 μM of mahanine in the absence or presence of 20 μM compound C (an AMPK inhibitor). Treatment with 2 mM metformin for 2 hour was used as a positive control. Data are presented as the mean ±SD of three independent experiments. *$p < 0.05$, compared to the control.

5.3.8 Effect of steviol, isosteviol and 7 β-OHisosteviol on cell viability

To determine the best concentration of steviol, isosteviol and 7 β-OHisosteviol that will be used for the further experiment. The viability of these compounds treatment were performed in L6 myotube cells using the MTT assay. The results of myotubes cell viability are shown in Figure 23, treatment with steviol, isosteviol and 7 β-OHisosteviol respectively. At a concentration up to 50 μM was appropriate for used in glucose uptake assays for L6 myotubes because this concentration did not affect cell viability after 24 hours of treatment. There for the results concluded that the substances showed highly safe to use in L6 myotube.

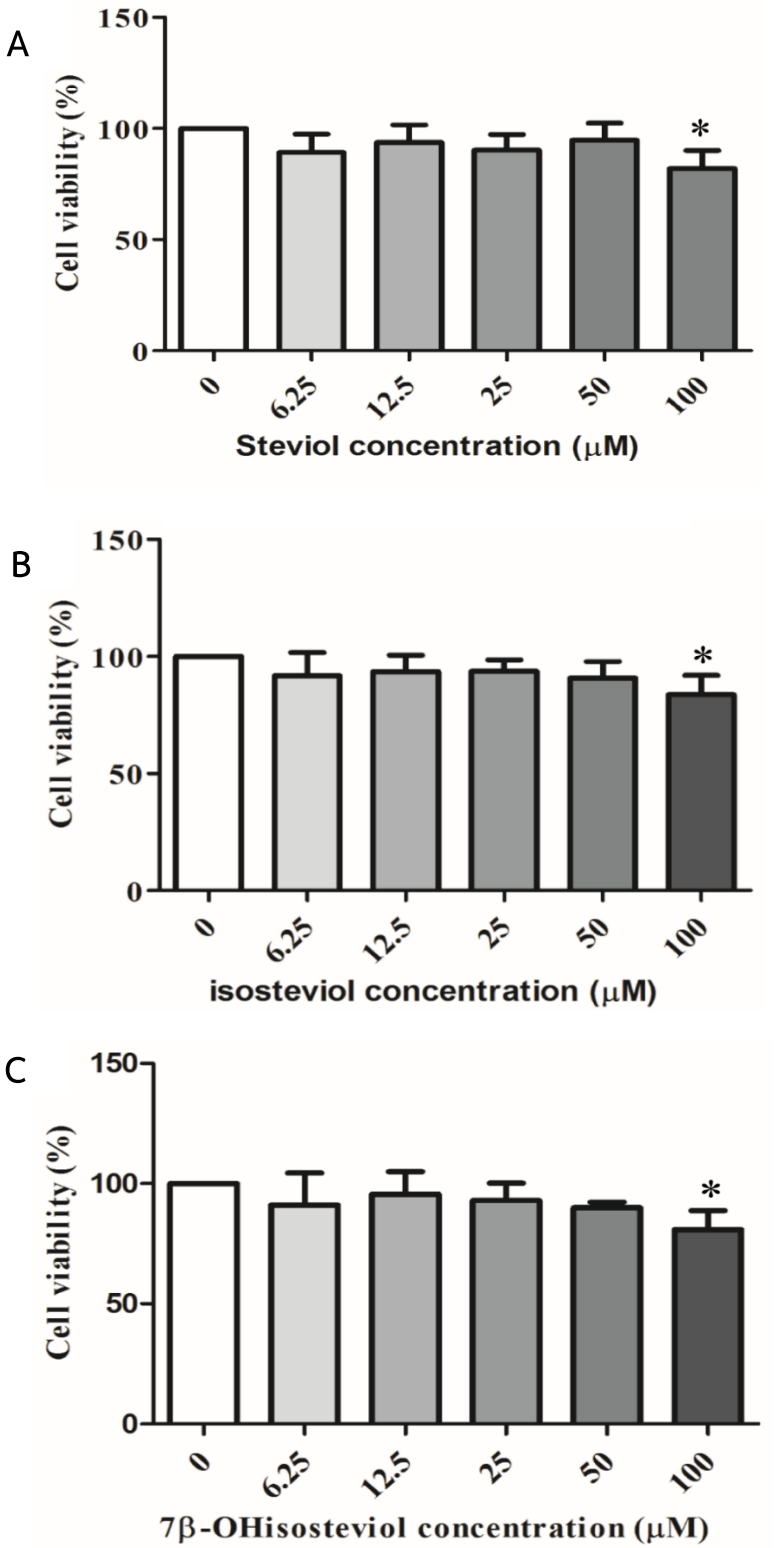

Figure 23: Myotube cells were treated with various doses of steviol, isosteviol and 7 β-OHisosteviol 0–100 μM for 24 h (A) (B) (C).

5.3.9 Steviol, isosteviol and 7 β-OHisosteviol stimulate glucose uptake in myotubes

The effect of steviol, isosteviol and 7 β-OHisosteviol induced glucose uptake into the cell was determined using a fluorescent glucose analogue (2-NBDG). Differentiated myotubes were treated with various concentrations of steviol, isosteviol and 7 β-OHisosteviol for 60 min or with 0.1 μM of insulin for 15 min, then 2-NBDG uptake was measured as a previous described protocol [161]. The results showed that steviol, isosteviol and 7 β-OHisosteviol increased glucose uptake. At the same concentration, it was observed that 50 μM of three compounds increased the glucose uptake by 174.3 ± 4.5%, 175.2 ± 11.0% and 169.8 ± 4.9% ,respectively when compared with control (Figure 24).

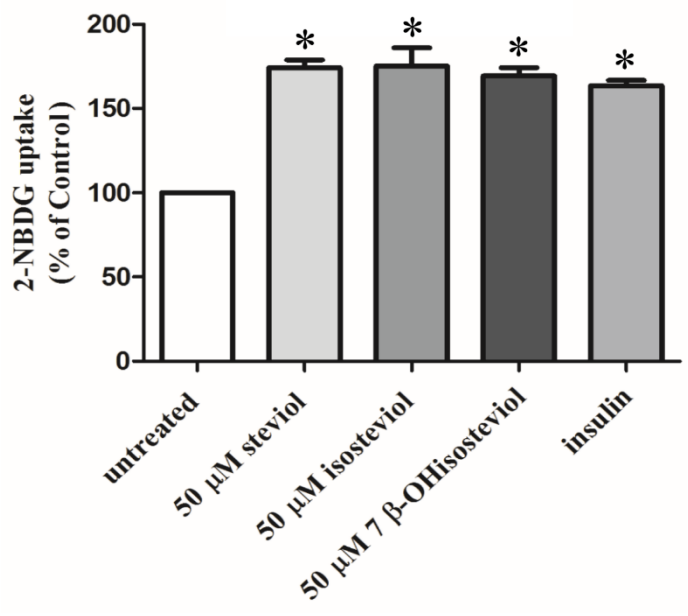

Figure 24: The effect of steviol, isosteviol and 7 β-OHisosteviol on 2-NBDG glucose uptake assay.

The effect of steviol, isosteviol and 7 β-OHisosteviol (50 μM) on 2-NBDG glucose uptake assay was performed in myotube cell using insulin (0.1 μM) as a positive control. Data represent the mean ± standard error of five separate experiments, each performed in triplicate, *p < 0.05 vs. control

5.3.10 Steviol, isosteviol and 7 β-OHisosteviol stimulate on GLUT4 translocation in myotubes

The effect of steviol, isosteviol and 7 β-OHisosteviol on GLUT4 translocation to the cell membrane was determination by western blot analysis. The results are shown in Figure 25, insulin, steviol, isosteviol and 7 β-OHisosteviol significantly increased GLUT4 translocation to the cell membrane as 2.73 ± 0.86, 2.11 ± 0.45, 2.58 ± 0.12, and 2.13 ± 0.28 fold of control, respectively. The total GLUT4 showed no significant difference when compared with the control group.

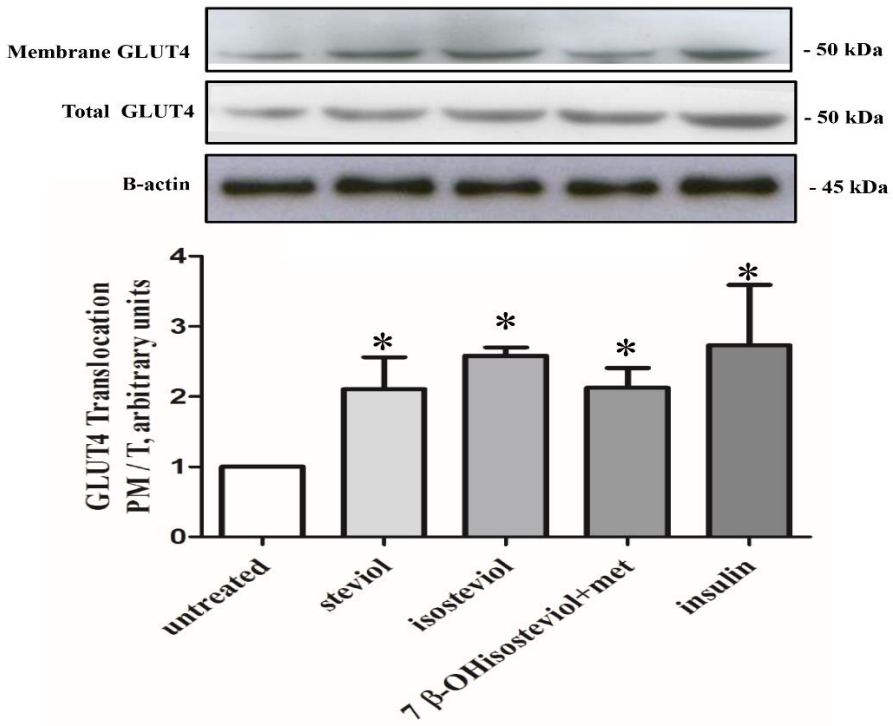

Figure 25: Effects of steviol, isosteviol and 7 β-OHisosteviol on GLUT4 translocation.

Myotubes were treated with 50 μM of three compounds for 60 min or 0.1 μM of insulin for 15 min. Plasma membrane and total GLUT4 ratio were used to assess the GLUT4 expression using western blot analysis. Treatment with 0.1 μM insulin for 15 min was used as a positive control. Data are presented as the mean ± SD of three independent experiments. *$p < 0.05$, compared to the control.

5.3.11 Steviol, isosteviol and 7 β-OHisosteviol stimulate glucose uptake is not regulated by the Akt pathway

To study the effect of steviol, isosteviol and 7 β-OHisosteviol on the Akt signaling pathway, the phosphorylation levels of Akt at Ser473 was examined. Insulin, the Akt activator, was used as a positive control with treatment for 15 min [163]. Results showed that steviol, isosteviol and 7 β-OHisosteviol treatment showed no significant difference when compared to the untreated group. This data suggests that steviol, isosteviol and 7 β-OHisosteviol stimulated glucose uptake in myotubes do not involve in the Akt pathway (Figure 26A), (Figure 26B), (Figure 26C).

A

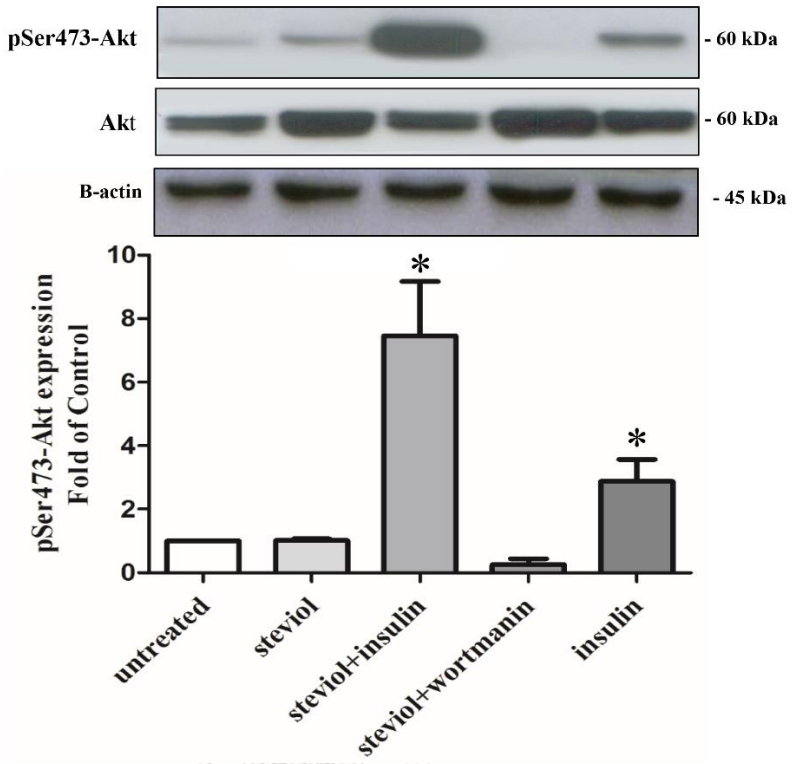
pSer473-Akt
- 60 kDa
Akt
- 60 kDa
B-actin
- 45 kDa
pSer473-Akt expression
Fold of Control
10
8
6
4
2
0
*
*
untreated
steviol
steviol+insulin
steviol+wortmanin
insulin

B

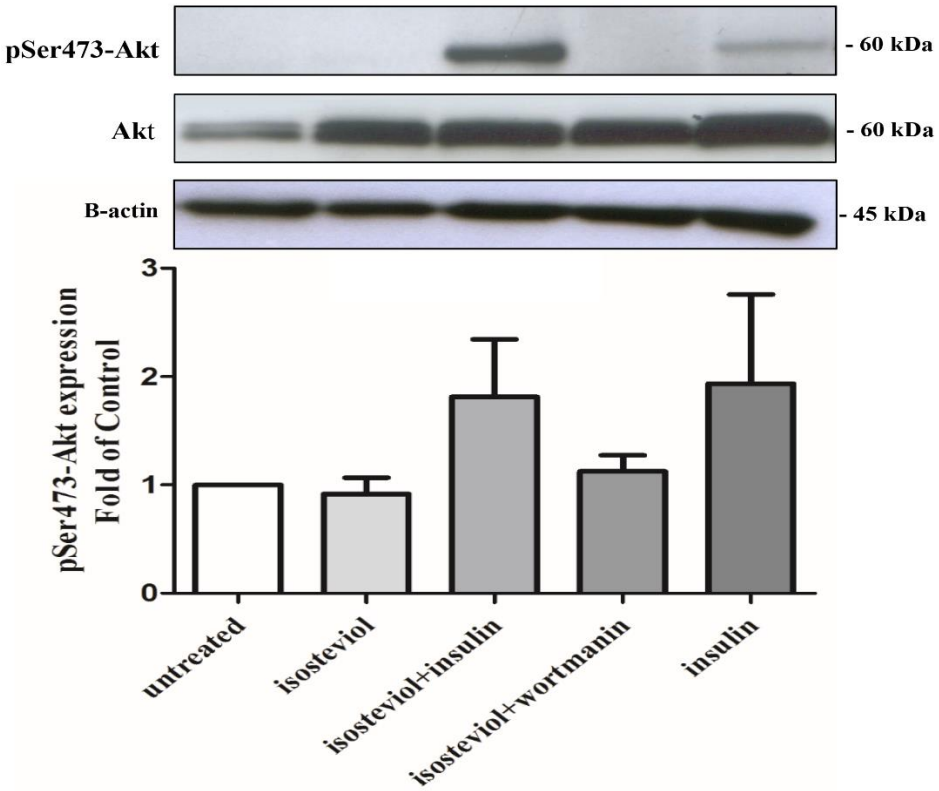
pSer473-Akt
- 60 kDa
Akt
- 60 kDa
B-actin
- 45 kDa
pSer473-Akt expression
Fold of Control
3
2
1
0
untreated
isosteviol
isosteviol+insulin
isosteviol+wortmanin
insulin

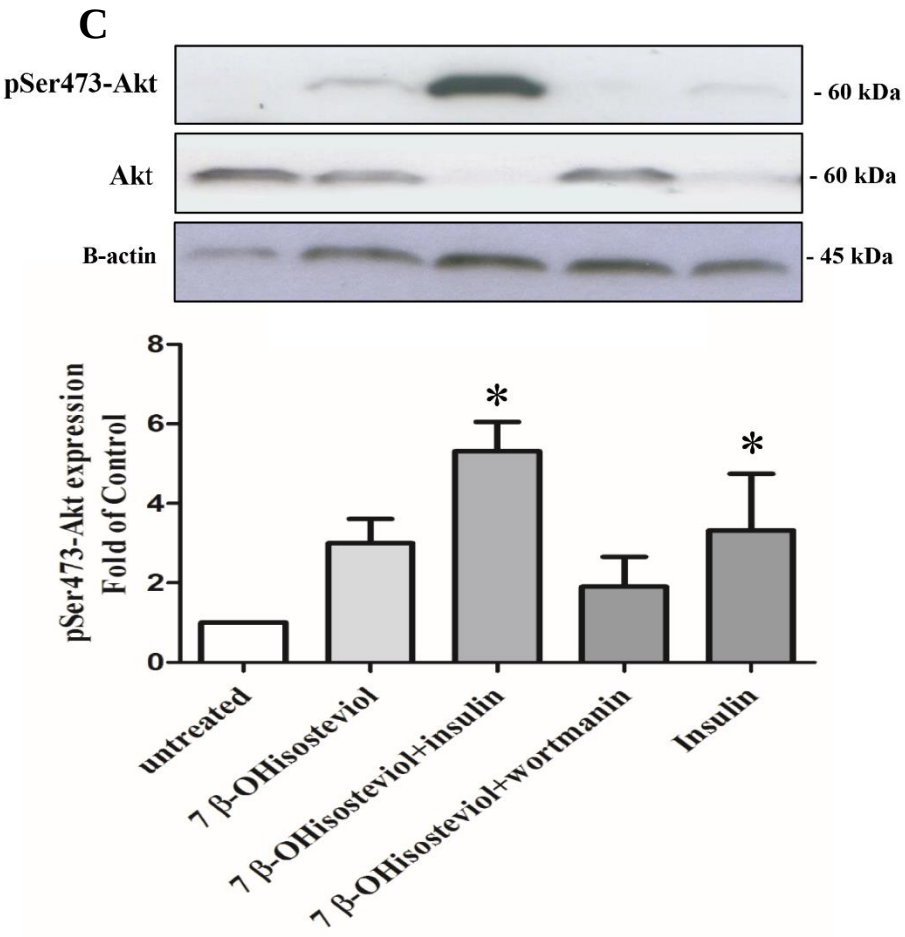

Figure 26: Effects of steviol, isosteviol and 7 β-OHisosteviol on the phosphorylation of Akt at Ser473 in myotube cells.

To study effect of steviol, isosteviol and 7 β-OHisosteviol on Akt signaling pathway**,** cells were treated with 50 μM of steviol, isosteviol and 7 β-OHisosteviol in the presence of 0.1 μM of wortmanin (an Akt inhibitor). Treatment with 0.1 μM insulin for the indicated time was used as a positive control. Data are presented as the mean ± SD of three independent experiments. *$p < 0.05$, compared to the control.

5.3.12 Steviol, isosteviol and 7 β-OHisosteviol stimulate glucose uptake is not regulated by the AMPK pathway

To study the effect of steviol, isosteviol and 7 β-OHisosteviol on the AMPK pathway signaling pathway, the phosphorylation levels of AMPK α at Thr172 was examined. Metformin, the AMPK activator, was used as a positive control with treatment for 2 hour [163]. Results showed that steviol, isosteviol and 7 β-OHisosteviol treatment showed no significant difference when compared to the untreated group. This data suggests that steviol, isosteviol and 7 β-OHisosteviol stimulated glucose uptake in myotubes do not involve the AMPK pathway (Figure 27A), (Figure 27B), (Figure 27C).

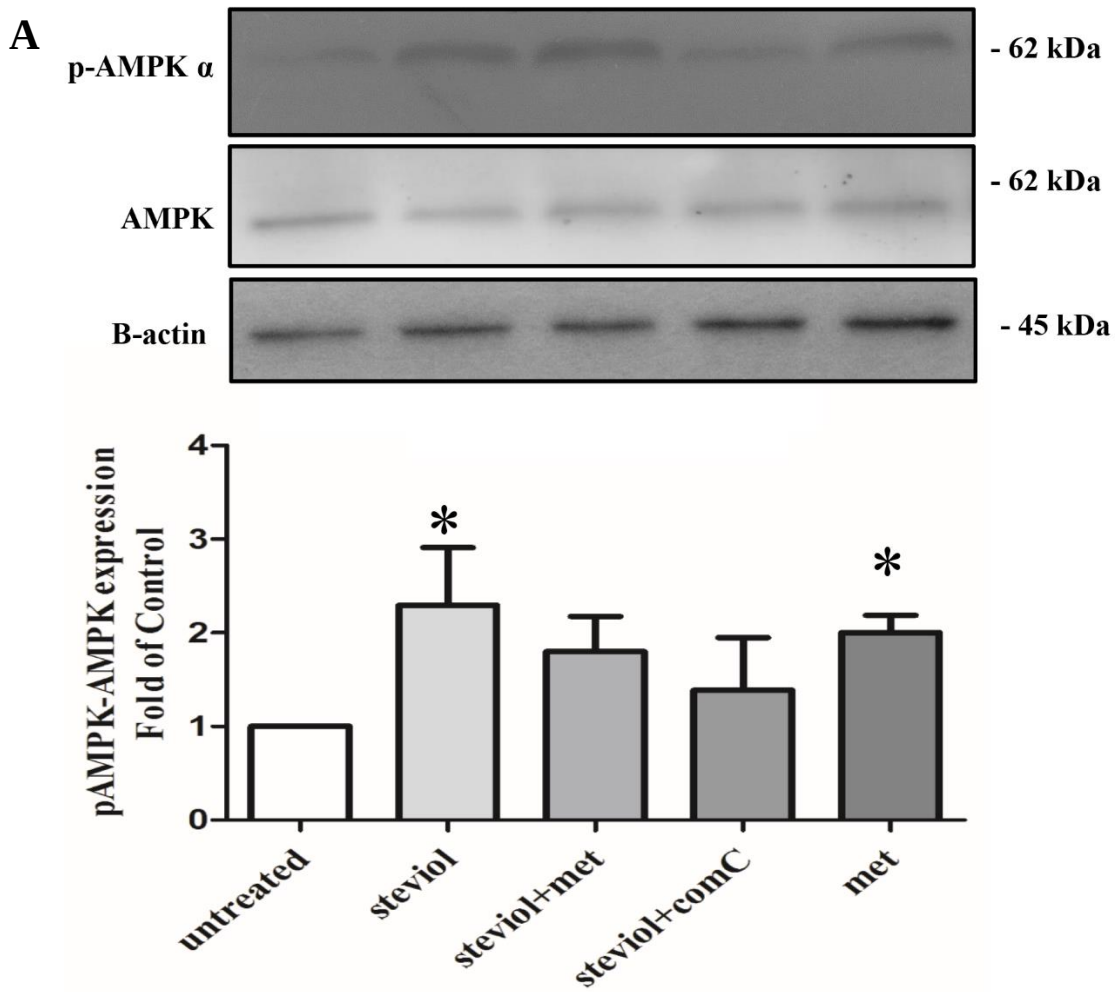

B

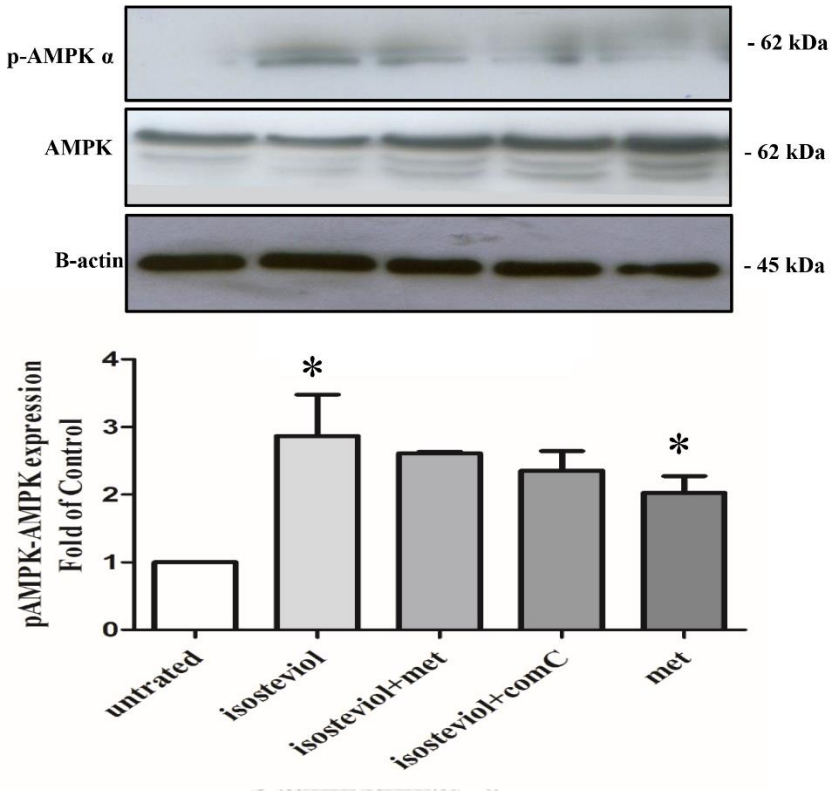
p-AMPK α
- 62 kDa
AMPK
- 62 kDa
B-actin
- 45 kDa
pAMPK-AMPK expression
Fold of Control
0
1
2
3
4
*
*
untrated
isosteviol
isosteviol+met
isosteviol+comC
met

C

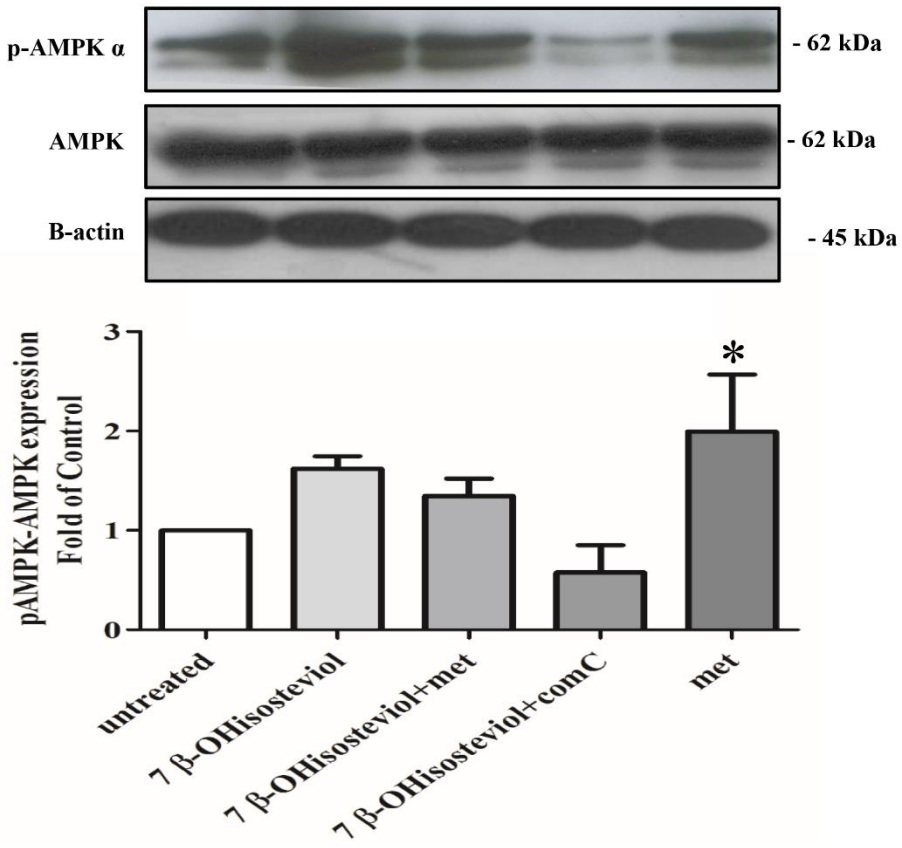
p-AMPK α
- 62 kDa
AMPK
- 62 kDa
B-actin
- 45 kDa
pAMPK-AMPK expression
Fold of Control
0
1
2
3
*
untreated
7 β-OHisosteviol
7 β-OHisosteviol+met
7 β-OHisosteviol+comC
met

Figure 27: Effects of steviol, isosteviol and 7 β-OHisosteviol on the AMP-activated protein kinase AMPK α at Thr-172 in myotube.

To study the effect of steviol, isosteviol and 7 β-OHisosteviol on AMPK signaling pathway, cells were treated with 50 μM of three compounds in the absence or presence of 20 μM compound C (an AMPK inhibitor). Treatment with 2 mM metformin for 2 hour was used as a positive control. Data are presented as the mean ± SD of three independent experiments. *$p < 0.05$, compared to the control.

5.4 Investigation for the antihyperglycemic mechanisms of bioactive compounds from Murraya koenigii related anticancer

5.4.1 Expression profiles of MITF and GLI1 in hepatocellular carcinoma

The findings with the hepatic cancer cell lines suggest that MITF expression may be differentially regulated, depending on the microenvironment of hepatocellular carcinoma and cholangiocarcinoma cells. Accordingly, we immunohistochemically analyzed the expression profiles of MITF in hepatocellular carcinoma and cholangiocarcinoma of the human liver cancer tissue array. Because we used two separate tissue arrays containing the same series of cancer specimens, it is not necessarily possible to analyze the consecutive tissue sections. GLI1 expression was also analyzed as a poor prognosis marker of hepatocellular carcinoma [164]. Figure 28 shows representative tissue sections of one hepatocellular carcinoma that was negative for both MITF and GLI1 immunoreactivities (tissue sections of panel A) and one sample that was positive for both MITF and GLI1 immunoreactivities (tissue sections of panel

B). Notably, MITF and GLI1 immunoreactivities were consistently detected in cytoplasm, but not detectable in cell nuclei.

The immunohistochemical analysis of 38 hepatocellular carcinoma specimens revealed the two groups of carcinoma (Table 9): cancer cells with undetectable MITF immunoreactivity (n = 32, 84%) and those with detectable MITF immunoreactivity (n = 6, 16%). Thus, MITF was expressed below the immunologically detectable levels in most cases of hepatocellular carcinoma. Importantly, three of the six MITF-positive hepatocellular carcinomas were categorized as poorly differentiated histology (50%), whereas eight of 32 MITF-negative hepatocellular carcinomas (25%) were categorized as poorly differentiated histology (Table 9). Thus, MITF immunoreactivity is associated with poor prognosis in patients with hepatocellular carcinoma (Table 9).

On the other hand, GLI1 immunoreactivity was detected in 55% of hepatocellular carcinoma specimens (21 out of 38 specimens) and undetectable in 45% specimens (17 out of 38 specimens; Table 10). Moreover, GLI1-positive hepatocellular carcinoma specimens showed poorly differentiated phenotypes (Table 10), whereas all of GLI1-negative hepatocellular carcinoma specimens showed moderately differentiated phenotypes. These results support the implication of GLI1 expression as a poor prognosis marker [164].

Importantly, MITF immunoreactivity was detected only in GLI1-positive hepatocellular carcinoma specimens (6 out of 21 GLI1-positive specimens, 29%; Table 11); namely, MITF immunoreactivity was undetectable in most of GLI1-positive

hepatocellular carcinoma (n = 15, 71%). These results are consistent in part with the notion that MITF expression is associated with poor prognosis in hepatocellular carcinoma. MITF expression may be correlated to GLI1 expression in a subset of hepatocellular carcinoma (Table 11). In other words, GLI1 may differentially influence MITF expression, depending on the microenvironment of hepatocellular carcinoma cells.

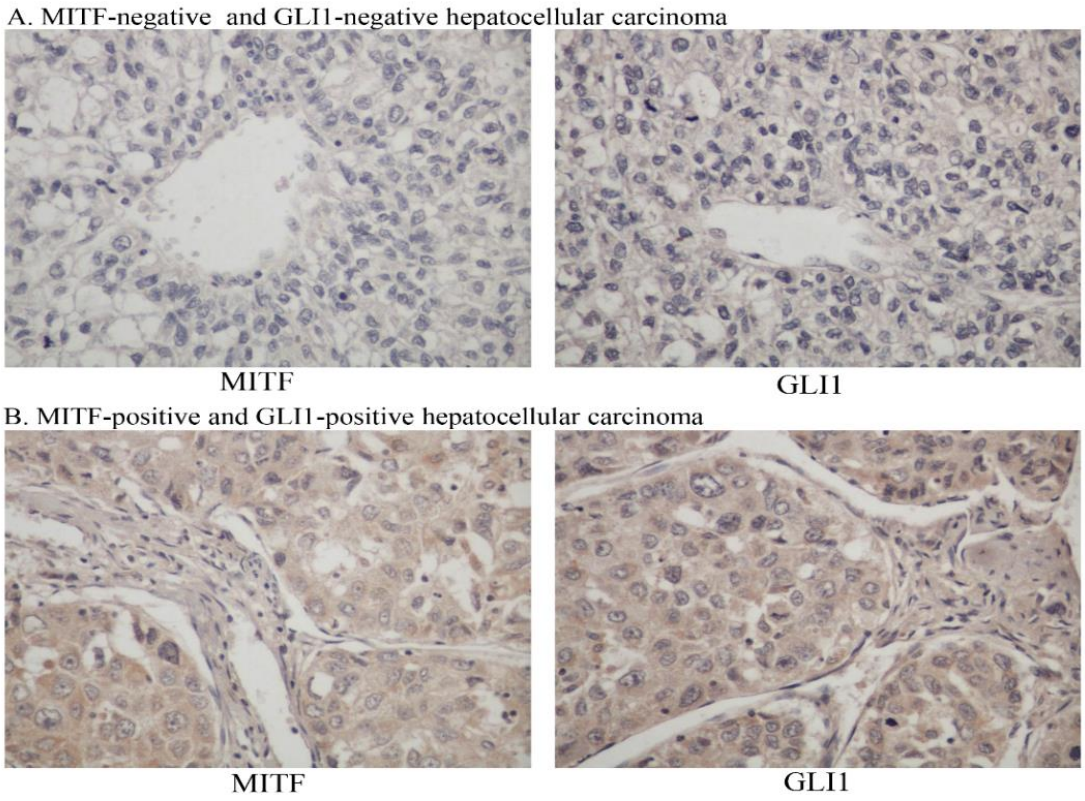

Figure 28: Expression profiles of immunoreactive MITF and GLI1 in hepatocellular carcinoma.

(A) One representative hepatocellular carcinoma specimen that is negative for MITF immunoreactivity (left) and GLI1 immunoreactivity (right) (magnification: x400), out of 17 double negative specimens. The presented hepatocellular carcinoma specimen was categorized as grade 2 (moderately differentiated) (see Tables 9 and 10); namely,

cells appear slightly different than normal. (B) One representative hepatocellular carcinoma specimen that is positive for MITF immunoreactivity (left) and GLI1 immunoreactivity (right) (magnification: x400), out of six double-positive specimens. The presented hepatocellular carcinoma specimen was categorized as grade 3 (poorly differentiated) (see Tables 9 and 10); namely, cells appear abnormal. Note that MITF immunoreactivity was detected only in GLI1-positive hepatocellular carcinoma.

Table 9: MITF expression in Hepatocellular Carcinoma

	MITF immunoreactivity		***P* value**
	positive (n = 6)	**negative (n = 32)**	
Age (years)*	52 ± 12	52 ± 11	0.97
Sex			
Male	6	28	
Female	0	4	0.99
Stage			
I	0	0	
II	3	16	
III	3	16	0.99
Histological grade			
1 (well)	2	0	
2 (moderate)	1	25	
3 (poor)	3	7	**0.0006**

*Data are presented as the mean ± SD. All other values represent the number of patients. P-values < 0.05 are considered to be significant, indicated bold.

Table 10: GLI1 expression in Hepatocellular Carcinoma

	GLI1 immunoreactivity		***P* value**
	positive (n = 21)	**negative (n = 17)**	
Age (years)*	52 ± 13	52 ± 9	0.60
Sex			
Male	21	13	
Female	0	4	**0.03**
Stage			
I	0	0	
II	10	9	
III	11	8	0.99
Histological grade			
1 (well)	2	0	
2 (moderate)	9	17	
3 (poor)	10	0	**0.0008**

*Data are presented as the mean ± SD. All other values represent the number of patients. P values < 0.05 are considered to be significant, indicated bold.

Table 11: Expression Profiles of MITF and GLI1 in Hepatocellular Carcinoma

	MITF immunoreactivity		***P* value**
	positive (n = 6)	**negative (n = 32)**	
GLI1 status			
positive (n = 21)	6	15	
negative (n = 17)	0	17	**0.02**

All other values represented the number of patients. P values < 0.05 are considered to be significant, indicated bold.

5.4.2 Expression profiles of MITF and GLI1 in cholangiocarcinoma specimens

We also analyzed the expression profiles of MITF and GLI1 in cholangiocarcinoma specimens (n = 7), because the Hedgehog signaling pathway is activated in cholangiocarcinoma, with GLI1 overexpression [94]. Representative tissue sections are shown in Figure 29, one cholangiocarcinoma that was negative for both MITF and GLI1 immunoreactivities (tissue sections of panel A) and one sample that was positive for both MITF and GLI1 immunoreactivities (tissue sections of panel B). MITF immunoreactivity were detected in cytoplasm of cholangiocarcinoma cells, except for a cholangiocarcinoma cell with the nuclear expression (Fig 29B). Although the sample size is small, MITF immunoreactivity was detected in two cholangiocarcinoma specimens (29%, 2 out of seven specimens). All of the seven cholangiocarcinoma specimens showed moderately differentiated phenotypes (Table 12).

GLI1 immunoreactivity was detected in six cholangiocarcinoma specimens (86%; 6 out of seven specimens) (Table 13). The clinical features of the cholangiocarcinoma patients are summarized in Tables 12 and 13. In this context, earlier reports showed that higher expression of GLI1 was associated with poor prognosis of patients with cholangiocarcinoma [94]. These results suggest that Hedgehog signaling may be aberrantly activated in most cases of cholangiocarcinoma, which is also associated with MITF expression in a subset of cholangiocarcinoma. Importantly, MITF immunoreactivity was detected in the GLI1-positive cholangiocarcinoma (Table 13), which is similar to the finding in hepatocellular carcinoma.

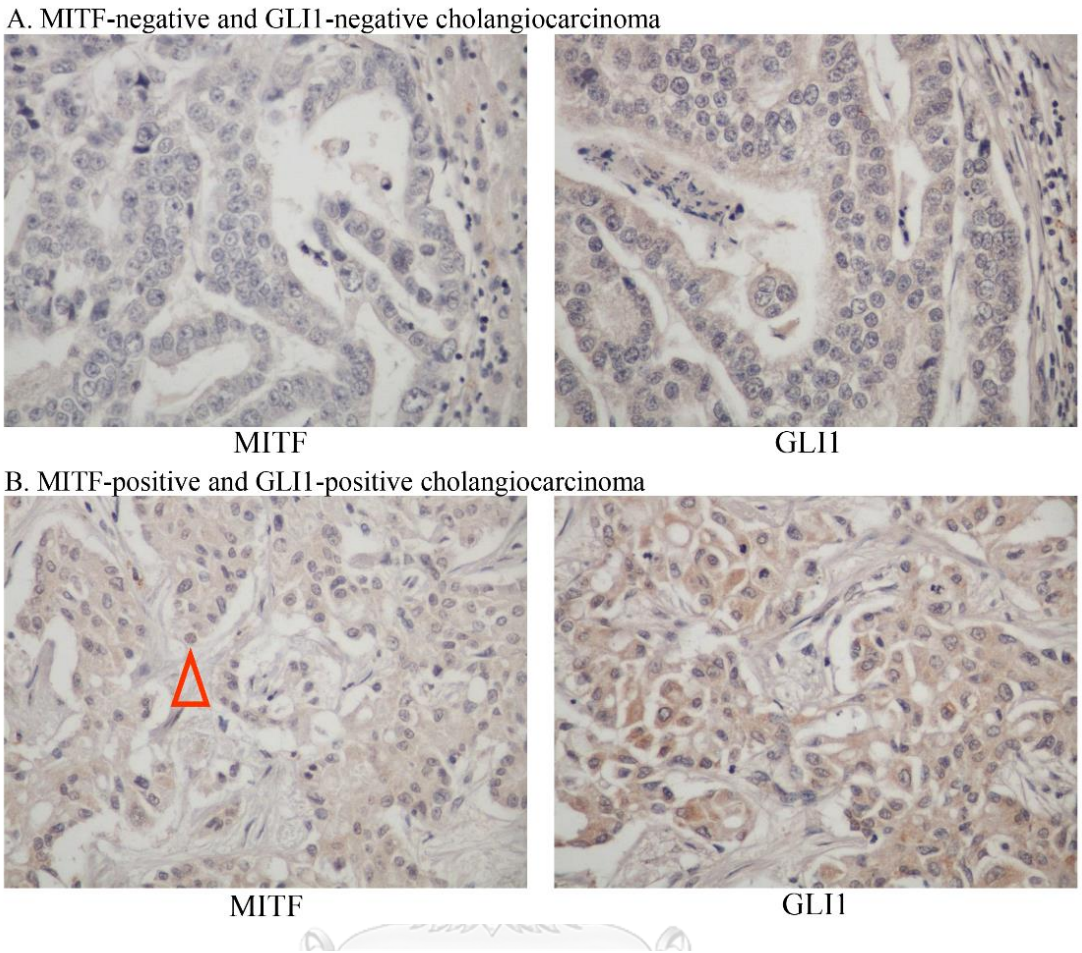

Figure 29: Expression profiles of immunoreactive MITF and GLI1 in cholangiocarcinoma.

(A) One cholangiocarcinoma specimen that is negative for MITF immunoreactivity (left) and GLI1 immunoreactivity (right) (magnification: x400). Among seven cholangiocarcinoma specimens, there was only one sample that is negative for both MITF and GLI1. (B) One cholangiocarcinoma specimen that is positive for MITF immunoreactivity (left) and GLI1 immunoreactivity (right) (magnification: x400). The tissue sections shown represent one of two cholangiocarcinoma specimens that are positive for both MITF and GLI1. Note that MITF immunoreactivity was detected in the nucleus of a single cholangiocarcinoma cell (indicated with red triangle). All of the

cholangiocarcinoma specimens were categorized as grade 2 (moderately differentiated) (see Table 12).

Table 12: MITF expression in Cholangiocarcinoma

	MITF immunoreactivity	
	positive (n = 2)	**negative (n = 5)**
Age (years)*	55	53 ± 8
Sex		
Male	1	2
Female	1	3
Stage		
I	0	0
II	0	2
III	2	3
Histological grade		
1 (well)	0	0
2 (moderate)	2	5
3 (poor)	0	0

*Data are presented as the mean ± SD. All other values represent the number of patients.

Table 13: GLI1 expression in Cholangiocarcinoma

	GLI1 immunoreactivity	
	positive (n = 6)	**negative (n = 1)**
Age (years)*	53 ± 8	55
Sex		
Male	3	1
Female	3	0
Stage		
I	0	0
II	3	0
III	3	1
Histological grade		
1 (well)	0	0
2 (moderate)	6	1
3 (poor)	0	0

*Data are presented as the mean ± SD. All other values represent the number of patients.

Table 14: Expression Profiles of MITF and GLI1 in Cholangiocarcinoma

	MITF immunoreactivity	
	positive (n = 2)	**negative (n = 5)**
GLI1 immunoreactivity		
positive (n = 6)	2	4
negative (n = 1)	0	1

All values represent the number of patients.

5.4.3 Differential effects of GANT61 on MITF expression in hepatic cancer cell lines

We previously reported that the treatment for 24 h with cyclopamine, a Hedgehog signaling antagonist, caused the induction of MITF expression in HepG2 hepatocellular carcinoma cells and HuCCT1 cholangiocarcinoma cells, but tended to decrease the MITF level in KKU-100 cholangiocarcinoma cells, as judged by Western blot analysis [[24]; data not shown]. To explore the role of the Hedgehog signaling in MITF expression, we analyzed the effects of GANT61, an inhibitor of GLI1-mediated gene transactivation, on the MITF expression in HepG2 hepatocellular carcinoma, HuCCT1 cholangiocarcinoma, and KKU-100 cholangiocarcinoma. The treatment for 24 h with GANT61 at 20 μM did not significantly influence the cell viability and MITF expression levels in these cell lines (data not shown). However, the treatment for 48 h with GANT61 at 20 μM significantly decreased the viability of HepG2 cells and HuCCT1 cells, but not KKU-100 cells (Figure 30A). Among these cell lines, HepG2 cells appeared to be more sensitive to the toxicity of GANT61, compared with HuCCT1 cells and KKU-100 cells. Importantly, the treatment for 48 h with GANT61 induced the MITF expression in HuCCT1 cells, but decreased MITF expression levels in HepG2 cells and KKU-100 cells (Figure 30B). We also analyzed expression levels of HO-1 that is an enzyme responsible for physiological heme catabolism [165], which also plays a cytoprotective role in cholangiocarcinoma cells [166]. GANT61 at 10 or 20 μM induced the expression of HO-1 in HepG2 cells, HuCCT1 cells, and KKU-100 cells, which may support the survival of

cancer cells. Because the effects of GANT61 were detected only after 48 h, we suggest that GANT61 may indirectly influence the MITF expression. Considering the seemingly consistent effects of GANT61 and cyclopamine, we assume that Hedgehog signaling may down-regulate MITF expression in HuCCT1 cholangiocarcinoma cells and may up-regulate MITF expression in KKU-100 cholangiocarcinoma cells. On the other hand, in HepG2 hepatocellular carcinoma cells, cyclopamine and GANT61 exerted the opposing effects on MITF expression, suggesting that cyclopamine or GANT61 may influence MITF expression through a mechanism that is unrelated to Hedgehog signaling. These results suggest the heterogeneity in the biological properties of hepatocellular carcinoma and cholangiocarcinoma cells.

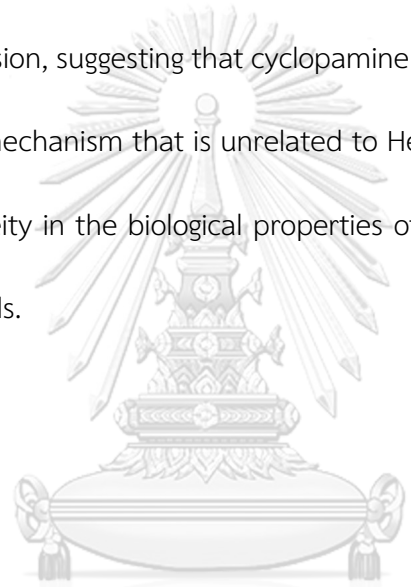

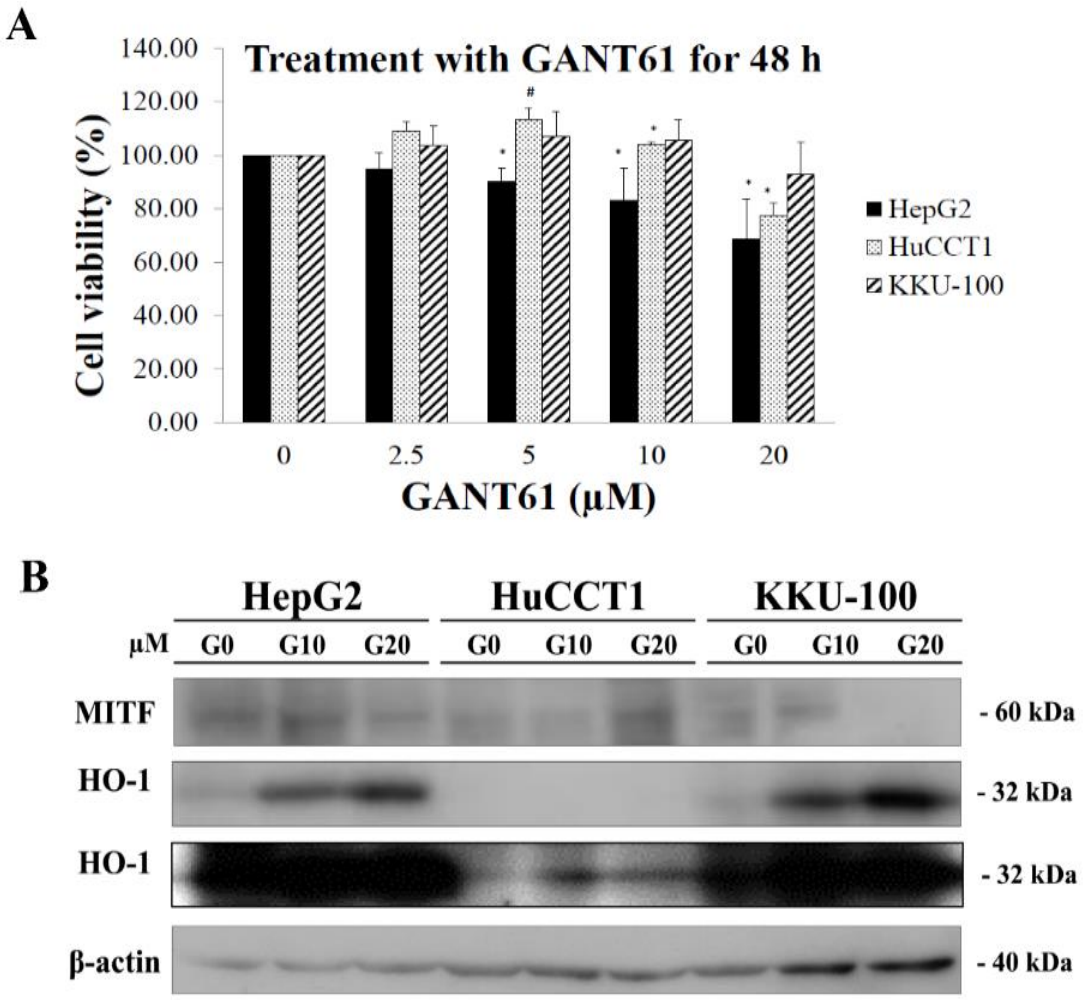

Figure 30: Induction of MITF by mahanine in hepatic malignant cells.

(A) The effect of mahanine on viability of HepG2 hepatocellular carcinoma cells and HuCCT1 and KKU-100 cholangiocarcinoma cells. Cells were incubated with mahanine at different concentrations for 24 h. MTT assay was used to determine the number of cell viability. Data represent mean ± S.D. of three independent experiments. $^{\#}P < 0.05$ compared to concurrent control. (B) Western blot analysis of MITF and HO-1. Cells were incubated with mahanine at different concentrations for 24 h. The data are shown from one of two independent experiments with similar results. Each lane contained cell

extracts (30 μg protein). Under the conditions used, MITF proteins were detected as a single band of about 60 kDa [93]. A 10% gel was used for detecting MITF and beta-actin (top and bottom).

5.4.4 Induction of MITF expression by mahanine in hepatic cancer cells

The findings with the hepatic cancer tissue array suggest that MITF may be over-expressed in subsets of hepatocellular carcinoma and cholangiocarcinoma, although MITF expression was undetectable in most of hepatocellular carcinoma and cholangiocarcinoma. To explore the cellular microenvironment that may influence MITF expression, we used three human hepatic cancer cell lines: HepG2 hepatocellular carcinoma, HuCCT1 cholangiocarcinoma, and KKU-100 cholangiocarcinoma. Among these cell lines, HuCCT1 cholangiocarcinoma cells were most resistant to cisplatin, compared with KKU-100 cholangiocarcinoma cells and HepG2 hepatocellular carcinoma cells [24]. Incidentally, KKU-100 cholangiocarcinoma cells were established from a Thai patient with liver fluke infection [167]. We therefore focused on mahanine, a carbazole alkaloid that has been used as folk medicine in Thailand. Mahanine was shown to induce cell death in human cancer cells through inhibiting the autophagic degradation activity, a mechanism different from cisplatin [39]. Treatment for 24 h with mahanine at 25 μM significantly decreased the viability of HepG2 hepatocellular carcinoma cells and HuCCT1 and KKU-100 cholangiocarcinoma cells (Figure 31A). Moreover, the treatment for 24 h with mahanine induced the MITF expression in all of the three cell lines (Fig. 31B). We also analyzed expression levels of HO-1 that is an enzyme responsible for physiological

heme catabolism [168] and also plays a cytoprotective role in cholangiocarcinoma cells [169]. Unexpectedly, MITF expression levels were increased in these dying cells treated with mahanine (Figure 31B). Moreover, the increase in the MITF expression levels was associated with the decrease in HO-1 expression levels, the latter of which may enhance the cell toxicity of mahanine, as reported for the antitumor effect of 5-fluorouracil and gemcitabinein on cholangiocarcinoma cells [165]. These results support the possibility that mahanine is a potential reagent for the treatment of hepatic cancer

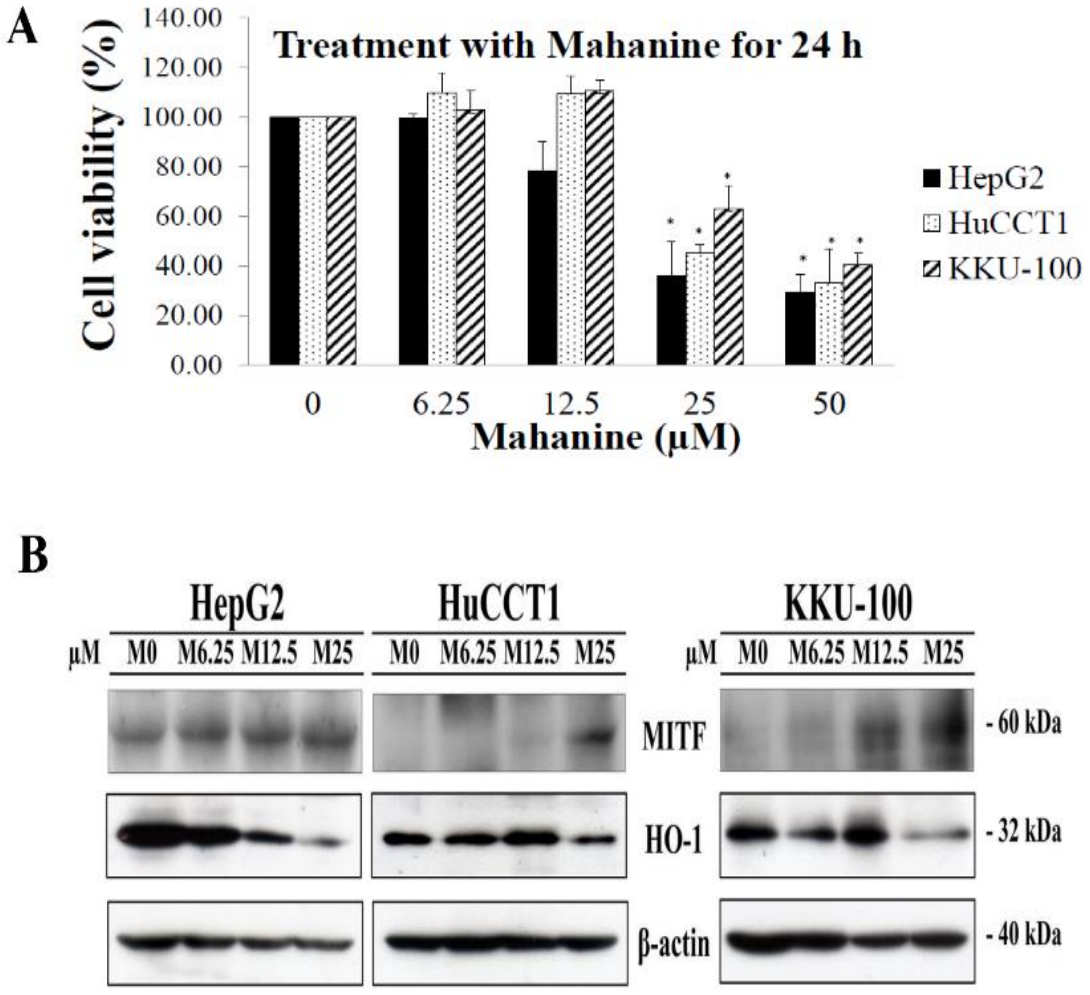

Figure 31: Induction of MITF by mahanine in hepatic malignant cells.

(A) The effect of mahanine on viability of HepG2 hepatocellular carcinoma cells and HuCCT1 and KKU-100 cholangiocarcinoma cells. Cells were incubated with mahanine at different concentrations for 24 h. MTT assay was used to *determine* the number of cell viability. Data represent mean ± S.D. of three independent experiments. $^{\#}P < 0.05$ compared to concurrent control. (B) Western blot analysis of MITF and HO-1. Cells were incubated with mahanine at different concentrations for 24 h. The data are shown from one of two independent experiments with similar results. Each lane contained cell extracts (30 μg protein). Under the conditions used, MITF proteins were detected as a single band of about 60 kDa [93]. A 10% gel was used for detecting MITF and beta-actin (top and bottom)

CHAPTER VI
DISCUSSION

Recently, many studies have focused on the prevention and treatment of chronic diseases including metabolic syndrome and its correlated health risks using natural compounds. *Murraya koenigii* and *Stevia rebuadiana* were showed the inhibition effects on rising of fasting blood sugar levels and improve metabolic condition in type 2 diabetic rat [170-173]. The present study was aimed to clarify the anti-diabetic mechanisms effect of mahanine from *Murraya koenigii*, steviol, isosteviol and 7 beta-OH –isosteviol from *Stevia rebuadiana* at the molecular and cellular levels enrolling RIN-m5F pancreatic beta-cells, L6 myotube and 3T3-L1 adipocytes . In addition the effect of mahanine after induction of MITF by mahanine in hepatic malignant cells were study. ROS may be play an important role in the study of diabetic mellitus. Ongoing beta-cell failure lead to impairment of insulin secretion, insulin resistance, and causes type 2 diabetes. Several study show the protective effect of antioxidative drugs from oxidative stress-induced in beta-cell lines and isolated pancreatic islets from rodents [174, 175]. Pancreatic islet cells are more susceptive to oxidative stress than cells in other tissue because they produce less antioxidant enzymes. Pancreatic beta-cells contain very low levels of antioxidant enzyme and accordingly they are exquisitely sensitive to ROS. This is consistent with physiological instruction of beta-cell function when ROS levels are low, but deleterious effects to the beta-cells occur when ROS levels are abnormally high [176]. Under diabetic situations, ROS levels are increased in numerous tissues and

organs, leading to the progression of beta-cell dysfunction in type 2 diabetes, since pancreatic islet cells express a moderately low amount of anti-oxidative enzymes such as glutathione peroxidase and catalase [177]. Hence, the model of pancreatic islet cells damage induced by high glucose is susceptible to study. *Murraya koenigii* (L.) Spreng leaves are well-known as curry leaves and have been used as one of the essential herbs of southern Indian for cooking as well as in folk medicine. Phytochemical studies of the leaves of this plant found that they contained various carbazole alkaloids [178]. A previous study suggested that the hypoglycemic effect of MK aqueous extract may be mediated through the stimulation and/or secretion of insulin from beta cells from pancreatic islet of Langerhans [179]. An aqueous extract of *Murraya koenigii* leaves contains a range of active pharmacological agents including carbazole alkaloids, flavonoids and tannins [138, 180, 181]. These compounds are known to be bioactive for the administration of diabetes [182-184]. It well known that certain alkaloids and flavonoids display hypoglycemic activity [185] and they are also known for their ability to regenerate beta cells [186-188]. Mahanine which has a hydroxyl group at the meta position, showed antioxidant activity against the oxidation of methyl linoleate in a bulk system, and radical scavenging activity [18]. The origin of ROS generation in insulin-secreting pancreatic beta-cells has commonly been examined to be the mitochondrial electron transport chain, but recent the study has focused on NOX enzymes as a likely source of ROS production [189]. The suppression of NADPH oxidase substantially restores the glucose-induced dysfunction of pancreatic cells [83]. NADPH oxidase is a

ubiquitous multi-subunit enzyme which creates superoxide from molecular oxygen using NADPH as an electron donor. Seven isoforms of the catalytic subunit NOX (NOX1-5, Duox1 and 2) with different cellular localization, tissue distribution and expression are known. RIN-m5F pancreatic beta cells (a sub-clone) express only NOX1 and NOX4 [190]. NOX4 is expressed and active, whereas NOX1, like the NOX2 isoform, requires other works for activity. In fact, Nox1 is constitutively connected with NOXO1 and NOXA1, the p47phox and p67phox homologues, respectively. In the present study, we investigated the effect of mahanine on RIN-m5F cells under hyperglycemia conditions, and its underlying mechanism. Induction the hyperglycemia condition was achieved by incubating cells with 33 mM glucose, as previously reported [83]. The high glucose induced ROS generation was eliminated by mahanine treatment in pancreatic beta cells as shown in Figure 11. Cell that were exposed to mahanine reversed the chronic hyperglyceamia induced ROS production and the impaired insulin secretion from beta cell. The effect of mahanine on gene expression in oxidative stress and insulin secretion were assessed and data are shown in Figure 12. Mahanine reversed the NOX1 and NOX4 gene expression that is known as a source of ROS production. Moreover, mahanine promoted insulin gene expression under the chronic exposure to a high glucose concentration. PDX-1 has important roles in pancreatic development and differentiation, but also regulates insulin gene transcription [191]. Chronic hyperglyceamia increases PDX-1 expression in the nucleus of pancreatic beta cells which is decreases the insulin secretion [191]. It has also been shown that depression of insulin secretion was inhibited

by antioxidant treatment. Mahanine restored the regulatory mechanisms of insulin secretion by increasing the levels of PDX-1, an insulin-related transcription factor, and insulin secretion. The results showed that treatment with mahanine reversed the high glucose induced translocation of PDX-1 from intranuclear to cytoplasm in RIN-m5F cells, as shown in Figure 13, and significantly increased the level of insulin secretion as shown in Figure 14. Consistent with the curry leaf from aqueous extract results, mahanine has the same effect on of antioxidant activity via inhibiting high glucose induced ROS production, the increasing PDX-1 translocation from the cytoplasm to the nucleus in RIN-m5F cells and promoting insulin secretion and attenuated pancreatic beta-cell function. However, *Stevia rebuadiana* crude extract and pure compound did not study the preventive effect on pancreatic beta-cells from high glucose-induced oxidative damage because it less affective on antioxidant activity.

One of the importance mechanism for diabetes mellitus control is prevention and treatment by increase the glucose uptake. GLUT4 protein translocation is necessary to maintaining glucose in the blood stream. The GLUT4 translocation in skeletal muscle and adipocyte cells could be regulated via an insulin dependent (Akt signaling pathway) or an insulin-independent (AMPK signaling pathway). AMP-activated protein kinase is suggested to play a role in improving insulin sensitivity by direct stimulation of glucose uptake in muscle independently of insulin signaling pathway [192, 193]. The stimulation of GLUT4 translocation by insulin requires the insulin receptor via tyrosine phosphorylation of insulin receptor substrate (IRS) proteins and PI-3-kinase activation

then Akt posphorylation, while the AMPK pathway has been shown to regulate GLUT4 translocation via an insulin-independent mechanism [63]. This study aimed to investigate the effects of mahanine from *Murraya koenigii*, steviol, isosteviol and 7 β-OHisosteviol from *Stevia rebuadiana* in facilitating glucose uptake in skeletal muscle and adipocyte cells. Initially, the hypoglycemic effect of mahanine on glucose uptake activity were elucidate. Our study demonstrated that mahanine could be effective in increasing glucose uptake in skeletal muscle and adipocyte cells. Mahanine significantly stimulated glucose uptake in myotube and adipocyte cells when comparable to untreated cells. Treatment with mahanine at 10 μM for 30 min revealed that glucose uptake was increased (Figure 17), this was mediated primarily by the rapid movement of GLUT4 from an intracellular compartment to the plasma membrane (Figure 18). The effect of mahanine is very similar to insulin, by mahanine significantly increasing the translocation of GLUT4 protein from intracellular vesicles into the plasma fraction. The investigation of the hypoglycemic effect of curry leaf also established the specific induction of glucose uptake in myotube cells [194]. Consistent with the curry leaf results, mahanine has the same effect on glucose uptake and GLUT4 translocation. The stimulation of glucose uptake by insulin in myocytes needs the insulin receptor-mediated tyrosine phosphorylation of IR substrate (IRS) family members and subsequent activation of PI3K and Akt. In addition to the PI3K pathway, the AMPK pathway has been shown to regulate glucose transport in muscle and adipocytes via an insulin-independent mechanism. In this study we also investigated biochemical mark to demonstrate that mahanine exerted

its insulin-like activities through activation of the Akt pathways. From the result it was shown that the anti-diabetic activities of mahanine by increasing glucose uptake and membrane translocation of glucose transporters, was through the activation of phosphorylation of Akt. In addition, the level of phosphorylation of Akt protein was decreased when co-treated with wortmanine (an Akt inhibitor). This result indicated that the effect of mahanine in glucose uptake and glucose transporters is through the activation of Akt signaling pathway. The *M. koenigii* crude extract has been shown to act as an insulin-mimetic in activating the Akt signaling pathways [194]. The AMPK pathway is an important therapeutic target for regulating whole-body energy balance. Compounds that activate AMPK showed improvement of hypoglycemic effect by helping glucose uptake and GLUT4 translocations. It has been shown that many compounds or drugs with helpful activity to metabolic syndrome are known to activate AMPK and metformin is a prominent example [195]. This study provides a mechanistic explanation for the increased glucose uptake, GLUT4 translocation, and GLUT4 gene expression in mahanine treated myotubes. The effects of mahanine on GLUT4 translocation were shown not to be associated with the activation of the AMPK signaling pathway.

As one of the most current traditional treatments used around the world, mahanine present as a promising candidate as an insulin-like natural medicine. However, the detailed mechanism of these compounds requires further investigation especially regarding the long-term effects of mahanine on diabetic patients. Our findings provide evidence of mahanine with marked insulin-like activity, has the potential for the

treatment of metabolic syndrome like diabetes. Another path of this study, we also investigated steviol, isosteviol and 7 β-OHisosteviol from *Stevia rebuadiana* on the Akt activation in vitro. The results shown that they did not promote AMPK signaling pathway. However, three compounds show the increasing of glucose uptake and increase endogenous GLUT4 translocation to plasma membrane in L6 myotubes, which was visually demonstrated by ELISA and western blot. This stimulatory tendency on glucose uptake level and GLUT4 translocation to plasma membrane was also observed *in vivo* and *in vitro* model when treated with *Stevia rebuadiana* crude extract [120, 196]. The limitation of our study is that we only have investigated the effects of steviol, isosteviol and 7 β-OHisosteviol from *Stevia rebuadiana* on signaling pathway only in i*n vitro* model. Further intensive studies such as measurement of the Akt and AMPK protein level of the glucose uptake and endogenous GLUT4 translocation to plasma membrane from skeletal muscle and adipose tissue in rat are required to verify their effect. Moreover, There are eight compounds have been isolated from *Stevia rebuadiana including* stevioside, rebaudioside A, B, C, D, E, dulcoside A and steviolbioside. Three compounds were investigated in this study from stevioside extraction so the result may be not cover for another metabolite. Adiponectin is the most widely reported adipokine in the research of metabolic disease. Serval datal and clinical studies shown that adiponectin improves insulin sensitivity [197]. Adiponectin helps increase glucose uptake in rat skeletal muscle and adipocyte cells [198]. From this result steviol, isosteviol and 7 β-

OHisosteviol may be play a role in the modulation of insulin sensitivity dependent on adiponectin in adipocyte cells.

High glucose in diabetes mellitus patents is associated with the progression in many types of cancer including liver cancer, pancreas cancer and breast cancer. Some diabetes mellitus medications are used to treat diabetes patient have a side effect in tumor growth so it is essential to having experience in wide range of idea. Therefore, this study was performed on the model that represent treatment of cancer with diabetes mellitus medication. Hepatocellular carcinoma and cholangiocarcinoma cell line were used in this study because the liver is an important glycogen storage and it originate for progression to be a bile duct cancer. Melanogenesis Associated Transcription Factor (MITF) protein was found to be involved in cancer. Cytoplasmic expression of MITF in hepatocellular carcinoma and cholangiocarcinoma was studied. Using the human liver cancer tissue array, we found the cytoplasmic expression of MITF in subsets of hepatocellular carcinoma and cholangiocarcinoma specimens. Importantly, MITF is co-expressed with GLI1, a poor prognosis marker for hepatic cancer [164]. The clinical data also support that MITF expression is a poor prognosis marker for hepatocellular carcinoma (Table 9). However, the impact of MITF expression in the prognosis of cholangiocarcinoma remains to be investigated, due to the limited number of cholangiocarcinoma specimens. On the other hand, MITF expression is undetectable in most of hepatic cancer specimens, irrespective of GLI1 expression (Tables 11 and 14). We are interested in the cytoplasmic expression of MITF in hepatic cancer cells,

because the cytoplasmic retention of MITF was reported in pancreatic cancer cells [166]. The nutritional starvation enhanced the nuclear translocation of MITF, which in turn could stimulate the processes of autophagy in pancreatic cancer [166]. We thus assume that the cytoplasmic expression of MITF may reflect the sufficient nutrition in hepatic cancer cells, which may be beneficial for cancer cell proliferation but may be predictive of poor prognosis in cancer patients. In this context, we have shown the cytoplasmic expression of Mitf in various cell types of the mouse kidney, except for the renal tubular epithelial cells with the nuclear localization of Mitf [33]. It is therefore conceivable that cytoplasmic MITF/Mitf may exert a hitherto unknown function essential for cellular homeostasis. Another question remains to be clarified is the identity of MITF isoform that is over-expressed in hepatocellular carcinoma and cholangiocarcinoma specimens, because MITF consists of multiple isoforms with different amino-termini [199]. Moreover, to the best of our knowledge, an MITF isoform-specific antibody is not available. In this context, using the real-time RT-PCR analysis, we have shown that among MITF isoform mRNAs, only MITF-A and MITF-H mRNAs were detected in the human liver [24], although their expression levels were about three-fold lower than those in HuCCT1 and KKU-100 cholangiocarcinoma cells [24]. In these cholangiocarcinoma cell lines, MITF-A and MITF-H mRNAs are similarly expressed [24]. Potential role of Hedgehog signaling for regulation of MITF expression. The earlier reports showed the activation of Hedgehog signaling in hepatocellular carcinoma [96-98] and cholangiocarcinoma [95, 99]. In fact, we have shown that GLI1 immunoreactivity was detected in 55% of

hepatocellular carcinoma (21/38 specimens) and 86% of cholangiocarcinoma (6/7 specimens) (see Tables 10 and 13). Furthermore, GLI1 has been shown as a poor prognosis marker for hepatic cancer [164]. Importantly, MITF is co-expressed with GLI1 only in subsets of hepatocellular carcinoma and cholangiocarcinoma. These results suggest that Hedgehog signaling may differentially regulate MITF expression in hepatocellular carcinoma and cholangiocarcinoma, depending on cellular microenvironment. We previously showed that the treatment for 24 h with cyclopamine, a Hedgehog signaling antagonist, caused the induction of MITF expression in HepG2 hepatocellular carcinoma cells and HuCCT1 cholangiocarcinoma cells, but tended to decrease the MITF level in KKU-100 cholangiocarcinoma cells, as judged by Western blot analysis [24]. It is therefore conceivable that Hedgehog signaling may down-regulate MITF expression or up-regulate MITF expression, depending on the microenvironment of hepatic cancer cells. In fact, sonic hedgehog, a glycoprotein, is expressed in HuCCT1 cholangiocarcinoma cells and HepG2 hepatocellular carcinoma cells [97]. HuCCT1 cells also expressed Smoothened [200]. However, it is also possible that cyclopamine may influence MITF expression through a mechanism that is unrelated to Hedgehog signaling, as evident from the mahanine-mediated induction of MITF. Mahanine as a potent inducer of MITF expression. Mahanine exerted the potent cell toxicity in the hepatic cancer cell lines, including HuCCT1 cells that were resistant to cisplatin [24]; namely, mahanine may kill hepatic cancer cells through the mechanism different from cisplatin. Recently, mahanine was shown to inhibit the autophagic degradation activity [39]. The

decrease in HO-1 expression may also contribute to the severe cell toxicity of mahanine in hepatic cancer cells. By contrast, the mahanine-mediated MITF induction may reflect the compensatory mechanism for restoring the cell survival. However, these unexpected findings need further experiments.

CHAPTER VII

CONCLUSION

Hyperglycemia or diabetes condition, induces the oxidative stress that leads to suppression of insulin biosynthesis and secretion, along with the reduction of nuclear PDX-1 expression, translocation and insulin gene expression [191]. Diabetic therapy is usually focused on reducing oxidative stress in diabetic patients by antioxidant treatments [176]. Our current study was confirmed that high glucose induces pancreatic beta cells damage, whereas mahanine inhibited high glucose induced pancreatic beta cell damage by suppressed ROS production. In addition, mahanine prevented the translocation of PDX1 from the nucleus to the cell membrane that promoting the insulin secretion and attenuated pancreatic beta-cell function. Moreover, mahanine treatment promoted a dose dependent increased glucose uptake in L6 myotubes and adipocyte cells via activation of the Akt signaling pathway. Mahanine induced Akt-activation was reversed by co-treatment with wortmannin, an Akt inhibitor. In addition, it was found that mahanine significantly enhanced GLUT4 translocation to the plasma membrane in L6 myotubes. These results suggest that increased activation of the Akt signaling pathway lead to increased plasma membrane GLUT4 content and increased glucose uptake. We have shown the cytoplasmic expression of MITF in subsets of hepatocellular carcinoma and cholangiocarcinoma specimens. Importantly, MITF immunoreactivity is detected only in the cancer specimens that also express GLI1 immunoreactivity. Subsequently, we showed that MITF expression was upregulated in dying hepatic cancer

cells treated with mahanine. Thus, MITF expression level may be determined by the balance between the activity of the Hedgehog signaling pathway and the degree of the cellular stress. Enhancement of the glucose uptake level and endogenous GLUT4 translocation to plasma membrane in L6 myotubes were found in steviol, isosteviol and 7 β-OHisosteviol treated group. However, the effect not related to Akt and AMPK signalling pathway but they may act as insulin enhance since co-treatment with insulin show very strong AKT activation. Hence the further studies needed to be performed to verify the mechanism of action.

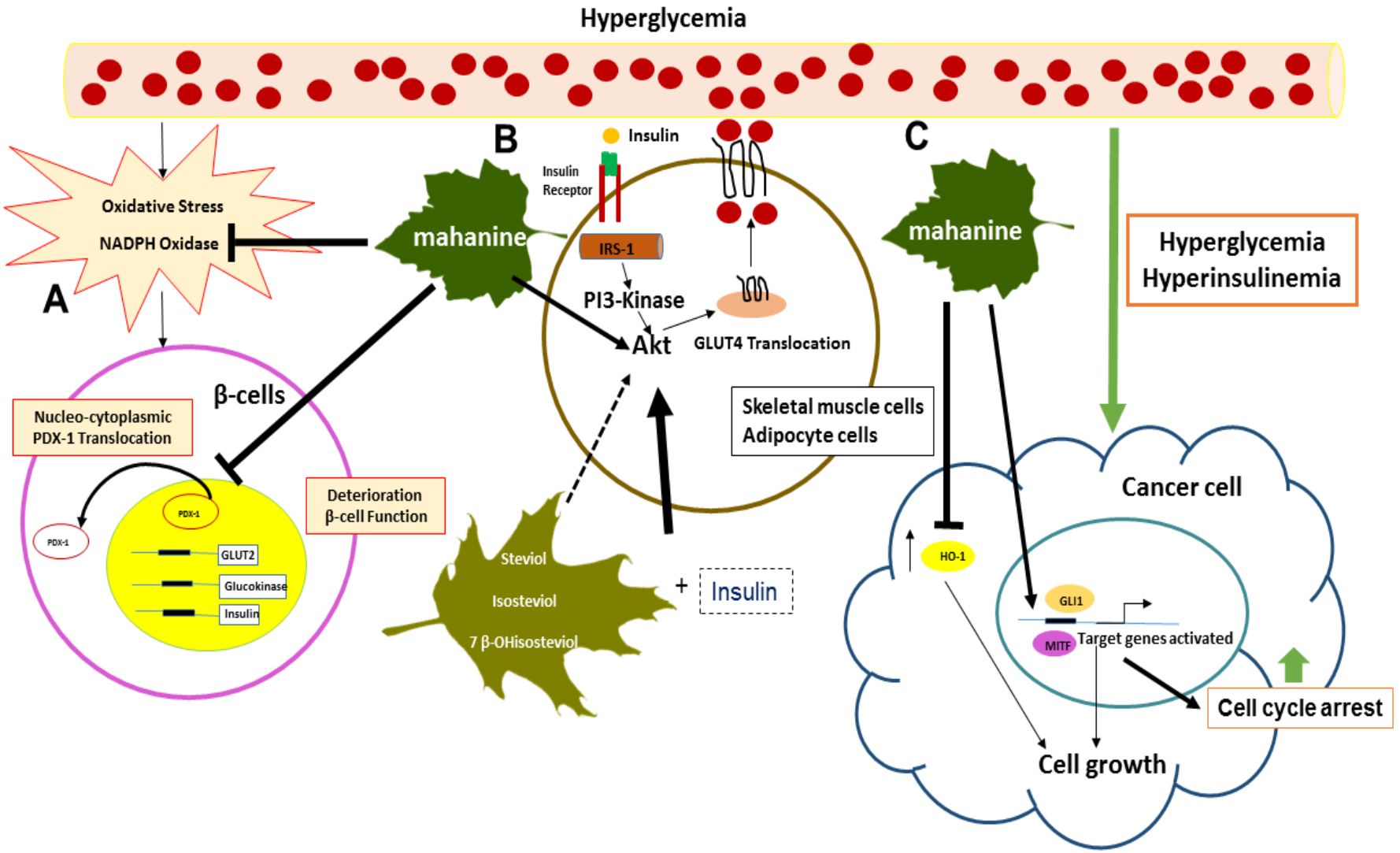
Hyperglycemia
A
Oxidative Stress
NADPH Oxidase
β-cells
Nucleo-cytoplasmic
PDX-1 Translocation
PDX-1
PDX-1
GLUT2
Glucokinase
Insulin
Deterioration
β-cell Function
B
Insulin
Insulin
Receptor
mahanine
IRS-1
PI3-Kinase
Akt
GLUT4 Translocation
Skeletal muscle cells
Adipocyte cells
Steviol
Isosteviol
7 β-OHisosteviol
+
Insulin
C
mahanine
Hyperglycemia
Hyperinsulinemia
Cancer cell
HO-1
GLI1
MITF
Target genes activated
Cell cycle arrest
Cell growth

Figure 32: Scheme of the pharmacological effect of mahanine, steviol, isosteviol and 7 β-OHisosteviol.

(A) The effect of mahanine from herbal extract in regulation of antioxidant mechanism. (B) The hypoglycemic effects of mahanine, steviol, isosteviol and 7 β-OHisosteviol through glucose uptake by using cultured myocytes and adipocyte. (C) Anti-cancer effect of mahanine in HepG2 hepatocellular carcinoma cells and HuCCT1 and KKU-100 cholangiocarcinoma cells.

7.1 Benefits from this study

1. To understand the mechanisms of diabetes and new knowledge that gain from the study could bring to further research.

2. To discover a new drug for treatment of diabetes without or less side effects than the present drugs and reduce the cost of the treatment.

3. The diabetic patient will have an alternative medication diabetes.

4. Expect to publish the results of this research project in the international journals.

7.2 Limitations of this study

1. In vitro methods or cells model are treated outside their normal environment such as no surrounding tissues, blood supply, normal supply of nutrients and hormone.

2. In vitro model can be stimulated by addition of specific chemical agents.

3. Enhanced reliability when same effect are also demonstrated in vivo

REFERENCES

[1] A. Misra, L. Khurana. Obesity and the metabolic syndrome in developing countries, The Journal of Clinical Endocrinology & Metabolism, 93 (2008) s9-s30.

[2] E. Phielix, M. Mensink. Type 2 diabetes mellitus and skeletal muscle metabolic function, Physiology & Behavior, 94 (2008) 252-258.

[3] J.J. Kannampilly. Continuous Glucose Monitoring System, Dostupné z: http://apiindia. org/medicine_update_2013/chap43. pdf.

[4] P. Vigneri, F. Frasca, L. Sciacca, et al. Diabetes and cancer, Endocr Relat Cancer, 16 (2009) 1103-1123.

[5] G. Shlomai, B. Neel, D. LeRoith, et al. Type 2 Diabetes Mellitus and Cancer: The Role of Pharmacotherapy, J Clin Oncol, 34 (2016) 4261-4269.

[6] D. Morgan, H.R. Oliveira-Emilio, D. Keane, et al. Glucose, palmitate and pro-inflammatory cytokines modulate production and activity of a phagocyte-like NADPH oxidase in rat pancreatic islets and a clonal beta cell line, Diabetologia, 50 (2007) 359-369.

[7] M. Nakayama, T. Inoguchi, T. Sonta, et al. Increased expression of NAD(P)H oxidase in islets of animal models of Type 2 diabetes and its improvement by an AT1 receptor antagonist, Biochem Biophys Res Commun, 332 (2005) 927-933.

[8] H. Yuan, Y. Lu, X. Huang, et al. Suppression of NADPH oxidase 2 substantially restores glucose-induced dysfunction of pancreatic NIT-1 cells, FEBS J, 277 (2010) 5061-5071.

[9] Y.C. Hu, D.M. Hao, L.X. Zhou, et al. 2',4'-Dihydroxy-6'-methoxy-3',5'-dimethylchalcone protects the impaired insulin secretion induced by glucotoxicity in pancreatic beta-cells, J Agric Food Chem, 62 (2014) 1602-1608.

[10] A.R. Saltiel, C.R. Kahn. Insulin signalling and the regulation of glucose and lipid metabolism, Nature, 414 (2001) 799-806.

[11] M.C. Towler, D.G. Hardie. AMP-activated protein kinase in metabolic control and insulin signaling, Circulation research, 100 (2007) 328-341.

[12] C. Loutradis, A. Skodra, P. Georgianos, et al. Diabetes mellitus increases the prevalence of anemia in patients with chronic kidney disease: A nested case-control study, World J Nephrol, 5 (2016) 358-366.

[13] M. Modak, P. Dixit, J. Londhe, et al. Recent Advances in Indian Herbal Drug Research Guest Editor: Thomas Paul Asir Devasagayam Indian Herbs and Herbal Drugs Used for the Treatment of Diabetes, Journal of clinical biochemistry and nutrition, 40 (2007) 163-173.

[14] V. Khan, A.K. Najmi, M. Akhtar, et al. A pharmacological appraisal of medicinal plants with antidiabetic potential, Journal of Pharmacy and Bioallied sciences, 4 (2012) 27.

[15] P. Gupta, A. Nahata, V.K. Dixit. An update on Murraya koenigii spreng: a multifunctional Ayurvedic herb, Zhong Xi Yi Jie He Xue Bao, 9 (2011) 824-833.

[16] D. Kumar, R. Ghosh, B.C. Pal. α-Glucosidase inhibitory terpenoids from Potentilla fulgens and their quantitative estimation by validated HPLC method, Journal of Functional Foods, 5 (2013) 1135-1141.

[17] M.K. Roy, V.N. Thalang, G. Trakoontivakorn, et al. Mechanism of mahanine-induced apoptosis in human leukemia cells (HL-60), Biochemical pharmacology, 67 (2004) 41-51.

[18] Y. Tachibana, H. Kikuzaki, N.H. Lajis, et al. Antioxidative activity of carbazoles from Murraya koenigii leaves, Journal of agricultural and food chemistry, 49 (2001) 5589-5594.

[19] R. Birari, V. Javia, K.K. Bhutani. Antiobesity and lipid lowering effects of Murraya koenigii (L.) Spreng leaves extracts and mahanimbine on high fat diet induced obese rats, Fitoterapia, 81 (2010) 1129-1133.

[20] J. Pandey, R. Maurya, R. Raykhera, et al. Murraya koenigii (L.) Spreng. ameliorates insulin resistance in dexamethasone-treated mice by enhancing peripheral insulin sensitivity, Journal of the Science of Food and Agriculture, 94 (2014) 2282-2288.

[21] A. Biswas, S. Bhattacharya, S. Dasgupta, et al. Insulin resistance due to lipid-induced signaling defects could be prevented by mahanine, Molecular and cellular biochemistry, 336 (2010) 97-107.

[22] J. Kasznicki, A. Sliwinska, J. Drzewoski. Metformin in cancer prevention and therapy, Annals of Translational Medicine, 2 (2014) 57.

[23] Y. Shaib, H.B. El-Serag. The epidemiology of cholangiocarcinoma, Semin Liver Dis, 24 (2004) 115-125.

[24] P. Samatiwat, K. Takeda, S. Satarug, et al. Induction of MITF expression in human cholangiocarcinoma cells and hepatocellular carcinoma cells by cyclopamine, an inhibitor of the Hedgehog signaling, Biochem Biophys Res Commun, 470 (2016) 144-149.

[25] M. Varjosalo, J. Taipale. Hedgehog: functions and mechanisms, Genes Dev, 22 (2008) 2454-2472.

[26] G.D. Dakubo, C. Mazerolle, M. Furimsky, et al. Indian hedgehog signaling from endothelial cells is required for sclera and retinal pigment epithelium development in the mouse eye, Dev Biol, 320 (2008) 242-255.

[27] C.A. Hodgkinson, K.J. Moore, A. Nakayama, et al. Mutations at the mouse microphthalmia locus are associated with defects in a gene encoding a novel basic-helix-loop-helix-zipper protein, Cell, 74 (1993) 395-404.

[28] H. Hozumi, K. Takeda, Y. Yoshida-Amano, et al. Impaired development of melanoblasts in the black-eyed white Mitf(mi-bw) mouse, a model for auditory-pigmentary disorders, Genes Cells, 17 (2012) 494-508.

[29] M.J. Hughes, J.B. Lingrel, J.M. Krakowsky, et al. A helix-loop-helix transcription factor-like gene is located at the mi locus, J Biol Chem, 268 (1993) 20687-20690.

[30] E. Steingrimsson, K.J. Moore, M.L. Lamoreux, et al. Molecular basis of mouse microphthalmia (mi) mutations helps explain their developmental and phenotypic consequences, Nat Genet, 8 (1994) 256-263.

[31] S.B. Smith, T. Duncan, G. Kutty, et al. Increase in retinyl palmitate concentration in eyes and livers and the concentration of interphotoreceptor retinoid-binding protein in eyes of vitiligo mutant mice, Biochem J, 300 (Pt 1) (1994) 63-68.

[32] M.A. Mazur, M. Winkler, E. Ganic, et al. Microphthalmia transcription factor regulates pancreatic beta-cell function, Diabetes, 62 (2013) 2834-2842.

[33] K. Ohba, K. Takeda, T. Furuse, et al. Microphthalmia-associated transcription factor ensures the elongation of axons and dendrites in the mouse frontal cortex, Genes Cells, 21 (2016) 1365-1379.

[34] K. Takeda, T. Adachi, F. Han, et al. Augmented chemosensitivity in black-eyed white Mitfmi-bw mice, lacking melanocytes, J Biochem, 141 (2007) 327-333.

[35] K. Ohba, K. Takeda, H. Yamamoto, et al. Microphthalmia-associated transcription factor is expressed in projection neurons of the mouse olfactory bulb, Genes Cells, 20 (2015) 1088-1102.

[36] M. Haswell-Elkins, S. Satarug, D. Elkins. Opisthorchis viverrini infection in northeast Thailand and its relationship to cholangiocarcinoma, Journal of gastroenterology and hepatology, 7 (1992) 538-548.

[37] H.R. Shin, J.K. Oh, E. Masuyer, et al. Epidemiology of cholangiocarcinoma: an update focusing on risk factors, Cancer Sci, 101 (2010) 579-585.

[38] M.K. Roy, V.N. Thalang, G. Trakoontivakorn, et al. Mechanism of mahanine-induced apoptosis in human leukemia cells (HL-60), Biochem Pharmacol, 67 (2004) 41-51.

[39] T. Utaipan, A. Athipornchai, A. Suksamrarn, et al. Carbazole alkaloids from Murraya koenigii trigger apoptosis and autophagic flux inhibition in human oral squamous cell carcinoma cells, J Nat Med, 71 (2017) 158-169.

[40] L. Guariguata, D. Whiting, I. Hambleton, et al. Global estimates of diabetes prevalence for 2013 and projections for 2035 for the IDF Diabetes Atlas, Diabetes Research and Clinical Practice, (2013).

[41] Diagnosis and classification of diabetes mellitus, Diabetes Care, 33 Suppl 1 (2010) S62-69.

[42] C.L. Triplitt. Examining the mechanisms of glucose regulation, Am J Manag Care, 18 (2012) S4-10.

[43] X. Guo, H. Li, H. Xu, et al. Glycolysis in the control of blood glucose homeostasis, Acta Pharmaceutica Sinica B, 2 (2012) 358-367.

[44] R. Botchlett, S.L. Woo, M. Liu, et al. Nutritional approaches for managing obesity-associated metabolic diseases, J Endocrinol, 233 (2017) R145-r171.

[45] G. Dimitriadis, P. Mitrou, V. Lambadiari, et al. Insulin effects in muscle and adipose tissue, Diabetes Res Clin Pract, 93 Suppl 1 (2011) S52-59.

[46] G. Wilcox. Insulin and Insulin Resistance, Clinical Biochemist Reviews, 26 (2005) 19-39.

[47] J. Shi, K.V. Kandror. Study of glucose uptake in adipose cells, Methods Mol Biol, 456 (2008) 307-315.

[48] M. Mueckler, B. Thorens. The SLC2 (GLUT) Family of Membrane Transporters, Molecular aspects of medicine, 34 (2013) 121-138.

[49] S.E. Leney, J.M. Tavare. The molecular basis of insulin-stimulated glucose uptake: signalling, trafficking and potential drug targets, J Endocrinol, 203 (2009) 1-18.

[50] S.R. Joshi, R.M. Parikh, A. Das. Insulin-history, biochemistry, physiology and pharmacology, Journal-Association of Physicians of India, 55 (2007) 19.

[51] N. Roopashree. Measurement Of Insulin Sensitivity In Men With Type Ii Diabetes Mellitus Using The Hyperinsulinemic Euglycemic Clamp, ST. JOHN'S MEDICAL COLLEGE, 2009.

[52] S. Farfari, V. Schulz, B. Corkey, et al. Glucose-regulated anaplerosis and cataplerosis in pancreatic beta-cells: possible implication of a pyruvate/citrate shuttle in insulin secretion, Diabetes, 49 (2000) 718-726.

[53] J.-C. Henquin. Triggering and amplifying pathways of regulation of insulin secretion by glucose, Diabetes, 49 (2000) 1751-1760.

[54] E. Cassani, R. Cilia, J. Laguna, et al. Mucuna pruriens for Parkinson's disease: Low-cost preparation method, laboratory measures and pharmacokinetics profile, J Neurol Sci, 365 (2016) 175-180.

[55] B.B. Kahn, J.S. Flier. Obesity and insulin resistance, Journal of Clinical Investigation, 106 (2000) 473-481.

[56] D. Lann, D. LeRoith. Insulin Resistance as the Underlying Cause for the Metabolic Syndrome, Medical Clinics of North America, 91 (2007) 1063-1077.

[57] J.E. Pessin, A.R. Saltiel. Signaling pathways in insulin action: molecular targets of insulin resistance, Journal of Clinical Investigation, 106 (2000) 165-169.

[58] Q. Liu, L. Chen, L. Hu, et al. Small molecules from natural sources, targeting signaling pathways in diabetes, Biochimica et Biophysica Acta (BBA)-Gene Regulatory Mechanisms, 1799 (2010) 854-865.

[59] Y. Zick. Insulin resistance: a phosphorylation-based uncoupling of insulin signaling, Trends Cell Biol, 11 (2001) 437-441.

[60] G. Boden, G.I. Shulman. Free fatty acids in obesity and type 2 diabetes: defining their role in the development of insulin resistance and beta-cell dysfunction, Eur J Clin Invest, 32 Suppl 3 (2002) 14-23.

[61] T. Mandrup-Poulsen. Apoptotic signal transduction pathways in diabetes, Biochemical pharmacology, 66 (2003) 1433-1440.

[62] B.B. Kahn. Glucose transport: pivotal step in insulin action, Diabetes, 45 (1996) 1644-1654.

[63] S. Huang, M.P. Czech. The GLUT4 glucose transporter, Cell Metab, 5 (2007) 237-252.

[64] Y.B. Kim, K. Kotani, T.P. Ciaraldi, et al. Insulin-stimulated protein kinase C lambda/zeta activity is reduced in skeletal muscle of humans with obesity and type 2 diabetes: reversal with weight reduction, Diabetes, 52 (2003) 1935-1942.

[65] S. Frojdo, H. Vidal, L. Pirola. Alterations of insulin signaling in type 2 diabetes: a review of the current evidence from humans, Biochim Biophys Acta, 1792 (2009) 83-92.

[66] D.D. Sarbassov, D.A. Guertin, S.M. Ali, et al. Phosphorylation and regulation of Akt/PKB by the rictor-mTOR complex, Science, 307 (2005) 1098-1101.

[67] E. Fayard, L.A. Tintignac, A. Baudry, et al. Protein kinase B/Akt at a glance, J Cell Sci, 118 (2005) 5675-5678.

[68] K. Bouzakri, A. Zachrisson, L. Al-Khalili, et al. siRNA-based gene silencing reveals specialized roles of IRS-1/Akt2 and IRS-2/Akt1 in glucose and lipid metabolism in human skeletal muscle, Cell Metab, 4 (2006) 89-96.

[69] M.E. Cleasby, T.A. Reinten, G.J. Cooney, et al. Functional studies of Akt isoform specificity in skeletal muscle in vivo; maintained insulin sensitivity despite reduced insulin receptor substrate-1 expression, Mol Endocrinol, 21 (2007) 215-228.

[70] Z.Y. Jiang, Q.L. Zhou, K.A. Coleman, et al. Insulin signaling through Akt/protein kinase B analyzed by small interfering RNA-mediated gene silencing, Proc Natl Acad Sci U S A, 100 (2003) 7569-7574.

[71] O. Tschopp, Z.Z. Yang, D. Brodbeck, et al. Essential role of protein kinase B gamma (PKB gamma/Akt3) in postnatal brain development but not in glucose homeostasis, Development, 132 (2005) 2943-2954.

[72] J.T. Brozinick, Jr., B.R. Roberts, G.L. Dohm. Defective signaling through Akt-2 and -3 but not Akt-1 in insulin-resistant human skeletal muscle: potential role in insulin resistance, Diabetes, 52 (2003) 935-941.

[73] L. Elghazi, L. Rachdi, A.J. Weiss, et al. Regulation of beta-cell mass and function by the Akt/protein kinase B signalling pathway, Diabetes Obes Metab, 9 Suppl 2 (2007) 147-157.

[74] K.A. Coughlan, R.J. Valentine, N.B. Ruderman, et al. AMPK activation: a therapeutic target for type 2 diabetes?, Diabetes, Metabolic Syndrome and Obesity: Targets and Therapy, 7 (2014) 241-253.

[75] D.G. Chandrashekarappa, R.R. McCartney, M.C. Schmidt. Ligand Binding to the AMP-activated Protein Kinase Active Site Mediates Protection of the Activation Loop from Dephosphorylation, The Journal of Biological Chemistry, 288 (2013) 89-98.

[76] R.R. Landgraf, D. Goswami, F. Rajamohan, et al. Activation of AMP-activated protein kinase revealed by hydrogen/deuterium exchange Mass Spectrometry, Structure (London, England : 1993), 21 (2013) 10.1016/j.str.2013.1008.1023.

[77] R.S. Lee-Young, J.S. Bonner, W.H. Mayes, et al. AMP-activated protein kinase (AMPK)α2 plays a role in determining the cellular fate of glucose in insulin-resistant mouse skeletal muscle, Diabetologia, 56 (2013) 608-617.

[78] U. Hostalek, M. Gwilt, S. Hildemann. Therapeutic Use of Metformin in Prediabetes and Diabetes Prevention, Drugs, 75 (2015) 1071-1094.

[79] B. Viollet, F. Andreelli, S.B. Jorgensen, et al. Physiological role of AMP-activated protein kinase (AMPK): insights from knockout mouse models, Biochem Soc Trans, 31 (2003) 216-219.

[80] M. Bensellam, D.R. Laybutt, J.-C. Jonas. The molecular mechanisms of pancreatic β-cell glucotoxicity: recent findings and future research directions, Molecular and cellular endocrinology, 364 (2012) 1-27.

[81] D. Morgan, H. Oliveira-Emilio, D. Keane, et al. Glucose, palmitate and pro-inflammatory cytokines modulate production and activity of a phagocyte-like NADPH oxidase in rat pancreatic islets and a clonal beta cell line, Diabetologia, 50 (2007) 359-369.

[82] M. Nakayama, T. Inoguchi, T. Sonta, et al. Increased expression of NAD (P) H oxidase in islets of animal models of Type 2 diabetes and its improvement by an AT1 receptor antagonist, Biochemical and biophysical research communications, 332 (2005) 927-933.

[83] H. Yuan, Y. Lu, X. Huang, et al. Suppression of NADPH oxidase 2 substantially restores glucose-induced dysfunction of pancreatic NIT-1 cells, FEBS journal, 277 (2010) 5061-5071.

[84] Y.-C. Hu, D.-M. Hao, L.-X. Zhou, et al. 2′, 4′-Dihydroxy-6′-methoxy-3′, 5′-dimethylchalcone protects the impaired insulin secretion induced by glucotoxicity in pancreatic β-cells, Journal of Agricultural and Food Chemistry, 62 (2014) 1602-1608.

[85] R. Pazdro, J.R. Burgess. The role of vitamin E and oxidative stress in diabetes complications, Mech Ageing Dev, 131 (2010) 276-286.

[86] H.F. Huseini, B. Larijani, R. Heshmat, et al. The efficacy of Silybum marianum (L.) Gaertn.(silymarin) in the treatment of type II diabetes: a randomized, double-blind, placebo-controlled, clinical trial, Phytotherapy research, 20 (2006) 1036-1039.

[87] S. Stranges, J.R. Marshall, R. Natarajan, et al. Effects of long-term selenium supplementation on the incidence of type 2 diabetes: a randomized trial, Annals of internal medicine, 147 (2007) 217-223.

[88] A. Satija, D. Spiegelman, E. Giovannucci, et al. Type 2 diabetes and risk of cancer, BMJ, 350 (2015) g7707.

[89] A.J. Klil-Drori, L. Azoulay, M.N. Pollak. Cancer, obesity, diabetes, and antidiabetic drugs: is the fog clearing?, Nat Rev Clin Oncol, 14 (2017) 85-99.

[90] J. Li, T. Han, L. Xu, et al. Diabetes mellitus and the risk of cholangiocarcinoma: an updated meta-analysis, Prz Gastroenterol, 10 (2015) 108-117.

[91] C. Saengboonmee, W. Seubwai, C. Wongkham, et al. Diabetes mellitus: Possible risk and promoting factors of cholangiocarcinoma: Association of diabetes mellitus and cholangiocarcinoma, Cancer Epidemiol, 39 (2015) 274-278.

[92] C. Phoomak, K. Vaeteewoottacharn, A. Silsirivanit, et al. High glucose levels boost the aggressiveness of highly metastatic cholangiocarcinoma cells via O-GlcNAcylation, Sci Rep, 7 (2017) 43842.

[93] K. Yasumoto, K. Takeda, H. Saito, et al. Microphthalmia-associated transcription factor interacts with LEF-1, a mediator of Wnt signaling, Embo j, 21 (2002) 2703-2714.

[94] D.M. Berman, S.S. Karhadkar, A. Maitra, et al. Widespread requirement for Hedgehog ligand stimulation in growth of digestive tract tumours, Nature, 425 (2003) 846-851.

[95] T. Kiesslich, C. Mayr, J. Wachter, et al. Activated hedgehog pathway is a potential target for pharmacological intervention in biliary tract cancer, Mol Cell Biochem, 396 (2014) 257-268.

[96] S. Huang, J. He, X. Zhang, et al. Activation of the hedgehog pathway in human hepatocellular carcinomas, Carcinogenesis, 27 (2006) 1334-1340.

[97] R. Al-Bahrani, S. Nagamori, R. Leng, et al. Differential Expression of Sonic Hedgehog Protein in Human Hepatocellular Carcinoma and Intrahepatic Cholangiocarcinoma, Pathol Oncol Res, 21 (2015) 901-908.

[98] M. Dugum, I. Hanouneh, T. McIntyre, et al. Sonic hedgehog signaling in hepatocellular carcinoma: A pilot study, Mol Clin Oncol, 4 (2016) 369-374.

[99] D. Riedlinger, M. Bahra, S. Boas-Knoop, et al. Hedgehog pathway as a potential treatment target in human cholangiocarcinoma, J Hepatobiliary Pancreat Sci, 21 (2014) 607-615.

[100] S.T. Lee, K.D. Welch, K.E. Panter, et al. Cyclopamine: from cyclops lambs to cancer treatment, J Agric Food Chem, 62 (2014) 7355-7362.

[101] S. Ikhlas, M. Ahmad. Metformin: Insights into its anticancer potential with special reference to AMPK dependent and independent pathways, Life Sci, 185 (2017) 53-62.

[102] S. Raptis, G. Dimitriadis. Oral hypoglycemic agents: insulin secretagogues, α-glucosidase inhibitors and insulin sensitizers, Experimental and Clinical Endocrinology & Diabetes, 109 (2001) S265-S287.

[103] B. Viollet, B. Guigas, N. Sanz Garcia, et al. Cellular and molecular mechanisms of metformin: an overview, Clinical Science (London, England : 1979), 122 (2012) 253-270.

[104] M. Foretz, S. Hébrard, J. Leclerc, et al. Metformin inhibits hepatic gluconeogenesis in mice independently of the LKB1/AMPK pathway via a decrease in hepatic energy state, The Journal of Clinical Investigation, 120 (2010) 2355-2369.

[105] G. Zhou, R. Myers, Y. Li, et al. Role of AMP-activated protein kinase in mechanism of metformin action, Journal of Clinical Investigation, 108 (2001) 1167-1174.

[106] X. Stephenne, M. Foretz, N. Taleux, et al. Metformin activates AMP-activated protein kinase in primary human hepatocytes by decreasing cellular energy status, Diabetologia, 54 (2011) 3101-3110.

[107] R.E. Soccio, E.R. Chen, M.A. Lazar. Thazolidinediones and the Promise of Insulin Sensitization in Type 2 Diabetes, Cell metabolism, 20 (2014) 573-591.

[108] C.E. Quinn, P.K. Hamilton, C.J. Lockhart, et al. Thiazolidinediones: effects on insulin resistance and the cardiovascular system, British Journal of Pharmacology, 153 (2008) 636-645.

[109] H. Kim, M. Haluzik, O. Gavrilova, et al. Thiazolidinediones improve insulin sensitivity in adipose tissue and reduce the hyperlipidaemia without affecting the hyperglycaemia in a transgenic model of type 2 diabetes, Diabetologia, 47 (2004) 2215-2225.

[110] F. Chiarelli, D.D. Marzio. Peroxisome proliferator-activated receptor-γ agonists and diabetes: Current evidence and future perspectives, Vascular Health and Risk Management, 4 (2008) 297-304.

[111] B. Cariou, B. Charbonnel, B. Staels. Thiazolidinediones and PPARgamma agonists: time for a reassessment, Trends Endocrinol Metab, 23 (2012) 205-215.

[112] S.K. Goyal, Samsher, R.K. Goyal. Stevia (Stevia rebaudiana) a bio-sweetener: a review, Int J Food Sci Nutr, 61 (2010) 1-10.

[113] O. Wonganan, C. Tocharus, C. Puedsing, et al. Potent vasorelaxant analogs from chemical modification and biotransformation of isosteviol, Eur J Med Chem, 62 (2013) 771-776.

[114] N.H. Mohd-Radzman, W.I. Ismail, Z. Adam, et al. Potential Roles of Stevia rebaudiana Bertoni in Abrogating Insulin Resistance and Diabetes: A Review, Evid Based Complement Alternat Med, 2013 (2013) 718049.

[115] H. Misra, M. Soni, N. Silawat, et al. Antidiabetic activity of medium-polar extract from the leaves of Stevia rebaudiana Bert. (Bertoni) on alloxan-induced diabetic rats, J Pharm Bioallied Sci, 3 (2011) 242-248.

[116] J. Hong, L. Chen, P.B. Jeppesen, et al. Stevioside counteracts the alpha-cell hypersecretion caused by long-term palmitate exposure, Am J Physiol Endocrinol Metab, 290 (2006) E416-422.

[117] P.B. Jeppesen, S. Gregersen, C.R. Poulsen, et al. Stevioside acts directly on pancreatic beta cells to secrete insulin: actions independent of cyclic adenosine monophosphate and adenosine triphosphate-sensitive K+-channel activity, Metabolism, 49 (2000) 208-214.

[118] J. Chen, P.B. Jeppesen, I. Nordentoft, et al. Stevioside improves pancreatic beta-cell function during glucotoxicity via regulation of acetyl-CoA carboxylase, Am J Physiol Endocrinol Metab, 292 (2007) E1906-1916.

[119] J. Chen, P.B. Jeppesen, I. Nordentoft, et al. Stevioside Counteracts Beta-Cell Lipotoxicity without Affecting Acetyl CoA Carboxylase, Rev Diabet Stud, 3 (2006) 178-188.

[120] J.C. Chang, M.C. Wu, I.M. Liu, et al. Increase of insulin sensitivity by stevioside in fructose-rich chow-fed rats, Horm Metab Res, 37 (2005) 610-616.

[121] J. Ma, Z. Ma, J. Wang, et al. Isosteviol reduces plasma glucose levels in the intravenous glucose tolerance test in Zucker diabetic fatty rats, Diabetes Obes Metab, 9 (2007) 597-599.

[122] D. Xu, M. Xu, L. Lin, et al. The effect of isosteviol on hyperglycemia and dyslipidemia induced by lipotoxicity in rats fed with high-fat emulsion, Life Sci, 90 (2012) 30-38.

[123] I. Nordentoft, P.B. Jeppesen, J. Hong, et al. Isosteviol increases insulin sensitivity and changes gene expression of key insulin regulatory genes and transcription factors in islets of the diabetic KKAy mouse, Diabetes Obes Metab, 10 (2008) 939-949.

[124] H.C. Bertram, P.B. Jeppesen, K. Hermansen. An NMR-based metabonomic investigation on effects of supplementation with isosteviol or soy protein to diabetic KKAy mice, Diabetes Obes Metab, 11 (2009) 992-995.

[125] V. Chatsudthipong, P. Jutabha. Effect of steviol on para-aminohippurate transport by isolated perfused rabbit renal proximal tubule, J Pharmacol Exp Ther, 298 (2001) 1120-1127.

[126] B.H. de Oliveira, R.A. Strapasson. Biotransformation of isosteviol by Fusarium verticilloides, Phytochemistry, 43 (1996) 393-395.

[127] F.E. Koehn, G.T. Carter. The evolving role of natural products in drug discovery, Nat Rev Drug Discov, 4 (2005) 206-220.

[128] G. Schmeda-Hirschmann, C. Aranda, M. Kurina, et al. Biotransformations of imbricatolic acid by Aspergillus niger and Rhizopus nigricans cultures, Molecules, 12 (2007) 1092-1100.

[129] S.F. Chang, L.M. Yang, C.H. Lo, et al. Microbial transformation of isosteviol and bioactivities against the glucocorticoid/androgen response elements, J Nat Prod, 71 (2008) 87-92.

[130] S.C. Saini, G.B.S. Reddy. A Review on Curry Leaves (Murraya koenigii): Versatile Multi-Potential Medicinal Plant, American Journal of Phytomedicine and Clinical Therapeutics [3][04][2015], (2015) 363-368.

[131] V. Prakash, C. Natarajan. Studies on curry leaf (Murraya koenigii L), Journal of Food Science and Technology, India, 11 (1974) 284-286.

[132] D. Iyer, U. Devi. Phyto-pharmacology of Murraya koenigii (L.), Pharmacognosy Reviews, 2 (2008) 180.

[133] S.K. Jain, R.A. DeFilipps. Medicinal plants of India, Reference Publications1991.

[134] Y. Tachibana, H. Kikuzaki, N.H. Lajis, et al. Comparison of antioxidative properties of carbazole alkaloids from Murraya koenigii leaves, Journal of agricultural and food chemistry, 51 (2003) 6461-6467.

[135] V. Mani, K. Ramasamy, A.B.A. Majeed. Anti-inflammatory, analgesic and anti-ulcerogenic effect of total alkaloidal extract from Murraya koenigii leaves in animal models, Food & function, 4 (2013) 557-567.

[136] S. Tembhurne, D. Sakarkar. Hypoglycemic effects of fruit juice of Murraya koenigii (L) in alloxan induced diabetic mice, Int J Pharm Tech Res, 1 (2009) 1589-1593.

[137] E. Mitra, A.K. Ghosh, D. Ghosh, et al. Protective effect of aqueous Curry leaf (Murraya koenigii) extract against cadmium-induced oxidative stress in rat heart, Food and chemical toxicology, 50 (2012) 1340-1353.

[138] Y.-S. Wang, H.-P. He, Y.-M. Shen, et al. Two New Carbazole Alkaloids from Murraya k oenigii, Journal of Natural products, 66 (2003) 416-418.

[139] S. Jagadeesh, S. Sinha, B.C. Pal, et al. Mahanine reverses an epigenetically silenced tumor suppressor gene RASSF1A in human prostate cancer cells, Biochemical and biophysical research communications, 362 (2007) 212-217.

[140] S. Sathaye, Y. Bagul, S. Gupta, et al. Hepatoprotective effects of aqueous leaf extract and crude isolates of Murraya koenigii against in vitro ethanol-induced hepatotoxicity model, Experimental and toxicologic pathology, 63 (2011) 587-591.

[141] C. Ito, M. Itoigawa, S. Onoda, et al. Chemical constituents of Murraya siamensis: three coumarins and their anti-tumor promoting effect, Phytochemistry, 66 (2005) 567-572.

[142] S.W. Pelletier. Alkaloids: chemical and biological perspectives, Springer1999.

[143] S. Syam, A.B. Abdul, M.A. Sukari, et al. The growth suppressing effects of girinimbine on HepG2 involve induction of apoptosis and cell cycle arrest, Molecules, 16 (2011) 7155-7170.

[144] K. Bhattacharya, S.K. Samanta, R. Tripathi, et al. Apoptotic effects of mahanine on human leukemic cells are mediated through crosstalk between Apo-1/Fas signaling and

the Bid protein and via mitochondrial pathways, Biochemical pharmacology, 79 (2010) 361-372.

[145] C. Ito, M. Itoigawa, K. Nakao, et al. Induction of apoptosis by carbazole alkaloids isolated from Murraya koenigii, Phytomedicine, 13 (2006) 359-365.

[146] B.A. Khan, A. Abraham, S. Leelamma. Murraya koenigii and Brassica juncea—Alterations on lipid profile in 1–2 dimethyl hydrazine induced colon carcinogenesis, Investigational new drugs, 14 (1996) 365-369.

[147] A.S. Shah, A.S. Wakade, A.R. Juvekar. Immunomodulatory activity of methanolic extract of Murraya koenigii (L) Spreng. leaves, (2008).

[148] A.N. Kesari, S. Kesari, S.K. Singh, et al. Studies on the glycemic and lipidemic effect of Murraya koenigii in experimental animals, Journal of Ethnopharmacology, 112 (2007) 305-311.

[149] P. Arulselvan, S.P. Subramanian. Beneficial effects of Murraya koenigii leaves on antioxidant defense system and ultra structural changes of pancreatic β-cells in experimental diabetes in rats, Chemico-Biological Interactions, 165 (2007) 155-164.

[150] M.B. Dusane, B.N. Joshi. Islet protective and insulin secretion property of Murraya koenigii and Ocimum tenuflorum in streptozotocin-induced diabetic mice, Canadian journal of physiology and pharmacology, 90 (2012) 371-378.

[151] S. Paul, T. Bandyopadhyay, A. Bhattacharyya. Immunomodulatory effect of leaf extract of Murraya koenigii in diabetic mice, Immunopharmacology and immunotoxicology, 33 (2011) 691-699.

[152] A.R. Shivashankara, A. Azmidah, R. Haniadka, et al. Dietary agents in the prevention of alcohol-induced hepatotoxicty: preclinical observations, Food & function, 3 (2012) 101-109.

[153] R. Gupta, D. Singh. Protective nature of Murraya Koenigii leaves against hepatosupression through antioxidant status in experimental rats, Pharmacologyonline, 1 (2007) 232-242.

[154] R. Birari, S.K. Roy, A. Singh, et al. Pancreatic lipase inhibitory alkaloids of Murraya koenigii leaves, Natural product communications, 4 (2009) 1089-1092.

[155] A. Chiabchalard, N. Nooron. Antihyperglycemic effects of Pandanus amaryllifolius Roxb. leaf extract, Pharmacogn Mag, 11 (2015) 117-122.

[156] J. Vattanarongkup, P. Piyachaturawat, P. Tuchinda, et al. Protective Effects of a Diarylheptanoid from Curcuma comosa Against Hydrogen Peroxide-Induced Astroglial Cell Death, Planta Med, 82 (2016) 1456-1462.

[157] E.C. Jensen. Quantitative Analysis of Histological Staining and Fluorescence Using ImageJ, The Anatomical Record, 296 (2013) 378-381.

[158] N. Nooron, A. Athipornchai, A. Suksamrarn, et al. Mahanine enhances the glucose-lowering mechanisms in skeletal muscle and adipocyte cells, Biochem Biophys Res Commun, 494 (2017) 101-106.

[159] B.C. Reed, M.D. Lane. Insulin receptor synthesis and turnover in differentiating 3T3-L1 preadipocytes, Proc Natl Acad Sci U S A, 77 (1980) 285-289.

[160] S.A. Yoon, S.I. Kang, H.S. Shin, et al. p-Coumaric acid modulates glucose and lipid metabolism via AMP-activated protein kinase in L6 skeletal muscle cells, Biochem Biophys Res Commun, 432 (2013) 553-557.

[161] J. Qiu, K. Maekawa, Y. Kitamura, et al. Stimulation of glucose uptake by theasinensins through the AMP-activated protein kinase pathway in rat skeletal muscle cells, Biochem Pharmacol, 87 (2014) 344-351.

[162] N. Fuse, K. Yasumoto, K. Takeda, et al. Molecular cloning of cDNA encoding a novel microphthalmia-associated transcription factor isoform with a distinct amino-terminus, J Biochem, 126 (1999) 1043-1051.

[163] W.H. Lee, R.J. Lin, S.Y. Lin, et al. Osthole enhances glucose uptake through activation of AMP-activated protein kinase in skeletal muscle cells, J Agric Food Chem, 59 (2011) 12874-12881.

[164] L. Che, Y.H. Yuan, J. Jia, et al. Activation of sonic hedgehog signaling pathway is an independent potential prognosis predictor in human hepatocellular carcinoma patients, Chin J Cancer Res, 24 (2012) 323-331.

[165] P. Samatiwat, A. Prawan, L. Senggunprai, et al. Repression of Nrf2 enhances antitumor effect of 5-fluorouracil and gemcitabine on cholangiocarcinoma cells, Naunyn Schmiedebergs Arch Pharmacol, 388 (2015) 601-612.

[166] R.M. Perera, S. Stoykova, B.N. Nicolay, et al. Transcriptional control of autophagy-lysosome function drives pancreatic cancer metabolism, Nature, 524 (2015) 361-365.

[167] B. Sripa, S. Leungwattanawanit, T. Nitta, et al. Establishment and characterization of an opisthorchiasis-associated cholangiocarcinoma cell line (KKU-100), World J Gastroenterol, 11 (2005) 3392-3397.

[168] S. Shibahara. The heme oxygenase dilemma in cellular homeostasis: new insights for the feedback regulation of heme catabolism, Tohoku J Exp Med, 200 (2003) 167-186.

[169] S. Kongpetch, V. Kukongviriyapan, A. Prawan, et al. Crucial role of heme oxygenase-1 on the sensitivity of cholangiocarcinoma cells to chemotherapeutic agents, PLoS One, 7 (2012) e34994.

[170] R.S. Kujur, V. Singh, M. Ram, et al. Antidiabetic activity and phytochemical screening of crude extract of Stevia rebaudiana in alloxan-induced diabetic rats, Pharmacognosy Research, 2 (2010) 258-263.

[171] R. Assaei, P. Mokarram, S. Dastghaib, et al. Hypoglycemic Effect of Aquatic Extract of Stevia in Pancreas of Diabetic Rats: PPARγ-dependent Regulation or Antioxidant Potential, Avicenna Journal of Medical Biotechnology, 8 (2016) 65-74.

[172] S. V. Tembhurne, D. M. Sakarkar. Anti-obesity and hypoglycemic effect of ethanolic extract of Murraya koenigii (L) leaves in high fatty diet rats, 2012.

[173] S.V. Tembhurne, D.M. Sakarkar. Influence of Murraya koenigii on experimental model of diabetes and progression of neuropathic pain, Research in Pharmaceutical Sciences, 5 (2010) 41-47.

[174] H. Kaneto, Y. Kajimoto, J. Miyagawa, et al. Beneficial effects of antioxidants in diabetes: possible protection of pancreatic beta-cells against glucose toxicity, Diabetes, 48 (1999) 2398-2406.

[175] M. Yamamoto, E. Yamato, S. Toyoda, et al. Transgenic expression of antioxidant protein thioredoxin in pancreatic beta cells prevents progression of type 2 diabetes mellitus, Antioxid Redox Signal, 10 (2008) 43-49.

[176] R.P. Robertson, H. Zhou, T. Zhang, et al. Chronic oxidative stress as a mechanism for glucose toxicity of the beta cell in type 2 diabetes, Cell biochemistry and biophysics, 48 (2007) 139-146.

[177] M. Tiedge, S. Lortz, J. Drinkgern, et al. Relation between antioxidant enzyme gene expression and antioxidative defense status of insulin-producing cells, Diabetes, 46 (1997) 1733-1742.

[178] M. Chakrabarty, A.C. Nath, S. Khasnobis, et al. Carbazole alkaloids from Murraya koenigii, Phytochemistry, 46 (1997) 751-755.

[179] M. Vinuthan, V. Girish Kumar, J. Ravindra, et al. Effect of extracts of Murraya koenigii leaves on the levels of blood glucose and plasma insulin in alloxan-induced diabetic rats, Indian journal of physiology and pharmacology, 48 (2004) 348-352.

[180] G. Gupta, S. Nigam. Chemical examination of the leaves of Murraya koenigii, Planta medica, 18 (1970) 83-86.

[181] D. Chakraborty, P. Bhattacharyya, S. Roy, et al. Structure and synthesis of mukonine, a new carbazole alkaloid from Murraya koenigii, Phytochemistry, 17 (1978) 834-835.

[182] B. Oliver-Bever. Medicinal plants in tropical West Africa, Cambridge university press1986.

[183] G. Shammas. Flavonoid heterosides of Teucrium polium L, Planta Medica Phytotherapia, 21 (1987) 144-148.

[184] K. Zaman. Medicinal plants with hypoglycemic activity, Journal of Ethnopharmacology, 26 (1989) 1-55.

[185] D. Pathak, K. Pathak, A. Singla. Flavonoids as medicinal agents-recent advances, Fitoterapia, 62 (1991) 371-389.

[186] M. Ahmad, M.S. Akhtar, T. Malik, et al. Hypoglycaemic action of the flavonoid fraction of Cuminum nigrum seeds, Phytotherapy research, 14 (2000) 103-106.

[187] B. Chakravarthy, G. Saroj, S. Gambhir, et al. Pancreatic beta cell regeneration–a novel antidiabetic mechanism of Pterocarpus marsupium roxb, Indian journal of Pharmacology, 12 (1980) 123.

[188] B. Chakravarthy, S. Gupta, S. Gambhir, et al. Pancreatic beta-cell regeneration in rats by (-)-epicatechin, The Lancet, 318 (1981) 759-760.

[189] P. Newsholme, D. Morgan, E. Rebelato, et al. Insights into the critical role of NADPH oxidase (s) in the normal and dysregulated pancreatic beta cell, Diabetologia, 52 (2009) 2489-2498.

[190] Y. Uchizono, R. Takeya, M. Iwase, et al. Expression of isoforms of NADPH oxidase components in rat pancreatic islets, Life sciences, 80 (2006) 133-139.

[191] H. Kaneto, G. Xu, K.H. Song, et al. Activation of the hexosamine pathway leads to deterioration of pancreatic beta-cell function through the induction of oxidative stress, J Biol Chem, 276 (2001) 31099-31104.

[192] Effect of intensive blood-glucose control with metformin on complications in overweight patients with type 2 diabetes (UKPDS 34). UK Prospective Diabetes Study (UKPDS) Group, Lancet, 352 (1998) 854-865.

[193] J.S. Fisher, J. Gao, D.H. Han, et al. Activation of AMP kinase enhances sensitivity of muscle glucose transport to insulin, Am J Physiol Endocrinol Metab, 282 (2002) E18-23.

[194] J. Pandey, R. Maurya, R. Raykhera, et al. Murraya koenigii (L.) Spreng. ameliorates insulin resistance in dexamethasone-treated mice by enhancing peripheral insulin sensitivity, J Sci Food Agric, 94 (2014) 2282-2288.

[195] M.J. Tan, J.M. Ye, N. Turner, et al. Antidiabetic activities of triterpenoids isolated from bitter melon associated with activation of the AMPK pathway, Chem Biol, 15 (2008) 263-273.

[196] N.H. Mohd-Radzman, W.I. Ismail, S.S. Jaapar, et al. Stevioside from Stevia rebaudiana Bertoni Increases Insulin Sensitivity in 3T3-L1 Adipocytes, Evid Based Complement Alternat Med, 2013 (2013) 938081.

[197] E. Esteve, W. Ricart, J.M. Fernandez-Real. Adipocytokines and insulin resistance: the possible role of lipocalin-2, retinol binding protein-4, and adiponectin, Diabetes Care, 32 Suppl 2 (2009) S362-367.

[198] R.B. Ceddia, R. Somwar, A. Maida, et al. Globular adiponectin increases GLUT4 translocation and glucose uptake but reduces glycogen synthesis in rat skeletal muscle cells, Diabetologia, 48 (2005) 132-139.

[199] T. Udono, K. Yasumoto, K. Takeda, et al. Structural organization of the human microphthalmia-associated transcription factor gene containing four alternative promoters, Biochim Biophys Acta, 1491 (2000) 205-219.

[200] Y. Kim, M.O. Kim, J.S. Shin, et al. Hedgehog signaling between cancer cells and hepatic stellate cells in promoting cholangiocarcinoma, Ann Surg Oncol, 21 (2014) 2684-2698.

APPENDIX

LISTS OF ABBREVIATIONS

α	Alpha
β	Beta
δ	Delta
°C	Degree Celsius
γ	Gamma
µg	Microgram
µl	Microliter
µM	Micro molar
µU	Micro Unit
%	Percent
Ab	Antibody
AKT	Protein kinase B (PKB)
ANOVA	Analysis of variance
ATCC	American type culture collection
AMPK	AMP-activated protein kinase
ATP	Adenosine triphosphate
BSA	Bovine serum albumin
cAMP	cyclic adenosine monophosphate
Ca	Calcium
Ca^{2+}	Calcium ion

LISTS OF ABBREVIATIONS (cont.)

cDNA	Complementary DNA
cGMP	Cyclic guanosine monophosphate
CH_2CL_2	Dichloromethane
cm^2	Centimeter
CREB	cAMP-response element binding protein
Ct	Cycle threshold
DCF	Dichlorofluorescein
ddH_2O	Double distilled water
DMEM	Dulbecco's modified Eagle's medium
DMSO	Dimethyl sulfoxide
DM	Diabetes mellitus
DNA	Deoxynucleic acid
EDTA	Ethylenediaminetetraacetic acid
e. g.	For example
FBS	Fetal bovine serum
FFA	Fatty acid
g	Gram
GAPDH	Glyceraldehyde-3-phosphate dehydrogenase
GCK	Glucokinase
GLI1	Glioma-associated oncogene 1

LISTS OF ABBREVIATIONS (cont.)

GLUT-4	Glucose transporter type 4
GSIS	Glucose-stimulated insulin secretion
h	Hour
HBSS	Hank's balanced salt solution
H_2DCFDA	2 ,7 –dichlorodihydrofluorescein diacetate
HO-1	heme oxygenase
H_2O_2	Hydrogen peroxide
HRP	Horseradish peroxidase
IC50	Fifty-percent inhibitory concentration
IL-1	Interleukin-1
IL-4	Interleukin-4
IL-1β	Interleukin-1 beta
IL-6	Interleukin-6
IRS-1 and IRS-2	Insulin receptor substrate
kDa	Kilodalton
LBs	Lewy Bodies
LDH	Lactic dehydrogenase
MAPKAPK 2/3	Mitogen activated protein kinase activated protein kinase 2 and 3
MAPKKK	Mitogen activated protein kinase kinase kinase

LISTS OF ABBREVIATIONS (cont.)

MAPKK	Mitogen activated protein kinase kinase
MAPK	Mitogen activated protein kinase
MEM	Modified Eagle's medium
MeOH	Methanol
ml	Milliliter
mg	Milligram
min	Minute
mm	Millimeter
mM	Millimolar
Mitf	Microphthalmia-associated transcription factor
MMP	Mitochondiral membrane potential
MTT	3-(4,5-Dimethylthiazol-2-yl)-2,5-diphenyltetrazolium bromide
MW	Molecular weight
NaCl	Sodium chloride
NAD^+	Nicotinamide adenine dinucleotide
NADPH	Nicotinamide adenine dinucleotide phosphate
NaF	Sodium fluoride
$NaHCO_3$	Sodium bicarbonate
Na_2HPO_4	Disodium hydrogen phosphate

LISTS OF ABBREVIATIONS (cont.)

nm	Nanometer
$O_2^{\cdot-}$	Superoxide
$OH^{\cdot}$	Hydroxyl radical
PAGE	Polyarcrylamide gel electrophoresis
PARP	Poly-ADP rinose polymerase
PBS	Phosphate-buffered saline
PBS-T	Phosphate-buffered saline tween
PDK1	Pyruvate Dehydrogenase Kinase 1
PDX-1	Pancreatic duodenum homeobox-1
PI3K	Phosphatydil-inositol-3-inase
PIP3	Phosphatidylinositol (3,4,5)-triphosphase
PKC	Protein kinase C
pmol	Picomole
PRE-INS	Pre-insulin
PPAR-γ	Proliferator-activated receptor-γ
S6K1	Ribosomal protein S6 kinase beta-1
ROS	Reactive oxygen species
Rpm	Revolutions per minute
RPE	Retinal pigment epithelium
RT-PCR	Reverse transcriptase PCR

LISTS OF ABBREVIATIONS (cont.)

s	Second
SAR	Structure-activity relationship
SDS	Sodium dodecyl sulfate
SDS-PAGE	SDS-polyacrylamide gel electrophoresis
SOD	Superoxide dismutase
TBS	Tris-buffer saline
TPS-T	Tris-buffer saline tween
TGF-α	Transforming growth factor-alpha
TNF-α	Tumor necrosis factor-alpha
T2DM	Type 2 Diabetes mellitus
UV	Utraviolet
V	Volt
WHO	World Health Organization

REAGENTS PREPARATION

A. Treatment reagents

1. Hydrogen peroxide (H_2O_2) 1 M

- H_2O_2 8.21 M 23 µL
- Serum free media 177 µL

Freshly prepare and protect from light

2. Ascorbic acid 100 mM in DMSO

- Ascorbic acid 17.613 mg
- DMSO 1 mL

Protect from light and store at – 20 °C

3. Wortmanin 100 mM in DMSO

- Wortmanin 1 mg
- DMSO 23 µL

Protect from light and store at – 20 °C

4. Compound C 100 mM in DMSO

- Compound C 5 mg
- DMSO 125 µL

Protect from light and store at – 20 °C

5. Metformin 100 mM in DMSO

- Metformin 150 mg
- DMSO 12 mL

Protect from light and store at – 20 °C

6. 2NBDG 10 mM in DMSO

- 2NBDG 5 mg
- DMSO 1.4 mL

Protect from light and store at – 20 °C

B. Experimental reagents

1. Reagents for using in cell culture

1.1 0.01 M Phosphate-buffered saline (PBS(-); 10X)

NaCl	80	g
KCl	2	g
Na_2HPO_4	14.4	g
KH_2PO_4	2.4	g

Add ddH_2O to 1000 mL and stored as stock solution

To prepare 1X 0.01M PBS, dilute to 100 mL 10X PBS with 900 mL H_2O and adjust pH to 7.4

1.2 MTT solution

MTT	0.01	g

Add 1X PBS to 10 mL and passed through 0.45 μM sterile filter membrane

Protect from light and stored at 4°C

1.3 0.25% Trypsin-EDTA

0.5% Trypsin-EDTA	2.5	mL
0.01M PBS	7.5	mL

1.4 0.1% Trypan Blue

0.4% Trypan Blue	2.5	mL
0.01M PBS	7.5	mL

2. Reagents for Western blot analysis

2.1 4X Running Gel Buffer (1.5M Tris-Cl, pH 8.8)

Tris	36.6	g
ddH_2O	200	mL

Adjust to pH 8.8 with HCl

Store up to 3 months at 4°C and protect from light

2.2 4X Stacking Gel Buffer (1.5M Tris-Cl, pH 8.8)

Tris	3	g
ddH_2O	50	mL

Adjust to pH 6.8 with HCl

Store up to 3 months at 4°C and protect from light

2.3 10% Sodium Dichosyl Sulphate (SDS)

SDS	10	g

ddH_2O	100	mL

2.4 10% Ammonium Persulfate (APS)

Ammonium Persulfate	0.1	g
ddH_2O	1	mL

Freshly prepare and protect from light

2.5 Loading/sample/dye buffer 6X, 1 mL

0.5 M TrisHCl pH 6.8	700	µL
10% SDS	0.1	g
Glycerol	300	µL
DTT	0.093	g
Bromophenol blue	0.0012	g

Add ddH_2O to 1 mL and store at 4 °C

2.6 10X Running Electrophoresis buffer

Tris base	30.28	g
Glycine	144.13	g
SDS	10	g
ddH_2O	1	L

Working concentration 1X

2.7 10X Transfer buffer

Tris-base	15.15	g

Glycine	72.1	g
ddH_2O	400	mL

To prepare 1X transfer buffer, mix 80 mL of 10X transfer buffer with 200 mL 100% methanol and 720 mL ddH_2O

2.8 1X phosphate buffer saline Tween-20 (1X PBST)

10X PBS	100	mL
ddH_2O	900	mL
Tween 20	1	mL

2.9 1X RIPA lysis buffer

1 M Tris pH 7.4	25	mL
3 M NaCl	25	mL
Triton X-100	5	mL
DOC	5	g
20% SDS	2.5	mL
Na_2HPO_4	2	g
NaF	1	g
EDTA	1	g
ddH_2O	440	mL

Before use, add 1 % protease inhibitor cocktail

2.10 Gel (12.5%) Preparation for 1.5 mm glass

Running gel

4X running gel buffer (1.5 M Tris-Cl, pH 8.8)	2.5	mL
Bis/acrylamide solution	4.2	mL
ddH_2O	3.2	mL
10% SDS	100	µL
10% APS	150	µL
TEMED	15	µL

Stacking gel

4X stacking gel buffer (0.5 M Tris-Cl, pH 6.8)	1.03	mL
Bis/acrylamide solution	440	µL
ddH_2O	1.822	mL
10% SDS	33	µL
10% APS	50	µL
TEMED	7.5	µL

2.11 Stripping buffer for 1 membrane

10% SDS	4	mL
4X stacking gel buffer (0.5 M Tris-Cl, pH 6.8)	2.5	mL
ddH_2O	13.5	mL
β-mercaptoethanol	140	µL

VITA

My name is Nattakarn Nooron. I graduated with a Bacherlor's degree in medical technology, Faculty of Allied Health Science, Thammasart University. Then I received the master degree in Clinical Biochemistry and Molecular Medicine program, Faculty of Allied Health Science, Chulalongkorn University. Now, I am studying of PhD program at the Chulalongkorn University with in Clinical Biochemistry and Molecular. My field of study is molecular of medical plants, especially on antioxidant and glucose -lowering mechanisms.